COLOUR MISMATCH IN COMPOUNDING OF PLASTICS: PROCESSING ISSUES AND RHEOLOGICAL EFFECTS

A Thesis submitted in partial fulfillment of the requirements for the degree of

Doctor of Philosophy

in

Mechanical Engineering

The Faculty of Engineering and Applied Science

University of Ontario Institute of Technology

By

Jamal Al-Sadi

Abstract

Demand for plastic products is continuously growing with population increase and higher living standards. Imparting colours to plastics is a combination of art and science and plays a key role in production of attractive products for a variety of consumer demands. It requires a good understanding of the processing parameters and formulation of compositions including colour pigments and their dispersion. This thesis presents experimental observations and statistical analysis to investigate scientific reasons for colour mismatches in compounded plastics. Material processing issues were investigated.

Six methods were used to study and improve the understanding of colour matching, colour stability, and consistency of compounded plastic materials in order to minimize wastage. The first was Data Mining, in which historical data was analyzed to select formulations, particularly for pigments and polycarbonate blends of compounded plastics that were known to suffer from colour mismatch. The second method involved the use of historical data and an artificial neural network (ANN) to predict the resultants colours based upon pigment formulations. In the third method, a parametric study was utilized to investigate issues in the dispersion of pigments due to the effects of processing conditions. Temperature and feed rate were found to have major effects on colour deviations. The fourth method involved studying the compounding process for blends of two polycarbonate resins (PC) of different melt flow index (MFI). It was also found that the PC composition of 30-70 wt.% was superior in terms of colour matching. The fifth method studied effects of rheology. The viscosity data collected allows predictions of viscosity changes with varying temperatures, which had a direct impact on polymer colour changes during processing of blends. The sixth method looked at the effects of processing parameters on dispersion, pigment size distribution (PSD), and the morphology of pigments in polycarbonate compounds. In general, the total colour difference decreased when processing parameters were increased. De-agglomeration occurred in zones of high shear and was found to significantly increase the number of particles and lower colour differences.

The results yield an optimum set of processing parameters for certain grades of plastic. The optimized measurements of processing conditions are typically in agreement with the minimum colour difference. Furthermore, many conclusions found here can be used to optimize compounding materials and generate an efficient dispersion process, and hence reduce colour mismatch so that wastage is minimized.

Keywords: Data Mining, Neural Network Modeling, Processing Parameters, Design of Experiments (DOE), Polycarbonate Blends and Rheology, Colour Matching and Morphological Dispersion

Acknowledgements

I would like to dedicate this work for my parents, who passed away during my study. My parents were the most beautiful things I ever had. I attribute my success in life to the moral, intellectual, and physical education I received from them. I would also like to show gratitude to my family for their support and encouragement throughout my research and higher education. This support has been vital, and I shall never forget it. Much love and thanks are extended to my friends and others who have lent their support and encouragement through this endeavour.

I would like to express my thanks to my supervisor Professor Ghaus Rizvi for his patient guidance, encouragement and useful critiques of this research work. I also want to extend my deepest appreciation to him for giving me every opportunity to enhance my graduate experience from introducing me to an industrial organization facility, to allowing me to attend conferences, seminars and workshops across North America and North Africa to present my work. I am thankful to my supervisory committee members Dr. Hossam Kishawy and Dr. Yuping He for their guidance and advice.

I am particularly grateful for the assistance given, not only for their technical knowledge, but also for showing me how to differentiate the important things and keep the most basic questions in mind. I would also like to express great appreciation to the people who helped and supported me during the preparation of this thesis. I also acknowledge the support and guidance by Professor Amir Hossein Behravesh. I would also like to take the time in expressing great thanks to my colleagues in our Mechanical Engineering Lab, Dr. Usman Saeed and PhD students Shahid and Rasel for their kind collaboration and efforts. Major funding for this research was graciously by SABIC IP and Natural Sciences and Engineering Research Council (NSERC) of Canada .I would like to extend my gratitude for support provided by the staff at SABIC IP Cobourg, Canada for their assistance in the experiments, lab tests: Daniel Ross. Joseph Wembley, James Price, and Richard Clarke. This journey

would not have been possible without their help and support. The material samples used throughout the experimental process were generously provided SABIC IP.

I would also like to thank Professor Hani Naguib of University of Toronto for use of the Minilab extruder and Dr. Reza Rizvi for his assistance in its operation.

Table of Contents

List of Figures

List of Tables

Nomenclature Symbols

Symbol	Description
ΔP	Delta pressure
$P1$	Pressure transducer
$\dot{y}_a$	Apparent shear rate (s-1)
R	Radius of rheometer plates (mm)
Ω	Angular velocity (rad/s)
f	Frequency (hertz)
ω	The fixed angular frequency of the oscillations (rad/s) ($\omega = 2\pi f$)
H	Gap between the rheometer plates (mm)
η^*	Complex viscosity (Pa x s)
η'	Dynamic viscosity (Pa x s)
n''	Elastic viscosity (Pa x s)
G'	Storage modulus (Pa)
G''	Loss modulus (Pa)
$R1$	Resin one
$R2$	Resin two
L	Screw length (mm)
D	Screw diameter (mm)
$Wt\%$	Weight percentage of PC (gm)
MFI	Polymer melt flow index (g/10 min)
MFR	Melt flow rate
MVR	Melt volume rate
S	Strain percentage

Symbol	Description
T	Temperature (°C)
T_m	Melting temperature (°C)
T_g	Glass transition temperature (°C)
LVR	Linear visco-elastic region
η	Shear viscosity (Pa x s)
η_0	Zero Shear Viscosity (Pa x s)
λ	Relaxation time (S)
$G'(t)$	Relaxation stress (Pa)
DSC	Differential scanning calorimetry
TGA	Thermal gravimetric analysis
DMA	Dynamic mechanical analysis
WOA	Without pigment and additives
WA	With pigment and additives
$WPNA$	With pigment, no additives
MB	Masterbatches
FCO	Forced convection oven
EVF	Extensional viscosity fixture
DOE	Design of experiments
μCT	Micro CT scanner
$ASTM$	Standard test method for MFI
LVR	Linear viscous-elastic region
DFS	Dynamic frequency sweep
$SSRS$	Steady shear rate sweep
SST	Strain sweep test
DOM	Digital Optical Microscope

Symbol	Description
M_w	Average molecular weight
PC	Polycarbonate
DE, dE^*	Colour differences with respect to target values in terms of dL*, da*, and db*
$LAOS$	Large amplitude oscillatory shear test
PP	polypropylene
PA	polyamide
PBT	polybutylene terephthalate
PPS	polyphenylene sulphide
ML	Minilab Extruder
SB	SABIC process (Coperion TSE & injection molding)
τ	Shear stress
$\dot{\gamma}$	Shear rate
R	Radius of rheometer plates (mm)
NN	Neural network
MLP	Multilayer perception
x_{ij}	The incoming signals or input
W_{ij}	Weights
b_j	Bias contribution
x_i	The connection weights between nodes
V_{ij}	The signal from node
F	A transfer function (when applied to the input of a node, determines its output)
F_i	The weighted sum of the input
GD	The batch gradient descent
GDX	Batch variable learning rate
SCG	Scaled Conjugate Gradient

Symbol	Description
LM	Levenberg–Marquardt algorithm has been used for the variants.
Sig	The sigmoid transfer function has been used in hidden layer
$Purelin$	Where the pure linear transfer function has been used in the output layer.
RMS	Root mean squared
R^2	Absolute fraction of variance or regression of coefficient
Ea	An actual result
Ep	A predicted result
Em	A mean value
N	The number of patterns
w_{ij}	Initialize all node connection weights
V_{im}	Input a training example
v_{iT}	Corresponding output values
M	The layer number
I	The node number
T	Represents the target or desired output state
V_i^{m-1}	Signal from node i and layer m − 1
β	Threshold or bias value of the node
(δ)	Compute the deltas for the output layer
GDM	The gradient descent with momentum
RP	Resilient back propagation
MSE	Mean squared error
$Tan\ \delta$	(G″/G′)
PSA	Particle size analyser
SEM	Scanning Electron Microscope
F	Additives

Symbol	Description
pph	Part per hundred
CCD	Digital cooled camera
VIF	Variance inflation factors
$DFFITS$	Difference of fits – a statistics helpful in detecting influential runs
PSD	Particle size distribution
ATR	The technique of Attenuated Total Reflectance
$FTIR$	Fourier Transform Infrared
RTD	Residence time distribution

Chapter 1: Introduction

1.1 Preamble

Plastics offer light weight, strength, and ease of molding into desired shapes, and are therefore preferred over metals in many daily applications. They can also take any colour, shape, and can be modified to look similar to a wide range of traditional materials, including steel and wood. Plastics generally offer attractive cost-saving opportunities due to their low material and manufacturing costs. Increasing performance demands and heightened competition are pushing plastic suppliers to produce higher quality products. Colour is an essential attribute of the product that highly affects the customer selection and attraction. Therefore, obtaining the desired colour is an important requirement in the manufacturing of plastics.

Each individual perceives colour differently, making variations in colour difficult to evaluate. To establish colour standards, various methods have been developed. Most of these define a 2D or 3D colour space, where colour variations are measured in terms of the spatial distance between the desired colour and the specimen colour. In this paper, CIE L*a*b* colour space is used and is described in Chapter 2 along with issues related to colour perceptions and its quantification. Colour of a compounded plastic batch is quantified utilizing a device called a spectrophotometer, which measures three numbers representing the tristimulus values (CIE L*a*b* values in this paper). These numbers should match the target colour values set by quality standards or by the customer. However, measured colour values, when compared with the target colour, may exhibit deviations from the target in terms of dE*, which indicates the spatial separation of the output colour compared to the target colour in the CIE L*a*b* colour space. If dE* exceeds a permissible limit, rejection of the whole lot produced may be warranted, resulting in wastage and delays in delivery time.

1.2 The Compounding of Coloured Plastic

Nearly all plastics used in manufactured products are coloured. The desired colour is obtained by compounding plastics, usually by dedicated compounding companies, where resins, additives, and pigments are blended together to produce coloured plastic under controlled processing conditions. Several compounding processes are available that share the same basic scientific principles and parameters. The primary compounding processes used in the industry are either continuous mixing or batch mixing, after which the material is processed by a single screw or twin-screw extruder. The output material strands are cooled and then cut into small pellets by a pelletizer. These pellets are sold to manufacturers to be used as raw materials for their products.

1.3 Reasons for Colour Mismatch

In the compounding industry, the main cause of material rejection is colour mismatch indicated by large deviations from the desired colour values. The colouring of plastic materials is not a simple process. There are many variables that must be dealt with and these variables often do not act independent of each other. In order to improve colour consistency in the plastic industry, there is a need to understand the effects of these variables and control them as much as possible. The problem of colour mismatch can arise mainly due to the following reasons:

- **Incorrect formulations:** This can be due to incorrect determination by the colour expert of the equipment used. The role of human error cannot be ignored too, and the problem multiplies due to measurement error.

- **Processing conditions:** Processing parameters such as temperature, feed rate, and shear rate (RPM) can also affect the colour of the final product.

- **Poor pigment dispersion:** Dispersion refers to the phenomenon of breaking clustered particles into tiny particles. In order to break the particles, sufficient shear energy is required. The compounding process should be designed to provide this energy.

- **Interaction between materials and processing conditions:** Like other chemicals, pigments have the potential to become involved in chemical reactions. If this occurs, the pigment is deemed as a failure for its intended purpose. Many polymer systems will yellow and/or darken with extended exposure to temperature. Similarly, an excess of shear stress can have adverse effects on pigments. [1]

- **Degradation during processing:** Degradation is a process of any harmful change in the polymer in terms of physical appearance, mechanical properties, chemical reaction, loss of clarity, change in colour, or increase in viscosity, to name a few. Often, degradation is caused by the regular intrusion of oxygen into polymer molecules, known as oxidation. The pigment in the polymer degrades as a result of elevated processing temperatures or environmental exposure due to the presence of UV light or weathering. One way to prevent degradation is to add stabilizers to the composition before processing. [2]

For large-scale compounders, the wastage due to mismatch is not a major issue as the correct formulation and processing conditions can be obtained during initial trials. The amount of wastage is only a minute proportion of the total production. But for compounders like SABIC IP, who cater to the needs of small lot size users such as for making prototypes or small-scale manufacturers, this wastage constitutes a significant loss. Getting the right colour in the first trial is crucial to their business model. This issue has not been as thoroughly studied by the plastic compounding industry as it has by the paint industry.

1.4 Saudi Basic Industries Corporation (SABIC)

Saudi Arabia Basic Industries Corporation (SABIC) was founded in 1976 when the government of Saudi Arabia decided to use the hydrocarbon gases associated with its oil production as the principal feedstock for the production of chemicals, polymers, and fertilizers. SABIC's businesses are grouped into Chemicals, Polymers, Performance Chemicals, Fertilizers, Metals, and Innovative Plastics. It is one of the recognized leaders in thermoplastics materials. The plant at Cobourg, ON, is the manufacturer of small lots of custom ordered coloured pellets and sheets (ABS, polycarbonate and other thermoplastic

resins) according to customers' specified colours. These are supplied to a large number of plastic manufacturers across the country and in the global market.

1.5 Collaboration between SABIC IP and UOIT

UOIT established a collaborative research project with the support of SABIC's Innovative Plastics to help understand the colour mismatch problem in short lot size compounding operations. Therefore, the principal objective of this research was to study and understand the colour mismatch issues during the colour compounding process. This included analysis of myriads of available processing data and conducting designed experiments at SABIC IP facilities. The resin most frequently compounded at SABIC IP is polycarbonate (PC); therefore, the focus of this collaborative research work was this resin.

1.6 Motivation

In the colour compounding industry, the most important cause of material rejection is colour mismatch. In order to improve colour consistency, it is essential to define, understand, and control as many influencing variables as possible. This paves the way to develop a scientific approach for improving colour matching, understanding the reason behind it, and finally, introducing possible solutions. SABIC uses a large number of materials and pigments to produce a variety of coloured products on a daily basis. They have 15 production lines; their basic input materials consist of approximately 15 to 20 resin grades, over 200 pigments, and a variety of other additives. To fulfil one order, on average, one or two resins and a combination of 4 to 8 pigments are used in addition to a number of additives. Hence, a very large number of compounded plastics are produced each day.

Due to the small batch sizes, producing the right product with minimum wastage, particularly when matching the colour is the principal goal, is highly challenging. Even a very small deviation in colour could cause rejection of the whole produced lot. Therefore, pinpointing the correct formulation in the first attempt is essential for reducing wastage. This requires a thorough knowledge of the key factors involved in colour matching.

1.7 Objective

The main objective of this research is to investigate major issues related to colour mismatch of compounded plastics that lead to high wastage.

To achieve this goal, the research was undertaken in two phases, each with their own objectives. The first phase utilized the historical data available at SABIC IP with the twin objectives of: a) identification of the various groups of materials and sets of processing conditions that cause colour mismatch issues by employing proper statistical tools; b) using the large set of formulation and the resulting product characteristics data available with SABIC to develop predictive models based on methods such as Artificial Neural Networks (ANN) in order to achieve correct colour formulations on the first attempt.

The second phase of research was based on scientific experimental studies for which the processing equipment at SABIC IP was used and characterizing work was carried out at both SABIC and UOIT. The main objectives of this work were threefold. The first objective was to elucidate the effects and interactions of the relevant material and processing parameters and subsequently develop a mechanism for proposing optimum formulations. This was done by studying the effect of processing parameters on the colour properties of polymers by using Design of Experiments (DOE) and by studying General Trends. The second objective was to carry out the characterization of rheological properties of polycarbonate blends with and without the addition of pigment and additives. Lastly, the third objective was to study the effects of processing parameters on the dispersion of pigments during the compounding process.

All in all, this research is intended to develop a broader understanding of the scientific mechanisms that result in colour variations when pigments are blended into plastic resins.

1.8 Thesis Organization

An introduction to colour compounding and compositions is presented in the first chapter. The mismatch issue in SABIC production lines, a statement of problem, and finally

the objectives of this thesis work are addressed in this chapter. The second chapter focuses mainly on the science behind the colouring of plastic. This will provide information about the factors, assessment, and the bases of colour quantification. Related information about the raw materials of plastic and principles of mixing are discussed. A review of literature published on the statistical analysis methods of data mining and design of experiments are also presented.

In the third chapter, a literature review is provided on the subjects relating to plastic resin (polycarbonate, PC), colouring of plastics**,** data mining and neural networks, design of experiments (DOE), rheology, pigment dispersion, and morphology. The fourth chapter includes experimental investigations through performing a series of experiments to study the effects of PC blends, processing parameters, and rheology on colour output. Experimental equipment and procedures are explained in this chapter. Experiments with two types of twin-screw extruders on various compounds are described here as well. The fifth chapter includes modelling of compounded plastic for optimised colour production. The main models used are NN, DOE, and viscosity (Carreau models). In this section, basic governing equations are also illustrated.

The sixth chapter presents the results and discussion for both phases of this research. A model is presented for predicting the final colour output based on input. In the seventh chapter, a summary of the thesis is given and the main findings are highlighted. Finally, a set of recommendations is presented for future research works in this area.

Chapter 2: General Review on Colouring of Plastics

2.1 Introduction

Plastics production is a key industrial sector in Canada. The plastics industry has grown substantially over the past few decades, in part due to the ease of manufacturing of plastic parts, relative to other materials. Complicated parts can be fabricated in fewer steps with lower resulting costs. In addition, plastics are recyclable and their manufacturing requires less energy than other conventional materials, and hence, are more eco-friendly than metals. Despite the current economic pressures, the North American plastic compounding industry sold 4.5-5.4 billion kg of compounded product in 2005, worth about $11 billion. [3, 4]. A vast benefit of using plastics is the immense array of colours that are available for enhancing the attractiveness of the products for consumers. However, generating the right coloured product with minimal wastage is a great challenge for plastic compounders. This is particularly true for short lead-time suppliers of small lot sizes who predominantly cater to the needs of prototype development. Quick realization of prototypes is a key component to the success of all innovative product development, and this capability is essential for Canada in order to maintain its leading place in the rapidly growing and competitive global markets.

One manufacturer facing such problems is SABIC Innovative Plastics (formerly GE Plastics), a recognized global industry leader, at its manufacturing plant in Cobourg, Ontario. A core component of SABIC's business is the supply of tailored plastics with customer specified colours, mostly in small unique lots for prototyping purposes. These are supplied to a large number of plastic manufacturers across the country and in the global market. Companies like SABIC play a very important role in rapid development of prototypes, and hence, facilitate innovation.

2.2 Background on Colour

Plastic resins are usually white or colourless when produced in petrochemical plants. Dyes and pigments are used for imparting colours into plastics. Dyes are soluble in plastics and they give a more transparent finish. On the other hand, pigments are insoluble and they must be properly dispersed in the plastic to achieve a uniform colour. When incident light falls on the plastic surface, a small fraction of the light reflects from the surface. Most of the light enters the plastic surface and then begins to pass through or is reflected from randomly shaped and oriented pigment particles. In the case of an opaque material, the colour is seen in the diffuse reflection and the gloss colour is usually seen in the specular reflection as shown in **Figure 2.1**.

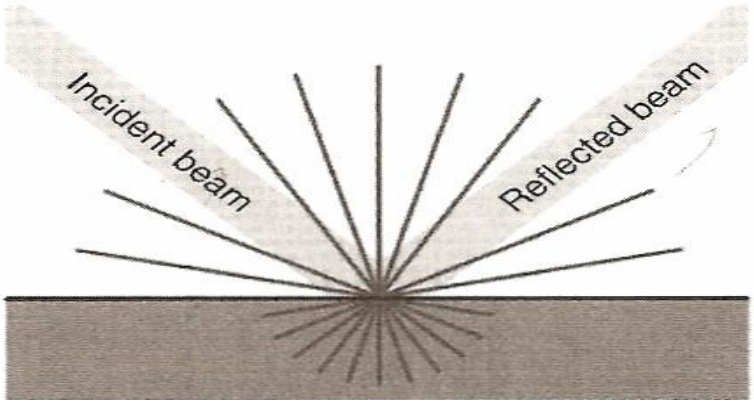

Figure 2.1. Incident and reflection of light on an opaque material [5]

The pigments absorb certain colours but reflect others in random directions based on their surfaces and orientations. Thus, in a multi-blend compound, the incident light is reflected by many pigment particles, usually of different colours, at different depths. Some pigments also exhibit fluorescence as they absorb energy in the UV range and emit it in the visual spectrum. The net result of all reflections and emissions imparts a colour to the plastic. Therefore, if there is no absorption and about equal amounts of scattering at all visible wavelengths, then the object will appear white; however, if the visible light is absorbed by the pigment, then the object appears coloured.

2.2.1 Interaction of Light with Colourants

When light strikes an object, it undergoes one or more of the following actions: refraction, absorption, reflection, and/or scatter. Interaction of light with colourants can be interpreted in terms of these actions.

- ***Refraction.*** When light travels from one medium to another, it changes direction due to changes in its velocity in the respective mediums. As a result, there is a change in its direction. The Refractive Index is the property of the material that determines the magnitude of this change.

- ***Absorption.*** If an object absorbs the entire visible spectrum of the light from a polychromatic source, the object will appear black. If the material absorbs only a portion of the light, then it will appear coloured. For example, if the object absorbs all but the green portion of the visible light, the object appears green. If however, the light source does not contain the green portion of the spectrum, the object will appear black. There are two basic laws in absorption: Beers law and Lamberts law. Lamberts law states that equal thickness of materials causes an equal amount of absorption, whereas Beers law states that the amount of light absorbed is proportional to the concentration of the absorbing material. [6]

- ***Reflection.*** Reflection occurs when light is incident upon a smooth surface, and it is returned or reflected back at an angle equal to the incidence angle.

- ***Scattering.*** Scattering occurs when light is reflected in random direction due to irregular surfaces or it is deflected due to passage through irregular particles. The amount of light scattered depends on two factors: the difference between the two refractive indices and the particle size of the pigment.

In conclusion, the appearance of colour of an object depends on the cumulative amount and type of scattering and absorption that takes place. Therefore, if there is no absorption and about equal amounts of scattering at all visible wavelengths, then the object

will appear white; and if the visible light is absorbed by the pigment, then the object appears coloured as shown in **Figure 2.2**. [7]

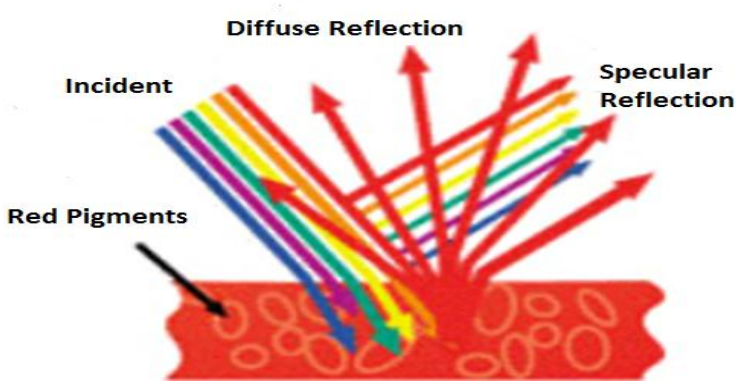

Figure 2.2. Scattering, absorption, transparency, and translucency of incident light [7]

2.2.2 Factors of Colours (The Triad)

There are three important factors referred to as the Triad of Colour that ought to be considered when discussing colour perception. This triad consists of a light source, an object, and an observer. The observer could be either the human eye or a photosensitive detector attached to a computer. A change in the light source, the object, and/or the observer will alter the final colour perception. [8]

- ***Light.*** A light source emits energy in the electromagnetic spectrum, and illuminates the viewed object. This includes X-rays, ultraviolet and infrared radiation, radio and TV waves, etc. The human eye can respond to electromagnetic radiation between 380 and 780nm of visible wavelength (the colourimeter range is 400-700nm). A light with a short wavelength appears blue or violet and as the wavelength increases, the colour changes through green, yellow, orange and red.

  Radiation combining all the wavelengths of the visible spectrum, in about equal amounts, is perceived as white as described in **Figure 2.3**. [9] It is essential to select a light source before defining colour tolerances, whether these are for use in visual assessment or in colourimetry. As a matter of fact, light sources can be described by their spectral power or energy distribution. This simply plots the amount of light (relative power) as a function of wavelength.

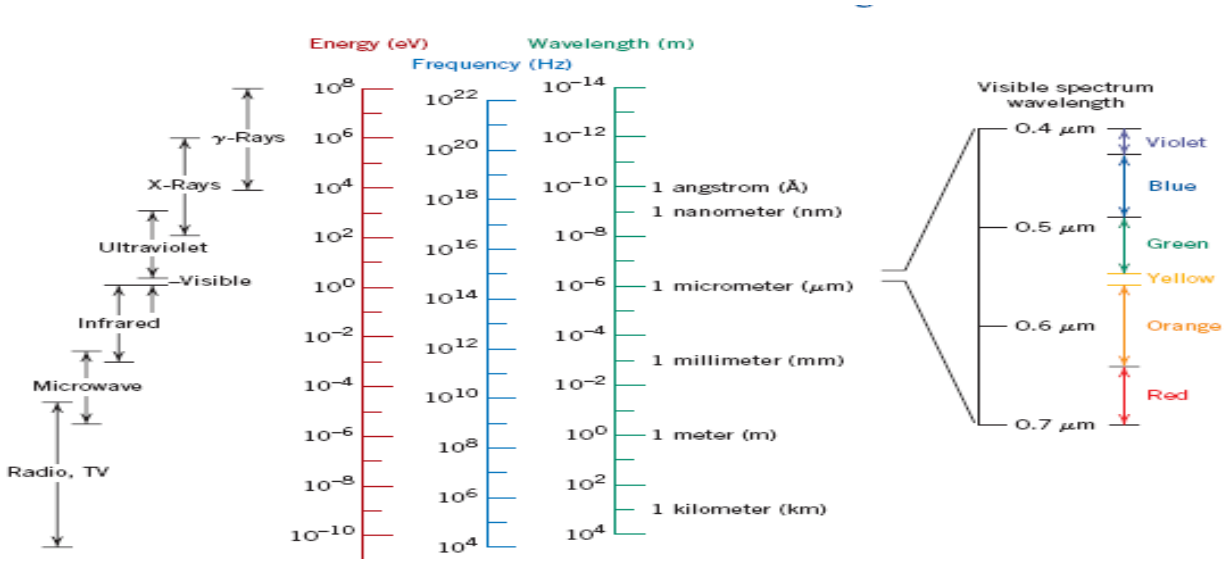

Figure 2.3. The Electromagnetic Spectrum (Optical Properties of Materials, 2007) [9]

- ***Object.*** The object is where the material interaction with the energy from the light source is addressed. In this paper, the material under study is polymeric in type. Generally, polymers are colourless or at best weakly coloured. The goal is to cover up the undesirable colour of the polymer in favour of the more desirable colour selected by the designer by adding pigments. The pigments absorb certain colours but reflect others, in random directions based on their surfaces and orientations. Thus, in a multi-blend compound, the incident light is reflected by many pigments, usually of different colours, at different depths.

- ***Observer.*** There are two types of observers; the human observer (human eye), and the instrumental observer (colourimetry).

  Human Observer. Human observation involves three phenomena: physiological, psychological, and vision deficiency. An object exhibits colour because it absorbs some wavelengths and reflects others. The reflected light passes to the pupil of the eye and then through the lens and is projected at the back of the eye with variable focal lengths onto the retina. The retina has two types of photosensitive receptors: rods and cones. The rods are responsible for colourless vision in condition of low light, and the cones are responsible for colour perception. The colour receptor cones are of three types: blue, green, and red. Each type of receptor cone has a different pigment making it sensitive to a

different colour of light. We see colour when the light and colour signal from the eye reach the brain. [5]

- *Psychological Response.* Colour has been used in fashion and art to reflect feelings of joy and sorrow. The reason behind this is that different wavelengths of light affect our brains differently. For instance, colours with longer wavelengths such as red stimulate and excite the nervous system more than colours with shorter wavelengths such as blue. Colour is generally used in business and advertising, which provides the best example of using colour in different functions to attract attention. [10]

- *Colour Deficiencies and Colour Blindness.* When receptors are unable to recognize a specific colour, they are classified as having a colour deficiency – scientifically known as dichromatism. Colour blindness, on the other hand, is the complete inability to recognize colour.

Instrumental Observer. Colourimetry is an attempt to quantify the colour observed by the human eye. Spectrophotometers analyze how objects interact with light by recording the spectral reflectance or transmission curve. The advantage of colourimetry is that it removes the subjectivity of human observation and provides quantitative measurements. Therefore, it provides the basis for statistical quality control and objective discussions between customers and suppliers.

Although there has been extensive progress made in recent years, the numerical expression of a sensory perception is still far from perfect. The lack of correlation of the current mathematical models of converting the spectrophotometer data to visual sensory perception is a major contributor to this issue. Further discussion on this matter will be addressed in the following chapters.

2.2.3 Colour Assessment

There are two methods for evaluation of colour: visual and instrumental.

- ***Visual Evaluation***. Visual evaluation has become more of a quality control tool rather than a tool for deriving colour formulas. Traditionally, even a well-trained and experienced colour matcher would follow the trial and error method. There are three decisive factors for visually evaluating colour: a normal vision, a viewing environment that is well controlled, and the experience of the colour matcher. Colour vision testing is rarely employed. Experience is what sets colour matchers apart.

- ***Instrumental Evaluation*.** Colour can be measured objectively utilizing instruments such as a spectrophotometer with higher accuracy and reliability. Spectrophotometers are usually equipped with special software and offer many advantages over visual colour evaluation. Different observer functions, illuminates, and formulae can be translated into the universal colour tristimulus attributes in terms of CIE L*a*b*, XYZ etc. Instrumental colour evaluation is faster, reproducible, and user friendly. The following issues should be addressed for the instrument and data evaluation:

    - Inspecting of the surface of the sample.
    - Categorizing the brand of instrument to be used to generate colour data.
    - Verifying transparency, translucency, or opacity of the sample.
    - Designating measurement illuminate(s).
    - Recognizing the observer function utilized, e.g. 2 degree versus 10 degree.

2.2.4 Understanding Metamerism

Metamerism is the phenomenon that occurs when two colours appear the same under one set of viewing conditions, but not under another set. There are three forms of metamerism: colourimetric, observer, and geometric.

- ***Colourimetric Metamerism***. When the difference in the colour observed is due to the difference in the spectral power distributions, this is called colourimetric metamerism.

Generally, colourimetric metamerism occurs because each sample has a different polymer or different colourant formulation or both.

- ***Observer Metamerism***. When two individuals differ in recognizing the same coloured sample or have different visions of colour, this is referred to as observer metamerism. The consequence is that two colours may match to one observer, but not to the second observer. [10]

- ***Geometric Metamerism***. This form of metamerism is important because it usually occurs when samples tested appear to match at one angle of illumination, but do not match if the angle of illumination or angle of viewing is changed. This sometimes happens due to the use of different instruments. Geometric metamerism may develop during processing due to the factors such as orientation of additives and colourants in the samples. [11, 12]

2.2.5 Observer Function

The observer function is the relative sensitivity of a human eye to various wavelengths of light. As mentioned earlier, there are three types of cone shaped receptors in the human eye sensitive to red, green, and blue light. Rod shaped receptors in the eye are responsible for night vision. When measuring colour from a fabrication process, therefore, the data typically needs to be processed further to take into account the three components that create colour: the object, the light, and the observer. This is accomplished by multiplying the reflectance curve of the spectral output by one of the two CIE (Commission Internationale de I' E'clairage) standard reflectance curves. The two standard observer curves are that of the 2° observer, defined in a 1931 study, or the 10° observer from a study conducted in 1964. The result of this multiplication are three distinct values, labeled X, Y, and Z, that position the colour within a three dimensional space. When plotted, XYZ will be in the form of three values, L*a*b*. The difference being that L*a*b* data is in the form of a Cartesian coordinate system and the systems plot within the same colour space. [10, 13] These functions quantify the sensitivity of the average human observer to red, green, and blue. The experiments were re-revised in 1964, resulting in the 1964 10° standard

observer, with a wider field of vision. The latter is recommended for better correlation with average visual assessments and is typical of most commercial applications (see **Figure 2.4**).

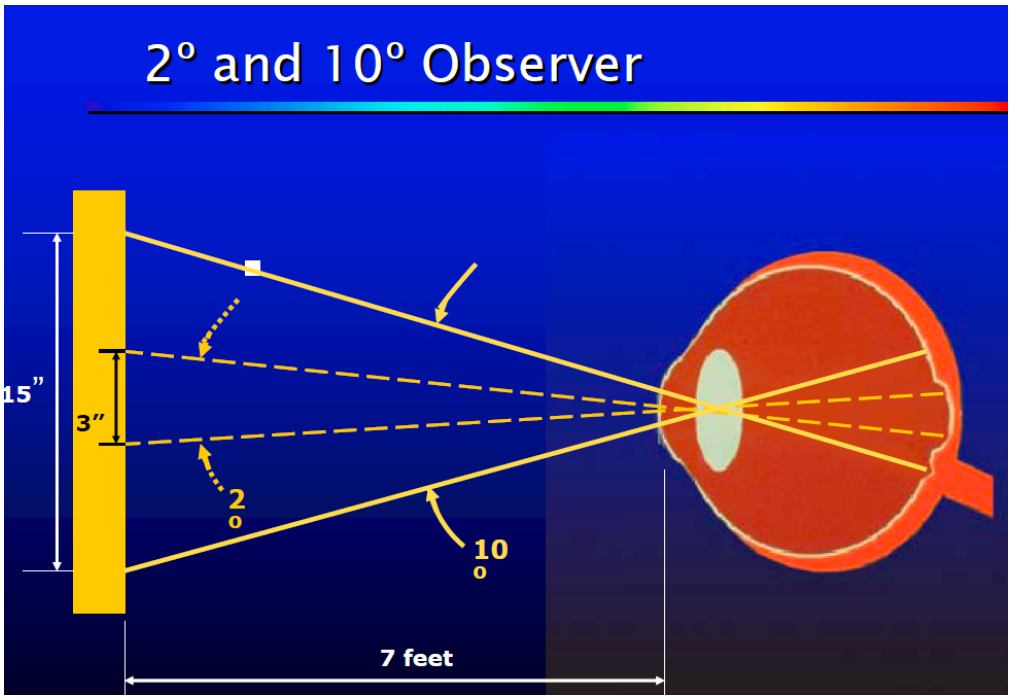

Figure 2.4. Two sets of observer functions with difference in field of vision [14]

2.2.6 Bases of Colour Quantification

To obtain a desired colour, usually a number of selected pigments are mixed with the main resin in specific proportions so that when light falls on the final compound, the net reflection will appear as the desired colour. However, colour appearance can vary with changes in light source, the object reflecting the light, and the observer. To standardize colour evaluation in the plastic compounding industry, the light source and observer are replaced with colour measuring instruments such as a colourimeter or spectrophotometer (see **Figure 2.5**). [15] This provides more consistent colour recognition as it is represented in codes or values.

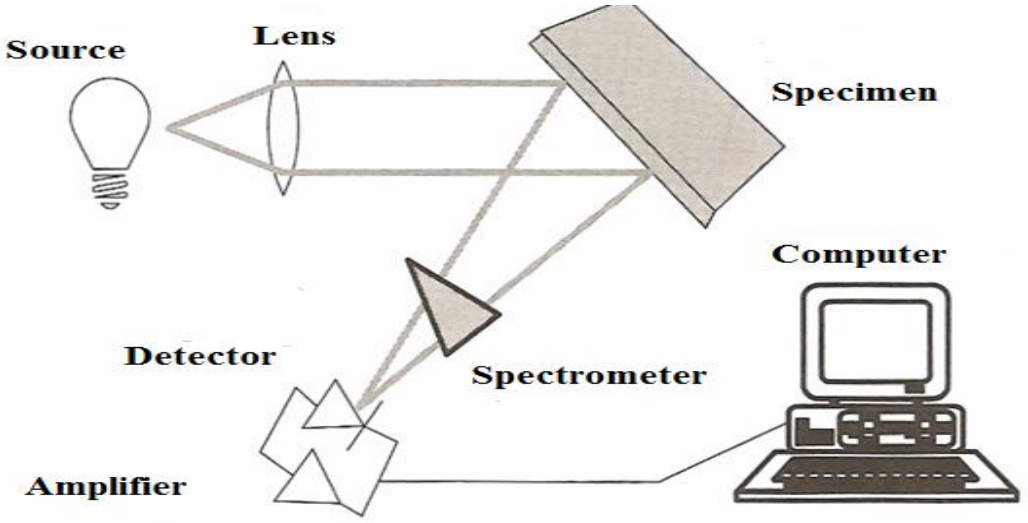

Figure 2.5. Schematic of a digital simulation of a visual colourimeter – spectrocolourimeter [13]

2.2.7 Colour Space and Tristimulus Values

Tristimulus values are mathematically derived from colour measurement and represent the amounts of red, blue, and green light content, recorded by the eye of a theoretical 'standard observer'. The first mathematical colour space was CIE XYZ 1931, created by CIE (Commission Internationale de l'E'clairage) in 1931. XYZ are called Tristimulus values.

The colour space was formed from experimentation and was derived from the CIE RGB model. It is ever so often referred to as the CIE XYY colour space. It is not critical to understand how the values of the CIE XYZ colour space are derived, but the following information is useful to know. The colour is the sum of the tristimulus values of the surface over the visible wavelengths. Since there are three tristimulus values at each wavelength, the result of the summation is three numbers, called the tristimulus coordinates of the colour. A plot of all conceivable tristimulus coordinates generates a space in three dimensions called the colour space. [13, 16]

2.2.7.1 Colour Space

The most commonly used colour space for plastics is CIE 1976 (L*a*b*), which characterizes colour in terms of a three-dimensional space. The L*-axis is known as the lightness and extends from 0 (black) to 100 (white). The other two coordinates, a* and b*,

represent redness-greenness and yellowness-blueness, respectively. Any colour can be characterized by three numbers or values and any attempts to reduce colour to a mathematical equation must utilize three dimensions (referred to as tristimulus). [17]

2.2.7.2 Munsell Colour System

Albert Munsell formulated a precise nomenclature for colour. He devised a three-dimensional colour system in the form of a tree, which classified shades according to the perceivable characteristics: hue, lightness, and saturation (represented in **Figure 2.6**). [10] In his model, "Value" (lightness) is indicated by the vertical position on the "Hue" branch, and "Saturation" (intensity) is indicated by how far the block is from the center. Intensity scales are of three types: (a) tints, the range from a pure hue to white; (b) shades, the range from a pure hue to black; and (c) tones, the range from a pure hue to any gray.

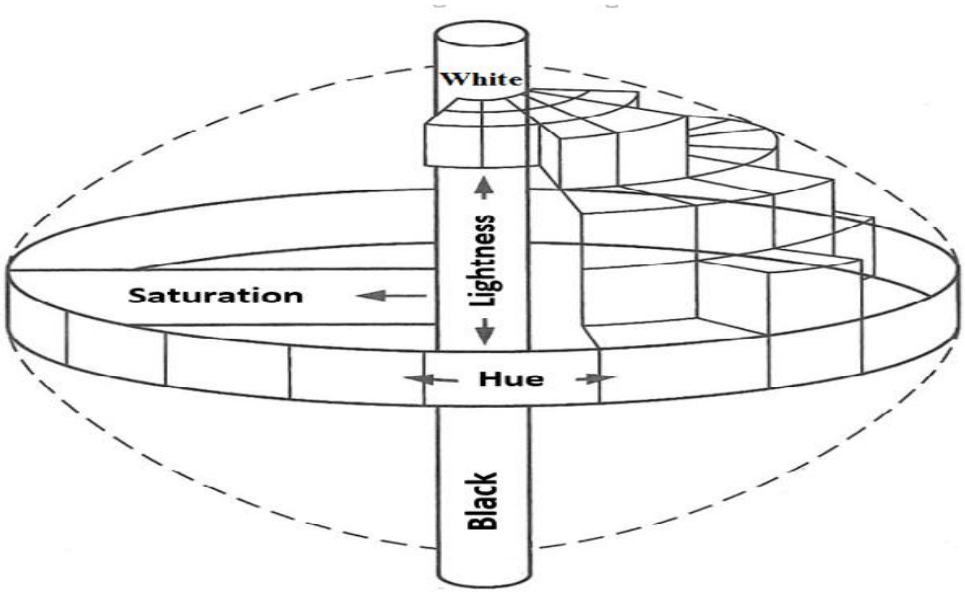

Figure 2.6. Three-dimensional colour space of hue, lightness, and saturation [10]

We can measure a colour quantitatively by creating scales for the hue, lightness, and chroma. Although there are many methods to quantify a colour, the most common is the L*a*b* colour space known as CIELAB. In this system, L* indicates lightness, and a* and b* are the chromaticity coordinates (see **Figure 2.7**). [18]

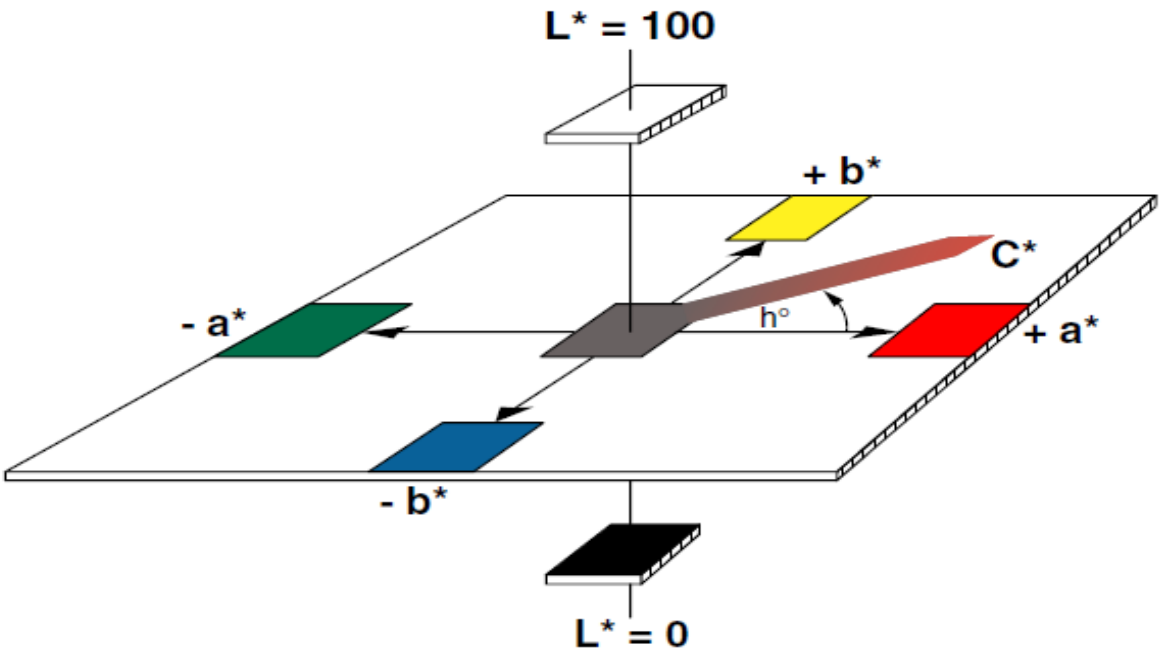

Figure 2.7. Colour in the CIE 1976 (L*a*b*) colour space [20]

It is important to note that these scales are simply mathematical attempts to simulate human colour perception and fall short of perfection.

2.2.7.3 Colour Difference (Delta E*)

A colourist may be asked to match a colour with a known reference colour or to compare two colours. Delta E* is a single number indicating the difference in colour between two readings and is based on the L*, a*, and b* colour space system. This is the geometric distance, delta E*, between two points in the three-dimensional space. But delta E* is not linear throughout colour space and is not a very good measure of colour perceptions. Therefore, more complicated computational methods have been developed to predict colour differences between two samples. [17]

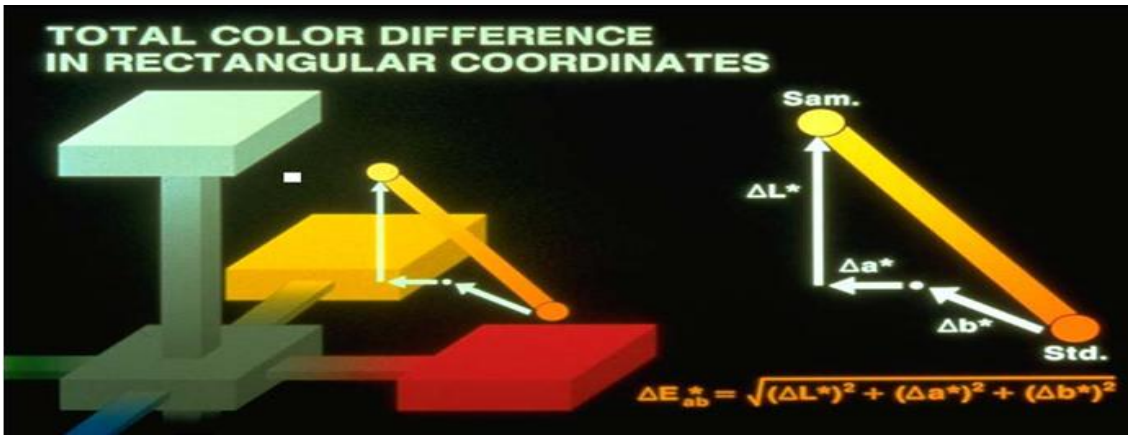

Figure 2.8. Colour guide [14]

In the figure above, the sphere represents the amount of acceptable difference (Delta E) between the sample and the measured standard in terms of colour output. Data that fall outside the tolerance sphere are unacceptable, while data that falls within the tolerance sphere represents an acceptable colour measurement. Delta E is calculated via the Pythagorean Theorem as follows:

$$\Delta E = \sqrt{(\Delta L)^2 + (\Delta a)^2 + (\Delta b)^2} \quad \textbf{(2.1)}$$

2.2.7.4 L-a-b Colour Scales

As mentioned earlier, measurement information can be used to control variations in observed colour. This is facilitated by characterizing a colour using three stimuli such as RGB or three attributes such as lightness, chroma, and hue (the three tristimulus values that combine to define or generate a specific colour). Colours will have different numerical values under Hunter and CIE colour scales, which are both mathematically derived from X, Y, and Z values. These scales are similar in organization and their colour differences are calculated as follows.

CIELAB Colour Scale (L* a* b*). The forward transformations are:

$$L^* = 116 \cdot f\left(\frac{Y}{Y_n}\right) - 16 \quad \textbf{(2.2)}$$

$$a^* = 500 \cdot \left[f\left(\frac{X}{X_n}\right) - f\left(\frac{Y}{Y_n}\right)\right] \quad \textbf{(2.3)}$$

$$b^* = 200 \cdot \left[f\left(\frac{Y}{Y_n}\right) - f\left(\frac{Z}{Z_n}\right)\right] \quad \textbf{(2.4)}$$

The current CIE recommendation is to use the CIE L*, a*, b* colour space. The reverse transformation is most easily expressed using the inverse of the function f above to calculate X, Y, and Z (tristimulus values). X_n, Y_n, and Z_n are the tristimulus values of the illuminant.

Hunter Scale (L, a, b). The forward transformations for this colour space are as follows, where L is the lightness axis, a is the red-green axis, b is the blue-yellow axis, K_a is a coefficient that depends upon the illuminant (for D65, K_a is 172.30), and K_b is also a coefficient that depends upon the illuminant (for D65, K_b is 67.20).

$$L = 100 \cdot \sqrt{\frac{Y}{Y_n}} \quad \textbf{(2.5)}$$

$$a = K_a \cdot \left[\frac{\left(\frac{X}{X_n} - \frac{Y}{Y_n}\right)}{\sqrt{\frac{Y}{Y_n}}}\right] \quad \textbf{(2.6)}$$

$$b = K_b \cdot \left[\frac{\left(\frac{Y}{Y_n} - \frac{Z}{Z_n}\right)}{\sqrt{\frac{Y}{Y_n}}}\right] \quad \textbf{(2.7)}$$

2.3 Fundamental Principles of Mixing

Different methods can be adopted to mix the colourant with a plastic resin. All options involve a two-stage process. The first is to ‘dry-blend’ the components followed by dispersing the colourant into the melted plastic. [19]

Powder blends can be mixed in low or high intensity mixers, which operate on the same principle. Mixing blenders consist of mixing blades that rotate at a high speed. Heat is generated due to intense mixing, developing a 3-dimensional mixing force inside the chamber. Mixing time is a function of product type. Mixing blenders work adequately for powders and small granules. They are also efficient for colour compounds.

2.3.1 Mixing Mechanisms

The mixing action is either induced by shear or elongation flow. The extent of the shear forces that occur in the extruder is a good determinant of the level of mixing. The mixing process occurs in all screw extruders. The distributive mixing process in screw extruders is of particular concern when dealing with plastics. Both distributive and dispersive mixing processes are not physically separated. [19]

2.3.1.1 Distributive Mixing

Distributive mixing is a low shear process that distributes particles uniformly throughout the melt. It is accomplished by breaking and recombining the melt stream. It is also referred to as non-dispersive mixing. Kneading blocks provide good distributive mixing. Distributive mixing occurs in solids as well as fluids. Distributive mixing is simpler to achieve than dispersive mixing because disruption of velocity profiles in the screw channel could cause distributive mixing to occur. The distributive mixing process is required when different polymers with very similar viscosities are blended together. [19]

2.3.1.2 Dispersive Mixing

This type of mixing is a high-shear process that breaks up large particles and disperses them as smaller particles throughout the melt. It is also referred to as intensive mixing. Dispersive mixing is a process used to blend two or more polymer resin systems and disperse pigments and liquid additives. [19]

2.3.1.3 Extruder Mixers

Extruders help to achieve a constant and uniform melt temperature and pressure, and thus, a homogeneous product. These factors all relate to polymer rheology. Different mixing

elements and screw geometries are used to accomplish each type of mixing. Mixing effectiveness or the level of mixing is dependent upon screw speed, percentage of fills in the screw elements and geometry, temperature, and shear rate. Shear rate and screw geometry also affect and influence the resin viscosity. [20]

Single screw extruders (SSEs) are widely used throughout the polymer industry. These extruders function by simple rotation of the screw in the extruder barrel. *SSEs are the most all-purpose type of mixers used for producing concentrates. They are capable of compounding practically all types of polymers.* Twin-screw extruders are probably the most efficient mixers for producing concentrates. They are mostly well suited for polymers that have very low melt viscosity such as acetals and nylons. [21]

2.4 Compounding Process

Extrusion is the most important compounding process involving several basic scientific principles and parameters. The primary compounding materials in the plastic industry are resins, pigments and additives. In terms of colour compounding, resins are classified in three categories: transparent, translucent, and opaque. The most transparent polymers such as polystyrene and polycarbonate do not scatter light and therefore can achieve a brilliant colour. Many resins such as polypropylene, polyamide, polybutylene terephthalate (PBT), acetal, and polyethylene fall into the class of translucent resins. However, very few resins such as polyphenylene sulphide (PPS) are found to be truly opaque. Opacity depends on the thickness of the polymer part. [15]

Colourants can be classified into pigments and dyes. Pigments are further classified as either inorganic or organic chemicals. Common classes of inorganic pigments include ultramarine, titanium dioxide, iron oxides, cobalt blue, and chrome oxides. The general components of organic pigments are phthalocyyanine, azo, polycyclic, or carbon black. Pigments are insoluble in the base polymer being used, whereas dyes are soluble. The physical and mechanical properties of the base resin can be affected by the colourant. As the particulates of pigments are insoluble in the polymer base, any agglomerates must be reduced

to the minimum particle sizes to improve colour development and minimize the negative influence on desired properties.

The greatest industrial challenge confronting the compounding processors is selecting the correct pigments and their ratios. The same challenges are faced with inorganic pigments as they typically work with small particle size fillers such as calcium carbonate, talc, barium sulphate, or mica. On the other hand organic pigments can be used in either an opaque or a transparent resin system. However, the most important disadvantage of organic pigments is that they are difficult to disperse. A compounder must then select an appropriate process to meet given requirements to provide the required mixing and control in order to achieve a quality product. Using a colour masterbatch during the compounding process may be beneficial because it can improve colour productivity and make for faster process cleanouts. This approach may be the best way to select a more cost-effective compounding process. [22]

2.5 Dispersion and Processing Conditions

Previous studies have investigated changes in dispersion and surface characteristics of pigments, and optical constants. One study investigated distributive mixing in the flow direction in a single-screw extruder and presented two significant conclusions: 1) increasing the screw speed (RPM) enhances longitudinal distribution; and 2) a modified screw with barrier flights, pin-elements, or high helix angle generates better longitudinal mixing than a conventional one. [23]

Academic researchers have evaluated both distributive and dispersive mixing techniques. The magnitude of generated shear stresses and the strength of the flow field were of particular importance. In a distributive mixing process, research indicates that a repeated rearrangement of the minor constituent would enhance system homogeneity. Moreover, in the process of continuous mixing, the uniformity of composition at the emerging stream is related to the material's residence time distribution (RTD). [24]

Experimental works on extruders conducted by other researchers demonstrated that single screw extruders could achieve a dispersive mixing capability just as good as that of twin-screw extruders. [19] Another study examined the colour mixing process using a 45mm diameter single-screw extruder having eight glass windows. [25] Using such an extruder enabled the researchers to identify where colour mixing started and ended. Their key finding was that the quality of mixing was directly related to the maximum processing pressure in the extruder.

In addition, previous studies have explored the effect of screw geometry and operating conditions on dispersion performance and torque loading during twin-screw compounding. [26] Researchers compounded three different grades of titanium dioxide pigments with different surface treatments into highly loaded polyethylene masterbatches. They found that optimum screw design and operating conditions were quite different for the three grades. It was noted that processing conditions or some combinations of modifiers and additives in the resin system could negatively affect the final desired colour. [27] The study also suggested that achieving the right colours, however, could have an adverse effect on other performance attributes such as UV stability, flammability, or mechanical properties. It indicated that colouring should be engineered taking other desired thermal and mechanical properties into consideration. Thus, the strategy could be either to formulate the desired colour to minimize property loss, or to achieve the most accurate colour while maintaining thermal and mechanical properties. [27]

2.6 Statistical Analysis Methods

In this research, statistical methods are required to be employed to analyze available data from SABIC to find the relationship between formulations and final colour matches/mismatches. Different methods were adopted with a focus on developing new predictive models and improving existing ones. These included:

- Data mining, in which selection of various formulations and processing parameters causing colour mismatches were made from historical data

- Neural Network (NN) investigations comprised of two phases. The first phase was involved error reduction in colour values for six grades, while the second employed colour modeling for lots.

- Response Surface Method (RSM) experiments, which also included two phases. The first phase was a three-level full factorial design; the second was a Box Behnken design (BBD).

2.6.1 Data Mining Techniques

Two data mining techniques were utilized. One was online analytical processing (OLAP) and the other was a decision tree classifier (DTC). OLAP helped to identify a relationship amongst variables resulting in unsuccessful batches; it identified parameters that had a high rate of adjustment. The DTC served to detect combinations of parameters potentially causing colour mismatch and was proposed as a decision support tool. The DTC will be used for exploring parameters likely to cause colour mismatch problems in compounded polymers. In the past, OLAP and data mining approaches have been used to discover such parameters. [28-30] However, in this research, DTC is used to discover whether a combination of certain parameters can cause problems. For example, a certain type of colour grade if processed through a certain type of extruder may likely generate higher colour mismatch. Therefore, DTC is used for parameters relationship discovery. Overall, in this research, DTC is used for exploration of possible relationships among the components of colour, grade, type, product, and line. Our literature review shows, to the best of our knowledge, that no research has used DTC for colour mismatch analysis. Some related manufacturing papers (semi-conductors) have use DTC. [31] Other researchers have tried to predict output colours based on historical data by using Neuro-Networks. [32]

2.6.2 Neural Network in colour values of polycarbonate (NN)

2.6.2.1 Error Reduction in Colour Values for Six Grades

In existing research, the artificial neural network (ANN) was used to reduce errors in colour values of polycarbonate. [33] The training data for ANN is obtained from

experimental measurements. There were twenty-two inputs and three tristimulus colour values, L*, a*, and b* that were used for the output layer. The neural network in this paper was used in order to reduce the errors in colour tristimulus values (L*, a*, b*), which directly affect DE calculated by **(2.1)**.

2.6.2.2 Colour Modeling for Lots

By considering the formulation, a neural network was implemented for prediction and optimization of polymer colour properties directly and accurately. The problem is especially complicated with the formulation of polymers to achieve desired physical properties. However, the neural network provides a possible method for the prediction of specific colour tristimulus values (L*, a*, b*).

2.6.3 Response Surface Methods (RSM)

The response surface methodology (RSM) is used when only a few significant factors are involved in optimization. Different types of RSM designs include the full factorial design, central composite design (CCD), Box-Behnken design, and D-optimal design. Design of Experiments (DOE) was conducted to determine the variables for successfully developing a process window model.

In this study, an experimental investigation of the processing parameters was conducted using DOE. DOE was utilized to determine the optimum number of experiments to be run so that sufficient data was available for analysis. The designs were prepared for three processing parameters: temperature, speed, and feed rate. The effect of the processing parameters on output response parameters was studied. Experimentation for various grades was carried out to observe the effect of controlled variation of different processing parameters on the colour attributes of compounded plastics. The results were analyzed to determine an optimum set of processing parameters in order to ensure minimum wastages and timely delivery of orders. Design of experiments proposed two different methods: a 3-level full factorial design and a Box Behnken design (BBD).

2.6.3.1 Three-Level Factorial Design

Plastics compounders need to understand the relationship between process variables and output colour. They should know the optimal process conditions needed to achieve consistency in output. Such a relationship was investigated for a polycarbonate resin-based plastic grade using a full factorial design of the response surface. This design provided a design space with accuracy within a tolerable range and involved a total of 27 runs. StatEase Design-Expert® software was used for the statistical analysis of data to evaluate and compare the effects of processing parameters.

2.6.3.2 Box Behnken Design (BBD)

This paper also utilized a DOE based on the Box-Behnken design (BBD). The aim was the same: to investigate the effect on output colour of a compounded plastic grade under varying processing conditions employed in the extrusion process. This design provided a design space with a total of 17 runs and with a higher range of input parameters than the full factorial design. It is more accurate and economic, and consequently consumes less time than the 3-level full factorial design. StatEase Design-Expert® software was used for the statistical analysis of data to evaluate and compare the effects of processing parameters. Permissible tolerance limits in terms of dL*, da*, db* or dE* are usually fixed by the customer; however for the plastic grade under study, limits were ≤ 0.6 for dL*, da*, db* and ≤ 1.0 for dE*.

Chapter 3: Literature Review

Producing plastic with a marketable colour requires adding one or more resins and pigments to the blend, but achieving the correct colour on the first attempt is highly challenging. Apart from pigment formulations, the colour properties of polymer are directly affected by processing parameters when compounding in an extruder. This includes parameters such as temperature, screw speed, feed rate, residence time, and screw configuration. A few studies have been carried out by various researchers regarding the effects of processing parameters on the resultant colour in the compounding of polymers. [23, 25]

A summary of the relevant literature works on colour mismatch in the compounding of plastics is presented below.

3.1 Data Mining

To achieve the right colour in plastic compounding, certain pigments with specific weight percentages (called a formulation) are mixed with the base resin (plastic). If the final colour does not match the target colour, a new batch of material is processed after adjusting the pigment formulations accordingly. This procedure may be repeated a number of times before the desired result (colour) is achieved.

As mentioned earlier, a large amount of data is available at SABIC IP on material formulations and processing parameters. Analysis of this data can provide valuable information for enhancing the colour matching process. A comprehensive study was conducted on the data in order to find any existing correlation between colour deviations and material formulations and/or processing parameters.

Two data mining techniques that were utilized in this paper are described: (1) Online Analytical Processing (OLAP) and, (2) Decision Tree Classifier **(**DTC). OLAP assisted to identify, in the un-successful batches, the variables with a high rate of adjustment. DTC served to detect combinations of parameters potentially causing colour mismatch. [28-30]

3.2 Neural Network (NN)

In the area of process system engineering, there has been a rapid increase in academic and industrial interests in neural networks. Neural networks have been used throughout various industries for solving problems related to the production of polymers [34], steel [35, 36], ceramics [37], semiconductors [38], and formulation of composites [39]. The functions include reaction and process monitoring, optimization, diagnosis, control, chemical composition analysis, characterization and modeling of materials properties, product design, and the classification of multicomponent materials. [40-45]

Thus, it seems the implementation of neural networks to model complicated processes has proven to be very successful. In an approach sometimes referred to as the formulation of compounds, an artificial neural network (ANN) is used to emulate the process and/or its inverse. [46-49] The goal of the system is to either provide a model that allows the investigation of the sensitivities of the input variables (optimization) or to use the model in a feedback loop for controlling the process. A natural extension of ANN-assisted modeling of a process is to use the model as a means for optimization. [50] By using the functional relationship between controllable input parameters and process responses, recipes for better performance can be determined.

The multilayer perception (MLP) neural network consists of one input layer, one output layer, and one or more hidden layer(s) (middle layers) between the input and output layer. Each layer employs several neurons (nodes), each of which is connected to the neurons in the adjacent layer with different weights. An optimization procedure adjusts the weights to minimize the difference between the output values and the target ones. The weights, after training, contain meaningful information (see **Figure 3.1**), whereas before training they are random and have no meaning. [51]

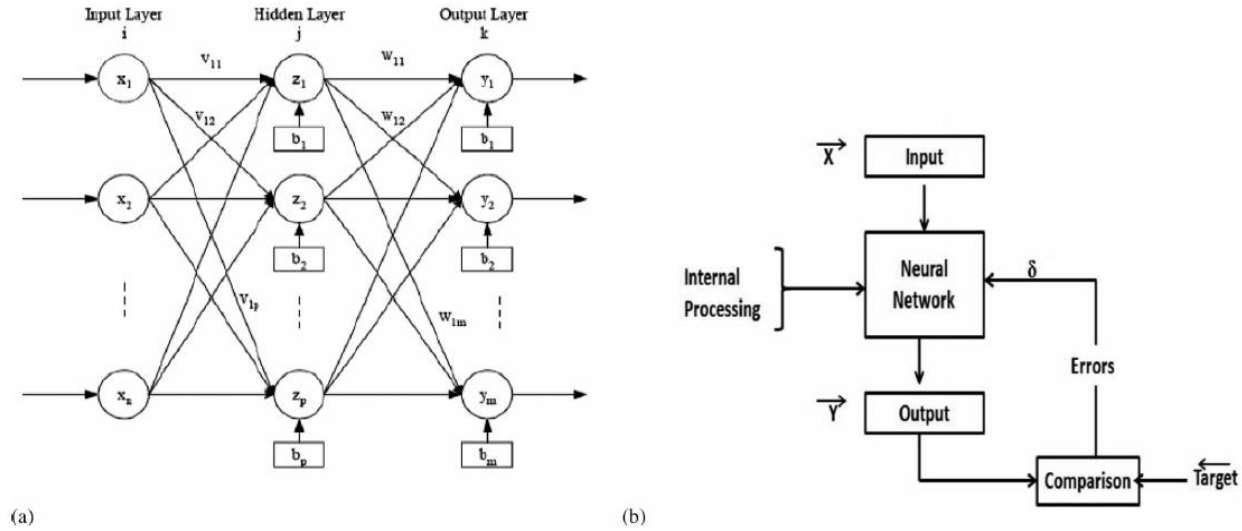

Figure 3.1. (a) Architectural graph of a multilayer perception (MLP) with one hidden layer. (b) Basic concepts of the CNN-supervised learning algorithm [51]

Backpropagation was the first practical method for training multilayer feed forward networks and is still the most popular learning algorithm. [52, 53] Researchers employed an artificial neural network (ANN), where the training data was obtained from experimental measurements. The neural network was used to reduce the errors in colour tristimulus values (L*, a*, b*), which directly affect dE*. There were twenty-two inputs and three tristimulus colour values (L*, a*, b*) were used as the output layer. The collected dataset was divided into three sets: 70% of data was used for training, 15% for validation, and 15% for testing the network. The total experimental dataset included 64 data points; this meant 44 observations were used for the training network, 10 for validation, and 10 were selected at random to test the performance of the trained network. [33, 54] The neural network consisted of sigmoid hidden units and a linear output unit arranged in a feed-forward-back-propagation architecture. The best result in terms of statistics was given by the LM algorithm, which had 16 neurons in the ANN model. It was concluded that the ANN provides a possible method for the prediction of specific colour tristimulus values. [54]

3.3 Design of Experiments (DOE)

Plastics compounders need to understand the relationship between process variables and output colour and how to optimize process conditions to achieve consistency in output.

Design of Experiments (DOE) is a planned approach that allows an experimenter to plan the experiments and determine cause-and-effect relationships. DOE is extensively used in numerous areas of science because it reduces the number of experiment that need to be performed.

The foremost reason for incorporating pigments in polymers is to introduce colour either for aesthetic reasons or due to functional needs. For optimal dispersion of these pigments, the optimization of extrusion process parameters is required. Researchers designed experiments to evaluate the effect of process parameters on colour properties of a compounded polycarbonate grade. A regression model was generated. Key factors that were shown to contribute to colour mismatch include: (1) poor mixing of colour pigments, both dispersive and distributive; (2) poor pigments formulation; (3) pigments particle size variation; and (4) particles/regions of varying refractive indices within polymeric resin causing scattering. Such factors need to be studied to understand their effect on output colour. [19, 23, 27]

Many experimental designs have been recognized as useful techniques to optimize process variables. A modified general factorial DOE has been employed for investigating the effect of changes in compounding process variables on gloss and surface appearance of a PVC sheet. [55] Fractional factorial and Plackett-Burman screening designs are among those that have been used for pre-formulation evaluations. Response surface methodology (RSM) is used when only a few significant factors are involved in optimization. Different types of RSM designs are available, including a factorial design, central composite design (CCD), Box-Behnken design, and D-optimal design. [56] The execution of a DOE involving the Box-Behnken design (BBD) has been reported to determine a relationship between processing parameters and viscosity variation for a wood-plastic compound. [57]

The BBD, being a combined array design, requires fewer runs than Taguchi's crossed array designs and allows estimation for significant interactions. [58] It is the most efficient design in terms of runs and requires only three levels of each factor in order to generate a quadratic model. [58, 59] To estimate curvature, other designs require either five levels of

each factor such as in a central composite design (CCD) or even more experimental runs such as in a three level factorial design.

Analysis-of-variance (ANOVA) is essential to validate the significance and fitness of the model; it explains, whether the developed quadratic model is meaningful. It investigated the bearing of process parameters and interaction of these parameters. The robustness of RSM designs is ensured by considering the propagation of error (POE). POEs, a measure of the standard deviation of the transmitted variability in the output response, are caused by fluctuations in significant controllable process variables during experimentation assuming uncontrollable factors (noise) to be zero. [60] When using the POE technique with an RSM design, levels of controllable input factors can be determined that would keep output responses close to their target values. It also reduces the variation transmitted by a lack of control over input factors. In other words, the POE technique makes a process less sensitive to variation in input factors.

3.4 Polycarbonate Blends and Rheology

Producing plastic with a marketable colour requires the addition of one or more resins; however achieving the correct colour in the first attempt is a challenge. Colour properties of polymers are directly affected by PC resin formulations. The actual MFI or viscosity may vary with formulations (i.e. the weight percent of resins, pigments, and additives in the blend) as well as processing parameters such as temperature, feed rate, and screw speed.

The amorphous PC provides impact resistance, toughness, stiffness, excellent transparency, and dimensional stability at elevated temperatures. It exhibits excellent weathering, creep, impact, optical, electrical, and thermal properties. [61] Studies have been carried out by various researchers regarding the effects of processing parameters for dynamic mixing in a screw extruder during the compounding of polymers. [23, 62] Pigment particles can be divided into three classes: primary particles (crystallites), aggregates, and agglomerates. The dispersion process involves the breakdown of associated particles into smaller particles and their distribution in a fluid. Dispersion of pigments in viscous polymeric

media proceeds in three distinct stages: (1) wetting; (2) de-agglomeration and distribution; and (3) stabilization. [63, 64]

In order to finely disperse pigment particles in a liquid, the particles must be 'wetted' by the liquid. Air incorporated in the pigment powder must be completely removed and the pigment particle must be completely surrounded by liquid. The wetting of pigment particles is influenced by the geometry of the particles, viscosity of the fluid, surface tension, and chemical character of the solvents. However, the breakdown of pigment particles can occur due to wetting (where there is a breakdown of the forces holding the agglomerates together) or due to a mechanical breakdown where the remaining agglomerates are broken down by transferring energy into the system. The energy is transferred due to the rotation of the extruder's screw, which generates shear forces for de-agglomeration.

The quality of the dispersion (or degree of dispersion) is dependent on the pigment volume concentration, residence or dwell time, energy input, and temperature. For optimum dispersion, temperature of the system has to be controlled. The stability of pigment dispersion depends on the overall interaction free energy between the two dispersed pigment particles. The overall interaction free energy is a combination of Van der Waals interactions, electrostatic interactions, and steric interactions. [65, 66] However, difficulties with the dispersion of pigments or in obtaining a uniform blend can be overcome by reducing the resin viscosity. [27, 67] If the viscosity of the blend is too high, the induced shear will be inadequate for optimum dispersion. However, viscosity is also an important indicator of the stability of a pigment concentrate. If it changes during storage, the pigments are usually inadequately stabilized. A system of additives and resins can be formulated to modify viscosity and improve thermal stability in order to attain better dispersion. [68] Researchers have studied the importance and effects of adding the pigment to the base resin; it has been shown that incorporating additives into polymeric materials during production often affects rheological and optical properties in an unpredictable way. [69-71] However, rheological properties are linked between processing steps and the final performance of the product. [72, 73]

Polymer blending is an important field of polymer science and has been reviewed by many scientists. The PC/PBT blends, are partially miscible blends. [73] These blends are transparent in the melt state and mostly transparent in the solid state. Researchers also studied the rheological properties of a blend made of virgin and recycled PCs. They stated that recycled PC could be added to virgin PC up to a level of 15 wt. % without significantly varying the properties of pure PC. [74] Other researchers characterized the blends of ABS and PC. [75] Some also studied the rheological and phase behaviour of PC/polyester blends. [76] The particle sizes, fillers (pigments and additives) and processing parameters such as temperature and pressure, have an effect on the rheology and on the colour of pigmented polymer. The significance of the processing variables was correlated with rheological results. [77]

The complex viscosity is measured from dynamic oscillatory tests. For polymer melts, the values of steady viscosity and complex viscosity are in a very good agreement. The benefit of complex viscosity is that reliable data can be obtained at 100 rad/sec, which corresponds to a shear rate of 100 1/sec (Cox-Merz rule). The empirical Cox-Merz rule is given by **(3.1)**.

$$\eta(\dot{\gamma}) = \eta^*(\omega) \qquad \textbf{(3.1)}$$

The rule states that the absolute value of the complex viscosity $\eta^*(\omega)$ at angular frequency, ω, matches the shear viscosity $\eta(\dot{\gamma})$ at shear rate, $\dot{\gamma}$. [78, 79]

Rheology, as a concept, is applicable to all types of materials (solid, semi-solid, and fluid) such as polymers and their composites. These experiments are devised with the objective of understanding the behaviour of material in different processes such as extrusion and injection-molding, which would further play an important role in developing better products.

Studying rheology of the resin, offers brighter prospects in predicting, controlling, and improving the colour matching process in plastic production. The physical properties of polymers and additives vary tremendously. They come in different forms, melting points, and thermal stabilities. The colour mismatch problem in the compounding process becomes

inherently prone to interaction effects, due to the large variation of available materials. [80] The relationship between time and temperature is known to affect both pigments and polymers. Many polymer systems will yellow or darken with extended exposure to temperature. Similarly, an excess of shear can have an adverse effect on pigments. [1]

Rheological properties can be considered as an important linkage between the processing steps and the final performance of the product. [68, 69, 81, 82]. Researchers have shown that, for certain polymers of industrial interest, Carreau and mainly the Cross viscosity models exhibit more acceptable agreement with the observed behaviour of polymer compared to other available models. [83]

In one study, polycarbonate compositions were first prepared in two different extruder machines having different screw configuration (Minilab (ML) at U of T and Coperion (SB) at SABIC IP), and thus had different blending efficiencies. The compounds were then rheologically characterized and modelled. The PC blends were rheologically characterized at 230, 255, and 280°C using the rotational rheometer and MFI tester. [84] All compounds made via both compounding extruders (ML and SB) were rheologically characterized using an ARES-G2 rheometer at three different dynamic modes: dynamic strain sweep (DSS), dynamic frequency sweep (DSFS), and strain sweep shear rate (SSSR) under nitrogen atmosphere at 230, 255, 280°C and with frequency varying from 0.01 to 79.43 Hz. [84] The third phase involved focusing on experimental studies conducted on the lab scale equipment to determine the various materials, processing parameters, and interaction effects that have an impact on colour mismatch. The focus was extended on the PC blend having a 30/70% composition of two resins, and the obtained viscosity data was correlated to colour changes. [84] The variation in polycarbonate content as well the temperatures in compounded formulations represented the most significant factors on rheological properties and colour model matching. The variation was conducted in order to obtain the optimum viscosity values and to simulate a design model. [84]

At higher frequencies, strain and shear rate cause the chains' entanglement network to come apart. At higher shear rates, the stresses may approach a maximum value as the chains disentangle (due to the shearing). [85-87] The shear stress parameter is dependent on the

viscosity and the velocity of thin melt film in the barrel wall. With low viscosity materials, low shear stresses are produced and less energy is dissipated in the melt. [88, 89] It has been shown that the melting rate increases with decreasing shear viscosity – that is, an increase in flow index. [88, 89] For the PC resin, the test results revealed that the maximum shear stress occurs at a temperature of about 230°C and the maximum melting rate at about 215°C. Later, researchers indicated that the shear stress at the interface increased with decreasing MFR for a PC resin; however, when shear viscosity is high, it is more likely to dissipate more energy and consequently to have a higher melting rate. [89] Others measured shear stress at the polymer-metal interface for a PC resin. [90] Subsequent processes are affected by the way in which the mixer is operated and the processing conditions that the PVC blend is subjected to. [91]

A micro-injection-molding machine was used for molding optimized melt-mixed multi-walled carbon nanotube (MWCNT)/polycarbonate. Micro-injection-molding features extreme injection pressure, high shear, high cooling rates, and shorter cycle times in comparison to conventional injection-molding. [92]

The transition from viscous to elastic behaviour was also observed for MWCNT/polystyrene (PS) composites, using a frequency sweep mode with an oscillatory rheometer at 210°C. This test indicated a physical gel formation described by a combination of entanglement of MWCNTs and interactions between the MWCNTs and the PS chains. [93]. The researchers claimed that the physical gel formation might provide an alternative method to determining the degree of dispersion of the MWCNTs in the polymer matrix. [93]

3.5 Dispersion and Effect of Processing Parameters

Pigment dispersion affects the colour difference and mechanical characteristics of an extruded polycarbonate compound. Poor dispersion into the PC compound can manifest in the form of large visible agglomeration, which can cause a large colour difference. Other colour variation problems that occur are poor gloss, low chroma, colour change, and poor opacity/transparency. Mechanical problems can be incurred due to poorly dispersed pigment in polymeric materials.

Appropriate processing parameters and shear rates are important for improving dispersion. Processing parameters such as temperature, screw speed, and feed rate can have significant influences on the colour and dispersion properties of pigments. Several researchers have conducted optimization studies of particles for the opacification of polymers in order to obtain suitable sized and shaped pigments for use in the plastics and paints industry. [94-99] To achieve optimum colour strength of pigment, it is necessary to obtain a full reduction in the primary particle size since smaller particles present a larger surface area and consequently stronger colour vision. [100, 101] There are two types of scenarios in which particle size is reduced: shear and collision. The degree of dispersion depends on pigment volume concentration, size, dwell time, rotation speed, mechanical energy, and temperature. [102, 103] A pigment particle size distribution (PSD) in the range of 50-500 nm exhibits a steady dispersion process and produces a stable colloidal system with colour strength, purity, gloss, and high opacity. [100-103] However, intensity of scattered light by a particle depends on molecular weight, size, and shape. [104] Particle size measurements will aid in establishing a terminology to describe pigment particles that comprise commercial products. Because pigments are metallic products, they do not exhibit exact and uniform size, but instead, they exist in a range of sizes. The ranges have been designated as crystals and crystallites, aggregates, and agglomerates. [105] Larger particles are more reflective and have more sparkle than smaller particles. On the other hand, smaller particles give more sheen and a satin finish.

Due to the effects of particles on absorption and scattering of incident light, changing a pigment particle size causes a change in the light hue. Narrower particle size distributions are superior for chroma. Since hue shifts with particle size, it is necessary for the pigment manufacturer to tightly control particles size. Pigments are generally produced in batches and then blended to meet a colour standard and uniformity. Blending a wide range of particles is in fact a blending of different hues, and therefore results in loss of chroma.

The properties of inorganic pigments influence their application. Control of particle size and distribution as well as their morphological structure determine a product’s chroma. The higher aspect ratio of a pigment, the higher the hiding power will be. Characteristically,

a narrow particle size distribution shows a cleaner effect and the wider the size distribution, the greater the hiding power. Particle geometry will also influence the visual effect. This mainly applies to metallic and spherical particles in use. Therefore, shapes offer different levels of reflectance and opacity. [106]

For a proper colour appearance, pigment dispersion is essential. Shearing forces are a requirement for overcoming the surface forces in the pigment particles that hold agglomerates intact. Additional related factors include the chemical composition and the structure of the particle, size, and distribution. Other related issues are viscosity, molecular weight distribution, the presence of additives in the pigment system, and interactions between the pigment and the polymer. [107, 108]

Scanning electron microscopy (SEM) and the digital optical microscope (DOM) have been widely used to observe and estimate pigment dispersion. These can provide direct information on pigment size distribution and the effect of processing parameters. It is important to evaluate the overall dispersion/distribution of pigment particles at the microscopic level using digital optical microscopy (DOM). Researchers suggested a statistical image examination method to describe the clay dispersion and the extent of agglomeration. [108] Their observation was based on TEM and OM, using histograms of the dispersion parameters for the tactoids of different classes. [109, 110]

As transparent polycarbonate does not scatter light, white pigment is added to create scattering, thus achieving a certain opacity level. It therefore affects the apparent colour strength. [27, 111, 112]

A high MFI (melt flow index) usually means a lower molecular weight. The presence of fillers may increase or decrease glass transition temperature (Tg). Moisture absorption, plasticizers, and contamination with impurities influence Tg. [113] Moreover, some other factors that may influence measured Tg, include the test method, test frequency, cooling/heating rate, and blending methods.

3.6 Measuring Dispersion

Dispersion quality can be determined by microscopy scanning. Particle analyzers are also useful. For example, a Microtrac S3500 permits users to measure complex particles with precision, which is difficult to measure with other particle analyzers. [114]

In general, organic pigments are more difficult to disperse than inorganic pigments. This is due to their smaller primary particle size. The smaller size allows for tighter packing thereby creating a larger surface area, which requires significantly more energy to break up the agglomerates of pigment encapsulated in the polymer. Shearing forces are required to overcome the surface forces in the pigment molecule that hold the agglomerates together. These forces are dependent on issues relating to pigment (chemical composition, particle size distribution), polymers (polarity, molecular weight distribution, viscosity), additives, and interactions between the pigment and the polymer.

Promoting dispersion, in general, is based on four objectives. The first objective is the reduction of pigment agglomeration. This is usually achieved through mechanical forces including, grinding actions, thermal crushing, or impingement. The second objective in pigment dispersion is to wet the pigment surface. The amount of energy required to wet the pigment surface depends on the interaction between the pigment and the binder, the size and geometry of the components, and the rheology of the medium. The third objective in dispersion is the distribution of the wetted pigment particles throughout the polymer medium. The final objective is generating a dispersed polymer system that is stable. Re-agglomeration and flocculation are to be avoided.

3.7 Closing Remarks

Colour matching has room for improvement in terms of its carbon footprint. If colour is integrated into a polymer with minimal colour difference, then wastage is reduced. This naturally leads to cost-effectiveness. As discussed earlier, optimizations through data mining, designed experiments (DOE), and neural network colour modelling serve to evaluate optimal processing parameters and colour properties of a compounded polycarbonate grade.

Processing parameters and the type of compounder affect the plastic colour. In this thesis, the effect of three processing parameters, namely, temperature, speed, and feed rate, on the colour of the final product was examined.

Polycarbonate blends with and without pigments and additives (WA&WOA) were initially prepared using different screw configurations and compounded plastics were rheological characterized and modelled through an experimental simulation of viscosity. In order to manufacture a compounded plastic with a certain colour, processing parameters must be controlled as well as the blend of polycarbonates with fillers. The effect of dispersion and rheology on colour matching must also be considered.

Chapter 4: Experimentation

This section describes the materials and the equipment used for experimentations and discusses the procedures adopted.

4.1 Materials

Due to a non-disclosure agreement signed with SABIC IP, we cannot publish the commercial names of the materials used, but can disclose chemical and physical properties. This research investigated two grades of PC resins, referred to as R1 and R2 here forth, each having a different melt flow index (MFI). R1 had an MFI of 25, and R2 an MFI of 6.5g/10min. The resins were manufactured by General Electric (GE) and traded under the name of Lexan. Colour pigments were in the form of powders; four different coloured pigments, black, white, red and yellow were used. In addition, three additives were also used called F1, F2, and F3. One was a stabilizer, another a light stabilizer, and the third offered weather resistant properties.

4.2 Equipment

Various equipment was employed for compound processing and sample preparation, rheological characterization, colour quantification, and microstructural characterization.

4.2.1 Compounding Equipment

Mixer. A 3-D material movement super floater, manufactured by KAWATA MFG CO. Ltd. and housed at SABIC was used for dry blending. The model was SFC-50. It produces a high degree of mixing of various materials of differing densities, and was used for the preparation of compounds prior to melt compounding in the extruders.

Compounding was carried out using two different extruders, one at SABIC IP in Cobourg, and the other in Prof. Naguib's lab at the University of Toronto.

Extruder 1. This system was located at the SABIC IP site in Cobourg. The extruder was an intermeshing co-rotating twin-screw extruder (TSE) manufactured by Coperion Germany. It had a 25.5 mm screw diameter, a L-to-D ratio of 37, and a 27kW motor. It also featured nine heating zones for the barrel along with one for the die. The system is shown in **Figure 4.1**. Upon exiting the die, the extrudate was quenched in cold water, dried using air and then converted into pellets via a pelletizer. The pellets were then molded via injection-molding into three rectangular colour chips (3x2x0.1"). The injection-molding machine used was manufactured by Kawaguchi Co. and was a KM100 model with a clamp tonnage of 85 ton as shown in **Figure 4.2**. It consisted of two main parts: an injection component and a clamping component. The KM100 was used to produce samples for further characterizations and colour quantification, and were processed at approximately 1,000 PSI (28 MPa) and 280°C. The specimen was then dried in the at lab room temperature for further optical microscopic tests and characterization measurements. For simplicity, the compounding process that involved this extruder is abbreviated '*SB*' in this document.

Extruder 2. The second extruder was located at the University of Toronto (U of T). It was a Thermo Haake Minilab II twin-screw micro compounder manufactured by Thermo Fisher scientific (**Figure 4.3**). It had a filling volume of 7 ml (5 gm), operating pressure of 200 bar, speed range of 10-360 rpm/min, two heating zones, maximum temperature of 350-420°C, and a screw diameter of 5/14 mm. In order to obtain a flow curve, the operating conditions of the extruder were held constant with a temperature of 255°C and a screw speed of 200 rpm. For simplicity, the compounding process employing this extruder is abbreviated '*ML*' here forth.

Figure 4.1. Coperion Co-Rotating twin screw extruder

Figure 4.2. Injection Molding Machine KM-100

4.2.2 Sample Preparation Equipment

Microscopic sample preparations were performed with a hot press or a microtome and are described below.

Hot press. A hydraulic Carvar Press with a manual jack unit was used for some sample preparations. Material was placed between thin aluminum sheets and was hot pressed under a load of 1.5 tons at a temperature of 230°C to achieve a 70 micron thickness. This press was also used to prepare disk-shaped specimens for rheological studies. The specimen were molded with a thickness of 1.2 mm and a diameter of 25 mm under a load of 1 ton at 245°C and for 3 minutes.

Microtome. For other samples, a fully automatic Slee rotary microtome (CUT 6062) was used to cut thin slices. This was able to yield very thin slices (up to 5-micron in thickness). Slices were cut into 50-micron thick chips for optical microscope scanning tests.

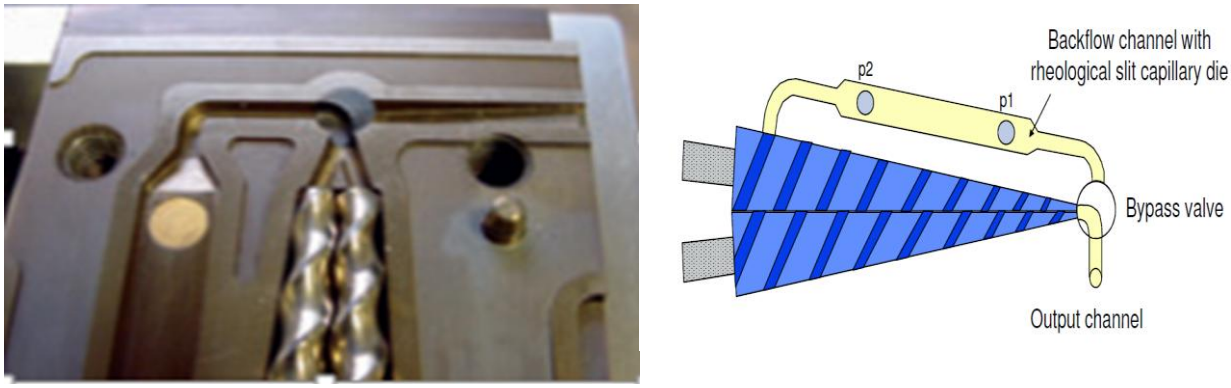

(a) **(b)**

Figure 4.3. (a) Haake Minilab system (Thermo Fisher Scientific), and (b) schematic of the design [115]

4.2.3 Rheological Characterization Equipment

Rheology can be quantified through the use of rheometers and melt flow indexers.

Rotational rheometer. The rheometer used was Ares-G2 from TA Instruments. It has a separate motor and transducer. It represents technology that allows taking pure rheological measurements. It is possible to mount the FCO (Forced Convection Oven) onto the side of the test station. The Ares-G2 is shown in **Figure 4.4**. There are three different modules for measuring the viscosity: (1) concentric cylinder; (2) cone and plate; and (3) parallel plate. We used the parallel plate geometry. The measurements of the dynamic viscosities were performed in a parallel-plate fixture with diameter 25 mm and gap size of 1.0 mm. The testing sample was sheared between the two plates. The measurement of the viscosity was the result of the ratio of the applied stress and the applied deformation rate. This rheometer is equipped with special software to program measurements, record data and display results. This rheometer offers a large range of new features including excellent accuracy with respect to data, fast data sampling, new TRIOS software and a new large amplitude oscillatory shear (LAOS) test.

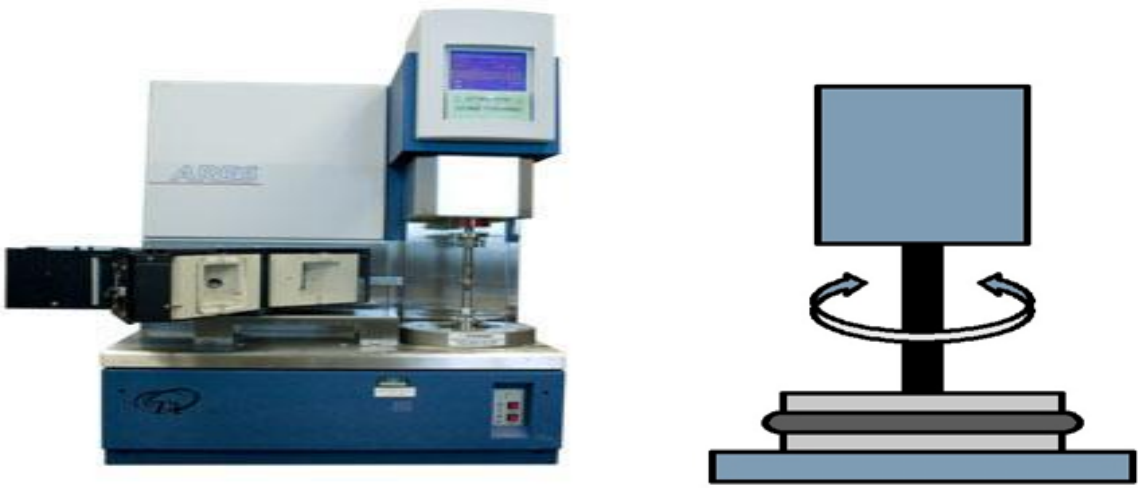

(a) **(b)**

Figure 4.4. Ares-G2 rotational rheometer: (a) photo, and (b) schematic diagram for the parallel plate (TA-Orchestrator software) [116]

Melt flow indexer. A melt flow measurement device manufactured by Tinius Olsen, Model MP600M (**Figure 4.5**), was used to investigate the rheological characteristics of different polycarbonate formulations. The MFI tests were performed in a SABIC IP lab according to ASTM D1238.

Figure 4.5. Tinius Olsen MP600M Et. Plastometer Melt [117]

Figure 4.6. X-rite-7000A-Spectrophotometer [118]

4.2.4 Spectrophotometer

A spectrophotometer is a photometric instrument that measures spectral transmittance, spectral reflectance or relative spectral emittance. Colour was quantified using a Spectrophotometer CE-7000A, equipped with X-RiteColour® Master software (**Figure 4.6**). The Standard Observer Function was 1964-10° and D65 light.

4.2.5 Microscopy

Microscopy examinations were carried out utilizing various equipment.

Digital optical microscope. A Keyence-Digital-Microscope-VHX-1000 (DOM) (see **Figure 4.7**) is the most common of the quick methods used to rate dispersion quality. This method was used to characterize the dispersion of pigments in transmission mode using a 70 micron thin hot pressed coupon, and a 50 micron slice cut by microtome from injection-molded rectangular samples. All samples were characterized using a block measurement method. The image accuracy of the digital microscope at 5000X was ±0.5 μm.

Scanning electron microscope. A Scanning Electron Microscope (SEM), Model Joel 5500 LV (see **Figure 4.8**), was employed to observe the microstructures of the produced compounds. Another SEM, Model JSM-600, was used with an acceleration voltage of 20 KV, working distance of 15 mm, and a magnification of 3000X. It was utilized to characterize raw pigment without coating in order to verify the presence of agglomerates in the four pigments (red, yellow, black and white) and the existence of primary particles in the vicinity of < 100 nm.

Figure 4.7. Keyence-Digital-Microscope VHX-1000 [119]

Figure 4.8. (SEM), Joel 5500 LV [120]

Figure 4.9. Microtrac S3500 Particle Size Analyzer (PSA) [121]

Figure 4.10. X-ray Micro-CT-scanner-Sky Scan 1172 [122]

4.2.6 Particle Size Analyzer

Particle size analyzer. A particle size analyzer (PSA) was used for raw pigment samples in a wet state for analysis of their size distribution. The model was a Microtrac S3500 manufactured by Microtrac (**Figure 4.9**). This model used three precisely placed red laser diodes to accurately characterize particles in the range from 0.086 μm to 1400 μm. In

order to perform wet test analysis, recirculation was used, which consisted of a reservoir where the sample was introduced, a fluid pump, and a valve to drain the system to disperse the material sample uniformly in fluid and deliver it to the analyzer. Pigments were suspended in deionised distilled water containing drops of the non-ionic surfactant, Triton X100 [C14H22O (C2H4O)n].

Micro CT scanner. For a three dimensional examination, an X-ray Micro CT Scanner, model Sky Scan 1172 μ CT scanner was used (**Figure 4.10**). The data was collected at 32kV and 187μA. The image was characterized on a high-resolution X-ray detector: 10 megapixel (4000 x 2300) and a 12-bit CCD camera.

4.3 Procedure

4.3.1 Compounding on Twin-Screw Extruder at SABIC IP (SB)

Experimentation was carried out at the SABIC IP plant in Cobourg, Canada (SB). The materials were extruded in an intermeshing, 25.5 mm, Coperion twin co-rotating screw extruder. The total weight of the colour additives (pigment and additive) was 0.86%. The two PC resins, R1 and R2, were used in a ratio of 30 and 70 wt. %, respectively. **Table 4.1** shows the formulation used. The additives and pigments were mixed with the resins at a 100:0.86 ratio and were batch blended by a super floater.

Table 4.1. Composition of compounding material (g3)

S.No.	Ingredients	Material Name	PPH	Weight	Unit
1	R1	Bisphenol A (BPA)	30	4.95	gm
2	R2	Bisphenol A (BPA)	70	10.05	gm
3	F 1	Weather Resistant (L)	0.035	0.00525	ml
4	F 2	Stabilizer (Liquid)	0.065	0.00975	ml
5	F 3	Light Stabilizer	0.2	0.03	gm
6	White	White Pigment	0.278	0.041625	gm
7	Black	Black Pigment	0.036	0.0054	gm
8	Red	Red Pigment	0.175	0.02625	gm
9	Yellow	Yellow Pigment	0.071	0.01065	gm

All material was supplied by SABIC IP and experiments were performed at their plant. The dry blended mixture obtained from the super floater was fed into a Brabender gravimetric feeder, which fed the material into the TSE for melt blending and mixing. The control process parameters were temperature, speed, and flow rate. The compounded material was extruded in the form of strands, which were cooled in water, air dried, and then pelletized.

These pellets were then molded using the injection-molding machine to produce rectangular colour chips (3x2x0.1" in dimensions). Injection pressure and temperature were maintained at about 28 MPa (1000 PSI), and at 280°C, respectively. Utilizing a spectrophotometer, colour measurements were carried out at three different spots in each specimen (coupon), to obtain the tristimulus values (L*,a*,b*). The target values for L*, a*, b* were defined as 68.5, 1.43, and 15.7, respectively. The colour differences were then measured as dL*, da*, db*, dE*, and dC*. For studying the dispersion using digital microscopy (DOM), thin sheets were prepared by molding the colour chips on a hot press, and by cutting a small piece of the coupon by microtome into thin slices. These were used to capture images with a DOM at the magnification of 1000X-5000X. A Scanning Electron Microscope (SEM) (JSM-600) was used to characterize the raw pigments (red, yellow, white, black) without coating in order to verify the presence of agglomerates. The acceleration voltage was 20 KV with a working distance of 15 mm, having a magnification of 3000X.

4.3.2 Compounding on Haake Minilab (ML)

To study the effects of the blending of two resins, a Thermo Haake Minilab II twin-screw micro compounder was used to prepare PC formulations with both resins individually as well as by varying the composition of the resins in steps of ten for a total of eleven blends. The concentration ratios between the two polycarbonate resins used in %R1/%R2 were 100%/0%), 90%/10%, 80%/20%, …, and 0%/100% (shown in **Table 4.2**). The Minilab was manufactured by Thermo Fisher. Experimentation was carried out at the University of Toronto (U of T).

The eleven batches were prepared both with and without pigments and additives (WA&WOA) for characterization of the viscosity. Strain shear rate (SSR), dynamic strain sweep (DSS), and dynamic frequency sweep (DFS) were used to study the material's rheological properties and simulate viscosity models. This helped in understanding the factors of rheology that have bearings on colour variations by studying the effect of rheology, particle size distribution, and the morphology on dispersion for the three processing parameters. **Figure 4.11** presents a schematic that summarizes the steps in the compounding process.

Table 4.2. Composition of R1-R2 (polycarbonate resins) blends

S.No	R1 (wt. %)	R2 (wt. %)
1	100	0
2	90	10
3	80	20
4	70	30
5	60	40
6	50	50
7	40	60
8	30	70
9	20	80
10	10	90
11	0	100

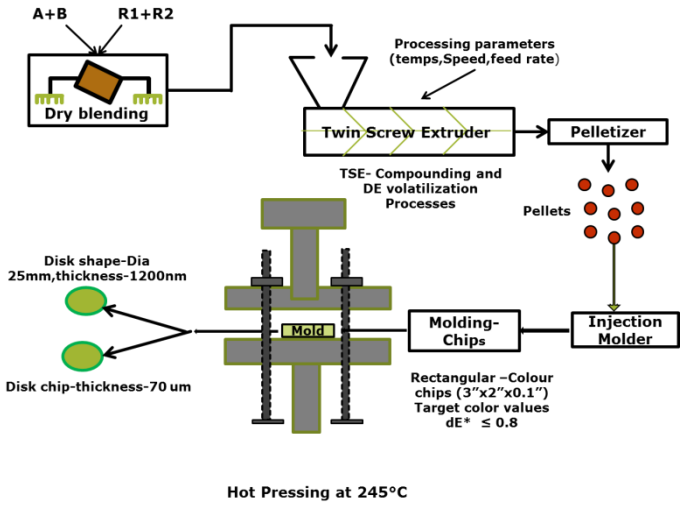

Figure 4.11. Schematic diagrams of process methods of plastics

4.4 Design of Experiments

4.4.1 General Trends (GT)

Three parameters including temperature, speed, and feed rate were varied individually at three different levels while maintaining all other parameters fixed. This was referred to as general trends (GT). The selected processing temperatures were 230°C, 255°C and 280°C with a speed and flow rate fixed at the middle values (750 rpm and 25 kg/hr, respectively). A similar procedure was followed for both speed and flow rate. The selected speeds were 700, 750 and 800 rpm and the selected flow rates were 20, 25, and 30 kg/hr. The following tables show the experimental processing conditions. The general trends (GT) experimental design is shown in **Table 4.3-Table 4.5**. [123-125]. SABIC IP's technology at its Cobourg Plant was used to execute the DOEs. Assuming that previously discussed variables were the same that were used, the present study suggests optimal values for process variables to achieve consistency in output colour of the plastic grade.

Table 4.3. Processing conditions with temperature variation

RPM	BZ1 (°C)	BZ2 (°C)	BZ3 (°C)	BZ4 (°C)	BZ5 (°C)	BZ6 (°C)	BZ7 (°C)	BZ8 (°C)	BZ9 (°C)	DZ1 (°C)	Feed Rate (kg/hr)
750	70	195	230	230	230	230	230	230	230	230	25
750	70	195	255	255	255	255	255	255	255	255	25
750	70	195	280	280	280	280	280	280	280	280	25

Table 4.4. Processing conditions with speed variation

RPM	BZ1 (°C)	BZ2 (°C)	BZ3 (°C)	BZ4 (°C)	BZ5 (°C)	BZ6 (°C)	BZ7 (°C)	BZ8 (°C)	BZ9 (°C)	DZ1 (°C)	Feed Rate (kg/hr)
700	70	195	255	255	255	255	255	255	255	255	25
750	70	195	255	255	255	255	255	255	255	255	25
800	70	195	255	255	255	255	255	255	255	255	25

Table 4.5. Processing condition with feed rate variation

RPM	BZ1 (°C)	BZ2 (°C)	BZ3 (°C)	BZ4 (°C)	BZ5 (°C)	BZ6 (°C)	BZ7 (°C)	BZ8 (°C)	BZ9 (°C)	DZ1 (°C)	Feed Rate (kg/hr)
750	70	195	255	255	255	255	255	255	255	255	20
750	70	195	255	255	255	255	255	255	255	255	25
750	70	195	255	255	255	255	255	255	255	255	30

The Design of Experiments (DOE) containing the 27 experimental runs was used to implement a Three-Level Full Factorial Design and a DOE containing 17 experimental runs was used to implement a Box-Behnken design (BBD) of response surface method (RSM).

4.4.2 Three- level Full Factorial Design

From the three process parameters, namely temperature, feed rate, and screw speed rpm, the experimental design level used is shown in **Table 4.6**. Parameters were varied and 27 different treatments with an additional center point for three levels of three factors (full factorial response method) was designed (**Figure 4.12**) to examine the effect of variables on colour. The additional centre point was added to estimate the experimental error.

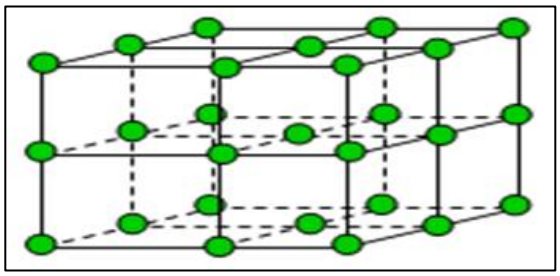

Figure 4.12. Experimental design of 3 level 3 factor

Table 4.6. Parameters and experimental design level used

Parameters	Units	3 Levels		
		Low	Medium	High
Temperature	^{o}C	230	255	280
Speed	rpm	700	750	800
Feed rate	kg/h	20	25	30

The desired colour output in terms of CIE L*, a*, b* values was L*= 69.59, a*= 1.43, and b*= 16.59. The Design-Expert® Software (Version 8, Stat-Ease Inc. USA) was used for the statistical analysis of data in order to evaluate and compare the effect of processing parameters. The analysis of variance (ANOVA) facilitated the identification of parameters that were significant and revealed any interaction between parameters. The ultimate goal was to derive an equation that could predict the tristimulus values of L*, a*, b* and to optimize the process parameter. ANOVA was performed to find interactions and to optimize the processing parameters related to colour properties. [126]

4.4.3 Box-Behnken Design (BBD)

For the three process parameters (temperature, feed rate, and screw rpm), the selected experimental design level is given in **Table 4.7**. Parameters were varied in 12 different treatments with additional 5 center points to observe the effect of variables on colour. The additional centre points were added to estimate the experimental error. The measured tristimulus values for the standard chip were found to be L*=70.04, a*=3.41, and b*=18.09.

Table 4.7. Experimental design level used for BBD

Parameters	**Units**	**3 Levels**		
		-1	**0**	**1**
Temperature	°C	230	255	280
Speed	rpm	650	750	850
Feed rate	kg/h	11	19	27

Chapter 5: Modelling and Optimization

There are different generalized simulation methods for colour modeling. Amongst the models available, Neural Network scheme (NN) is the one found to be efficient to model colour values of the compounds. One can apply this scheme utilizing MATLAB software package (e.g., Version 6.5) with Neural Network Toolbox. [33, 54] One other model is analysis of variance (ANOVA) which can be applied to find the interactions between different processing parameters and their effects on colour difference, dE* or (L*, a*, b*) output. Design Expert® Version 8 of Stat Ease Inc. can be used for the statistical analysis of regression models of design of experiment (DOE). [126, 127] For viscosity Carreau model has shown to conform to the behaviour observed in certain polycarbonate grades that are of interest to the industry. Orchestrator software is used to plot the rheological characteristic curves, simulated viscosity carreau models and finding the four parameters (C1, C2, C3, and C4) corresponding to the model. [84] The analysis is based on statistical and experimental analyses, and historical data were applied to the developed models. In this subsequent section, the basics of the governing equations are illustrated.

5.1 Neural Network (NN)

The artificial neural network (ANN) is used to approximately mimic the manner in which the brain processes a large number of inputs having unknown functions and processes them based upon prior knowledge of their behaviour. These are particularly useful to model systems with large number of inputs. A widely used neural network (NN) model called the multilayer perception (MLP) NN is shown in **Figure 3.1**. The MLP-type neural network (NN) consists of one input layer, one or more hidden layer (s) (middle) in between input and output layers, and one output layer. Each layer employs several neurons (nodes), and each neuron in a layer is connected to the neurons in the adjacent layer with different weights.

The weights, after training, contain meaningful information, whereas before training they are random and have no meaning. [52] Signals flow into the input layer, pass through the hidden layer(s), and arrive at the output layer. With the exception of the input layer, each neuron receives signals from the neurons of the previous layer. The incoming signals or input (x_{ij}) are multiplied by the weights (v_{ij}) and summed up with the bias (b_j) contribution. Mathematically, it can be expressed as follows:

$$\mathrm{net}_j = \sum_{i=1}^{n} x_i v_{ij} + b_j \text{ and } v_{ij} = F(\mathrm{net}_j)_i \quad \textbf{(5.1)}$$

where F is a transfer function (a function that, when applied to the input of a node, determines its output). F is usually taken as a sigmoid function, most commonly the logistic function:

$$F_i = \frac{1}{1 + e^{-E_i}} \quad \textbf{(5.2)}$$

where F_i is the weighted sum of the inputs and E_i is the weighted sum of the input. This function is continuous and varies monotonically from a lower bound of 0 to an upper bound of 1 and has a continuous derivative. The output of a neuron is determined by applying an activation function to the total input and calculated using **(5.2)**. [128] If the computed outputs do not match the known (i.e., target) values, the NN model is in error. Then, a portion of this error is propagated backward through the network. This error is used to adjust the weight and bias of each neuron throughout the network, so the next iteration error will be less for the same units. The procedure is applied continuously and repetitively for each set of inputs until there are no measurable errors, or the total error is smaller than a specified value.

An important stage of a neural network is the training step, in which an input is introduced to the network together with the desired output: The weights and bias values are initially chosen randomly, and the weights are adjusted so that the network produces the desired output. After training, the weights contain meaningful information, contrary to the

initial stage where they are random and meaningless. When a satisfactory level of performance is reached, the training stops and the network uses the weights to make decisions. In the current work, the neural network was used to reduce the errors in colour tristimulus values (L*, a*, and b*), which directly affect the DE calculated using colour difference equations.

The usual approach is to prepare a single dataset and differentiate it by a random selection. The learning algorithm called backpropagation was employed for the single hidden layer. The batch gradient descent (GD), batch variable learning rate (GDX), resilient backpropagation (RP), scaled conjugate gradient (SCG), and Levenberg–Marquardt (LM) algorithms have been used for the variants. The NN has been optimized using MATLAB version 6.5 Neural Network Toolbox.

The standard on-line backpropagation scheme works as followings:

(a) Initialize all node connection weights w_{ij} to some small random values

(b) Input a training example V_{im} and corresponding output values v_{iT} where m is the layer number, i is the node number, and T represents the target or desired output state.

(c) Propagate the initial signal forward through the network using

$$NET_j^m = \sum W_{ij}^m V_i^{m-1} + \beta_j \;\; while \;\; V_j^m = F\left(NET_j^m\right) \qquad \textbf{(5.3)}$$

where w_{ij} is the connection weight between nodes i and j, V_i^{m-1} is the signal from node i in layer m − 1, β is the threshold or bias value of the node, and F is a transfer function (a function that, when applied to the input of a node, determines its output), usually a sigmoid function, the most commonly used logistic function, mathematically represented as:

$$F\left(NET_j^m\right) = 1/\left[1 + exp^{\left(-NET_j^m\right)}\right] \qquad \textbf{(5.4)}$$

This function is continuous and varies monotonically from a lower bound of 0 to an upper bound of 1 and has a continuous derivative. However, in theory, any non-

polynomial function that is bounded and differentiable can be used as a transfer function without altering the ANN capabilities of universal approximation. [51]

(d) Compute the deltas (δ) for the output layer, which are defined as follows:

$$\delta_i^0 = -\delta E/\delta NET_i^0$$
$$\delta_i^0 = -(\delta E/\delta V_i^0)(\delta V_i^0/\delta NET_i^0)$$
$$\delta_i^0 = F(NET_i^0)(V_i^T V_i^0) \quad \textbf{(5.5)}$$

For the logistic function, the derivative is:

$$F'(NET_i^0) = \delta FNET_i^0/\delta NET_i^0 = FNET_i^0[1 - FNET_i^0] \quad \textbf{(5.6)}$$

(e) Compute the deltas for the preceding layers by propagating the errors backward:

$$\delta_i^{m-1} = F(NET_i^{m-1})\left[w_{ij}^m \delta_j^m\right] \quad \textbf{(5.7)}$$

For all m, m-1, m-2… for each layer.

(f) Using:

$$\Delta w_{ij}^m = n\delta_i^m V_j^{m-1} \quad \textbf{(5.8)}$$

Renovate the connection weights to:

$$\Delta w_{ij}^{new} = w_{ij}^{old} + \Delta w_{ij} \quad \textbf{(5.9)}$$

(g) Return to step b, and repeat for another input.

The process is continued until the output of the network satisfies the determined criteria. In practice, this type of the iterative approach can often take a number of epochs (cycles through the whole dataset) before a reasonable error is reached. This is one of the disadvantages of the standard backpropagation algorithm.

With the results produced by the network, statistical methods were used to investigate the prediction performance of NN results. Several performance measures are used to assess the prediction performance of a network. These include statistical analysis in terms of root mean squared (RMS), absolute fraction of variance (R^2) or regression of coefficient, as well as mean error percentage values as defined in **Equation (5.10)** through **Equation (5.12)**, corresponding to **Figure 3.1**. [129]

$$\mathrm{RMS} = \sqrt{\frac{\sum_{i=1}^{i=n}(E_a - E_p)^2}{N}} \quad \textbf{(5.10)}$$

$$\text{Mean Percentage Error } = \frac{1}{N}\sum_{i=1}^{i=N}\left[\frac{\left|E_a - E_p\right|}{E_a} \times 100\right] \quad \textbf{(5.11)}$$

$$\text{Regression } R^2 = 1 - \left[\frac{\sum_{i=1}^{i=n}(E_a - E_p)^2}{\sum_{i=1}^{i=n}(E_a - E_M)^2}\right] \quad \textbf{(5.12)}$$

In the equations above, E_a is an actual result, E_p is a predicted result, E_m is a mean value, and N is the number of patterns. The regression coefficient multiple-R^2 compares the accuracy of the model to the accuracy of a trivial benchmark model.

5.2 Design of Experiments (DOE): Regression Models

Process optimization was performed utilizing response surface methods (RSM): 3-level factorial design and box behnken design (BBD). In this approach, the first step is to properly design the experiments in order to evaluate the parameters of the model, efficiently, after performing the experiments. Second step is to develop a second order polynomial mathematical model for the responses. [59]

$$y = \beta_o + \sum_{i=1}^{k}\beta_i x_i + \sum_{i=1}^{k}\beta_{ii}x_i^2 + \sum_i\sum_{j>i}\beta_{ij}\,x_i x_j + \varepsilon \quad \textbf{(5.13)}$$

where y is the predicted response, β_0 is a constant, β_i is the *i*th linear coefficient, β_{ii} is the *i*th quadratic coefficient, β_{ij} is the *i*th interaction coefficient, x_i is the independent variable, k is number of factors and ε is error. Any difference between target colour and the output colour, which exceeding the permissible limits, can be reported as colour mismatch in terms of delta values, i.e. dL, da, db, or dE (the Euclidean distance of colour deviation in the 3D colour space). [130]

Permissible tolerance limits in terms of dL, da, db or dE are usually fixed by the customer's needs. However, for the plastic grade under study, limit values were given as less

or equal to 0.6 for dL, da, db, and less than or equal to 1.0 for dE. However, the POE technique is beneficial when RSM reveals curvilinear relationships between input factors and output responses, and the transmitted variation is reduced by approaching a plateau [131]. The mathematical expression for POE is given below. [132]

$$POE = \sqrt{\sigma_Y^2} = \sqrt{\left[\left[\frac{dy}{dx_i}\right]^2 \sigma_{x_i}^2 + \sigma_{resid}^2\right]} \quad \textbf{(5.14)}$$

It takes partial derivatives of the response polynomials (y) with respect to the input variables (xi) and incorporates variation in input variables (σ_{x_i}) and the unexplained residual, i.e. experimental noise (σ_{resid}). The variation in process variables observed during experimentation and incorporated in RSM design were 10°C for temperature, 1 rpm in screw rotational speed, and about 0.01 kg/hr in feed rate. Response polynomials, used to calculate POEs, are expressed as predictive model equations given in **Table 5.1** and **Table 5.2** in non-coded units.

5.2.1 Three- Level Factorial Design

Three process parameters were selected: temperature of the heating zones, feed rate to the extruder, and the screw speed (rpm). The experimental design levels are shown in **Table 4.6**. Parameters were varied on 27 different treatments for three levels of three factors with full factorial response method (**Figure 4.12**). The additional centre point was added to estimate the experimental error. Due to the results of the ANOVA analysis, multiple linear regression analysis was generated to determine the predicted response for L*, a* and b* functions as presented in **Table 5.1**. The parameters and their interactions, integrated in the regression model, have strong impact on the predicted tristimulus values.

Table 5.1. Regression model (3-level factor design)

Response	Regression Model
L^*	$+111.17$ $-0.026 \cdot Temp$ $-0.063 \cdot Speed$ $-1.153 \cdot FeedRate$ $+1.68E^{-004} \cdot Temp \cdot Speed$ $+2.40784E^{-003} \cdot Temp \cdot FeedRate$ $+6.98387E^{-004} \cdot Speed \cdot FeedRate$ $-3.28740E^{-004} \cdot Temp^2$
a^*	$+16.18499$ $-0.018688 \cdot Speed$ $-0.47864 \cdot Feed\ rate$ $+6.06028E^{-004} \cdot Speed \cdot FeedRate$
b^*	$+19.76757$ $-4.79457E^{-003} \cdot Speed$ $-0.030560 \cdot FeedRate$

The polynomial equations represent the quantitative effect of process variable (temperature, speed, and feed rate) and their interactions on the responses. The values of the coefficients are correlated to the degree of the effect of the corresponding variables on the responses. Coefficients in terms with more than one factor or higher order represent interaction terms and quadratic relationship, respectively. A positive value represents an effect that favours the optimization, while a negative value indicates an antagonistic effect.

5.2.2 Box-Behnken design (BBD)

Table 5.2 gives the regression models for the colour values based on the three process parameters. The experimental design levels are shown in **Table 4.7** . Parameters are varied in 12 different treatments with additional 5 center points to experience the effect of variables on colour. The additional centre points were added to estimate the experimental error.

Table 5.2. Regression model (BBD)

Response	Regression Model
L^*	$+83.3$ $-0.011 \cdot Temp$ $-0.021 \cdot Speed$ $-0.22 \cdot FeedRate$ $+0.0003 \cdot Speed \cdot FeedRate$ $+0.00001 \cdot Speed^2$
a^*	-29.45 $+0.19 \cdot Temp$ $+0.023 \cdot Speed$ $+0.64 \cdot FeedRate$ $-0.0002 \cdot Speed \cdot FeedRate$ $-0.0004 \cdot Temp^2$ $-0.0002 \cdot Speed^2$ $-0.0026 \cdot FeedRate^2$
b^*	$+3.89$ $+0.141 \cdot Temp$ $-0.005 \cdot Speed$ $-0.105 \cdot FeedRate$ $+0.00025 \cdot Speed \cdot FeedRate$ $-0.0003 \cdot Temp^2$ $-0.002 \cdot FeedRate^2$

The parameters and their interactions integrated in the regression model have a strong impact on the predicted tristimulus values.

5.3 Rheological Behaviour: Modelling and Experimental Simulation

The effect of viscosity on dispersion and colour shift was studied. Shear is an important parameter for pigment dispersion in plastics. Shear rate in the channel of the screw extruder is given by:

$$(\dot{\gamma}) = \frac{\pi \cdot D \cdot N}{60 \cdot h} \tag{5.15}$$

Significant shear is required during processing to fully disperse pigment in plastic. Shear, on the other hand, may also damage pigments or other particulate materials in the plastic such as fillers and other additives. Pigments, as particulate matter, may be fractured by shearing. Pigment properties depend upon their specific particle shape and size. If this

distribution is changed, the rheological characteristics (viscosity) and the observed colour can also change.

$$(\tau) = \eta\,\dot{\gamma} \tag{5.16}$$

The Carreau model is selected as a description for viscosity behaviour of the compounds as it performs high regression values at various temperatures from 230, 255, and 280°C. Orchestrator software was used to plot the rheological characteristic curves and to simulate the Carreau viscosity model by finding the four coefficients (C1, C2, C3, and C4), as expressed below in **(5.17)**.

$$\eta = c_1(1 + (c_2 x)^{c_3})^{(c_4-1)/c_3} \tag{5.17}$$

Chapter 6: Results and Discussion

The main objective of this research is to improve colour matching on the PC grades. This involved investigating the effect of incorrect formulations, processing conditions, poor pigment dispersion, interaction between materials and processing conditions, and degradation during processing. Different scientific methodologies were developed and applied as shown in the flow chart in **Figure 6.1**.

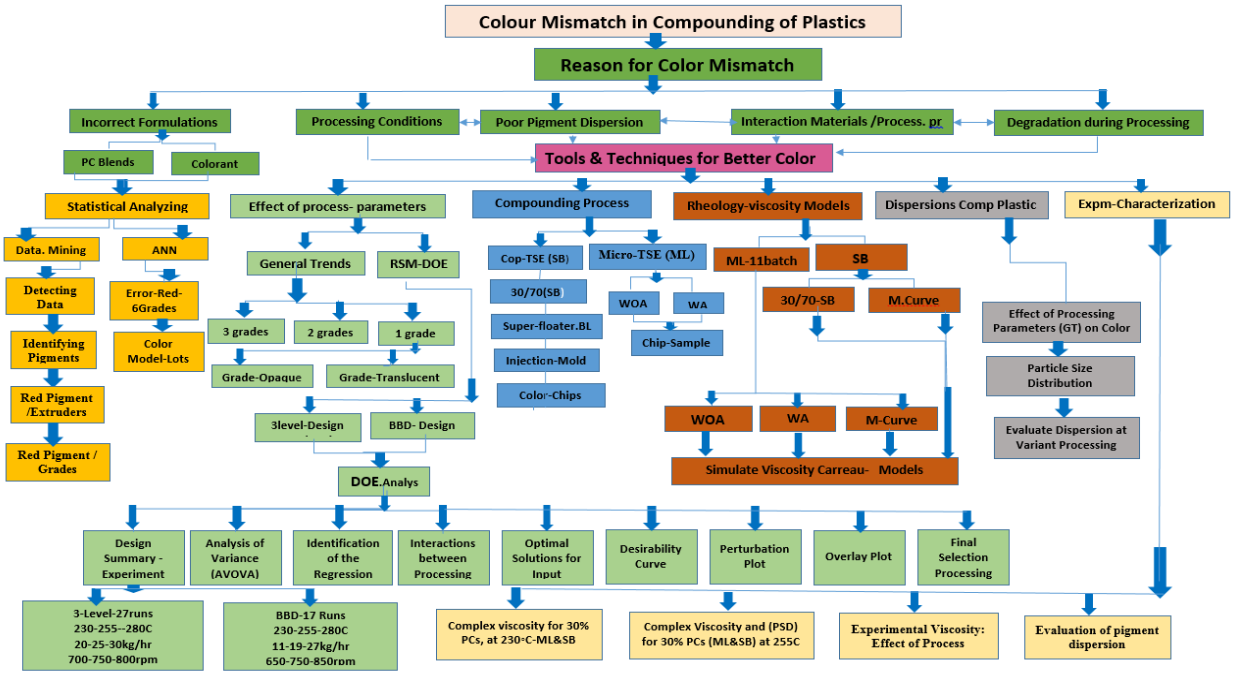

Figure 6.1. Overall flow chart for colour mismatch analysis of the compounded plastic

6.1 Data Mining

Diagnosis and Detecting Processing Data. Data mining techniques were applied using MS Excel with OLAP to detect patterns of adjustments for the runs conducted in 2009. Trends in the data that could explain the causes of colour mismatches and formulations were sought. The results obtained from data analysis techniques described above are given in **Table 6.1**. Out of 9,598 lots, 17.7% required adjustments in formulations at least one or more times.

Table 6.1. Demonstrating the percentage of adjustment of the lots run in 2009

#	No. of Adjustments	No. of Lots	Percentage
1	0	7,896	82.30%
2	1	1,186	12.40%
3	2	358	3.70%
4	3+	158	1.60%
Total		9,598	100%

The analysis of data revealed that red pigment caused the most adjustment and their corresponding lots were identified. In terms of the pigments used, around 7,395 pigments used experienced at least one adjustment, while 83,519 pigments did not require an adjustment. The top 13 pigments that required most adjustments on a percentage basis are summarised in **Table 6.2**. Red pigment with colour code P1 (commercial name cannot be used per agreement with SABIC) had the highest rate of adjustment of 40.60% and another red pigment with colour code P13 had around 27% adjustment rate. This indicated that the red pigments were causing the highest number of adjustments.

Table 6.2. Pigments requiring the highest percentage of adjustments

Pigments	Total No. of Lots	No. of Lots with Adj.	No. of Lots without Adj.	Pct. Lots with Pigment having Adj.
P1	101	41	60	40.60%
P2	134	45	89	33.60%
P3	185	62	123	33.50%
P4	312	104	208	33.30%
P5	602	194	408	32.20%
P6	347	109	238	31.40%
P7	117	36	81	30.80%
P8	506	151	355	29.80%
P9	385	114	271	29.60%
P10	338	96	242	28.40%
P11	99	28	71	28.30%
P12	107	30	77	28.00%
P13	185	50	135	27.00%
Total	9,073	1652	7,421	

Red Pigment and the Extruder Lines. Various extruder lines, with different screw geometry, are used for compounding at SABIC IP. The analysis of data on the effect of line on the frequency of mismatch or adjustment was also investigated. The focus was on the red pigment P1, which, as mentioned earlier, was involved in the highest mismatch, as shown in **Table 6.3**. Lines NF and NG caused the highest rate of adjustment. The adjustment rate was 80.0% and 75.0%, respectively. However, Line NT seemed to experience a very low rate of adjustment with pigment P1, with only 5.6% of lots requiring adjustments. Unfortunately the screw configuration is a closely guarded secret and was not available for further evaluations.

Table 6.3. Percentage of adjustment of the lines caused by red pigments

Lines	NA	NC	NF	NG	NH	NT	NW	Total
Adj.	6	3	4	12	9	1	6	41
Not Adj.	9	3	1	4	16	17	10	60
% Adj.	40%	50%	80%	75%	36%	5.6%	37.5%	40.6%

Red Pigment and the Polymer Grades. SABIC IP produces many grades of PC. Grades are either a single resin, or more commonly, a blend of resins formulated to impart specific properties to the final reins. Based on the historical records, the grades formulated with red pigment (P1) or diluted red pigment (P1L01) and requiring the highest rate of adjustment were identified and are shown in **Table 6.4**. As an example, the translucent grade (g3) including the diluted red pigment (P1L01) underwent the highest rate of adjustment amongst the grades with diluted red pigment (P1L01). Note that designation L01 indicates that the pigment content is 10%, the rest being resin.

Table 6.4. Percentage of adjustment of grades formulated with red pigments

#	Grades	% Adj. caused by P1	% Adj. caused by P1L01	No. of Adj. Lots
1	g1	21.95%		9
2	g2	19.51%		8
3	**g3**		19.44%	7
4	g4		11.11%	4
5	g5	9.75%		4
6	g6		8.33%	3
7	g7		8.33%	3
8	g8	7.32%		3
9	g9	7.32%		3
10	g10	4.88%		2
11	g11		2.78%	1
12	g12	2.43%		1
13	g13	2.43%		1
14	g14	2.43%		1

The table shows the fourteen grades containing P1 that had the highest rate of adjustment. Six of these grades were selected for additional statistical and experimental investigations to study the effects of the formulations on the colour shift. The sample grades are illustrated in **Figure 6.2**.

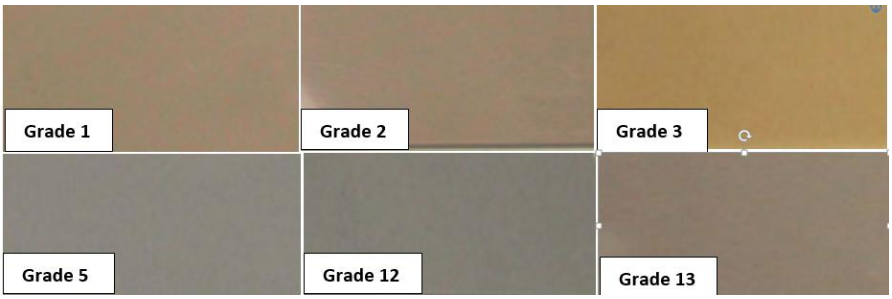

Figure 6.2. The six grades with the highest rate of adjustment

6.2 Neural Network Analysis

ANN Applied to the Data for the Six Grades. Initially the MLP model of NN was applied to a small set of data pertaining to the six grades selected in the previous study. Statistical analysis in terms of Root-Mean-Squared (RMS), absolute fraction of variance (R2), as well as mean square error was used to investigate the performance of the ANN. The best result was presented by the LM algorithm with fourteen neurons in the designed ANN model.

The usual approach is to prepare a single dataset, and obtain numerous random samples from it. Process parameters, additives and pigments were selected for the input layer, while colour tristimulus values (L*, a* & b*) were used for the output layer. The Neural Network was optimized using MATLAB Version 6.5 Neural Network Toolbox. In the training stage, the number of neurons in the hidden layer was increased step-by-step (i.e. 10, 12, 14, 16, 18, and 20). After the successful training of the network, the network was tested with the test data. [35]

The results are presented in **Table A–1** (Appendix A: Neural Network). All input and output values were normalized before running NN. Validation values were used early in the training stage to avoid overtraining. After eight training cycles, the level of error was shown to be satisfactory and further cycles had no significant effect on error reduction. This is evident in **Figure 6.3**.

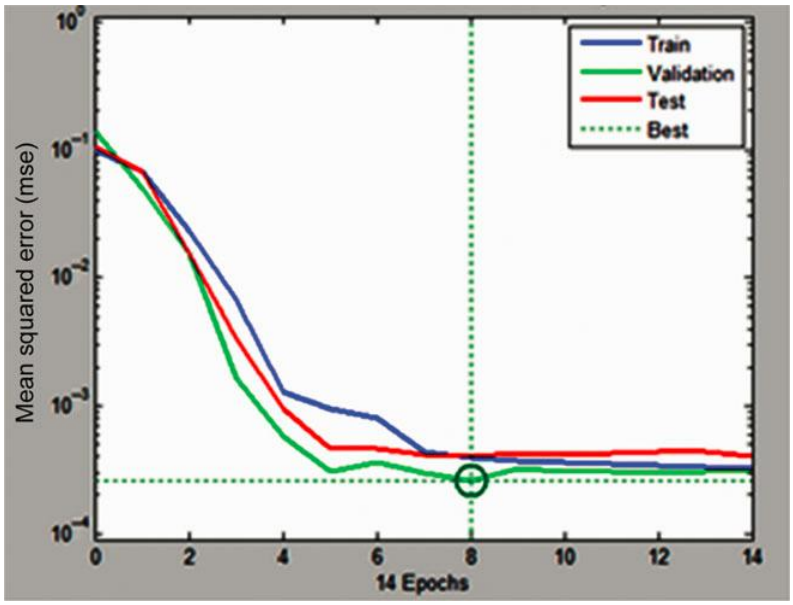

Figure 6.3. Network training cycle

The comparison of different trained neural networks algorithm is shown in **Figure 6.4**. The performance of the batch gradient descent GD and batch variable learning rate GDX were not adequate, and the statistical values were out of the desired range. The accuracies of algorithms RP and SCG have shown to be more satisfactory, but not consistent when varying the number of neurons. The Levenberg–Marquardt algorithm (LM) exhibited good performance accuracy and consistency when changing the number of hidden neurons. The best network was found to be the LM algorithm with 14 hidden neurons. The adjusted weights between input layers and hidden output layers for the 14 neurons that have a strong impact on the output values are given in **Table A–2** (Appendix A: Neural Network).

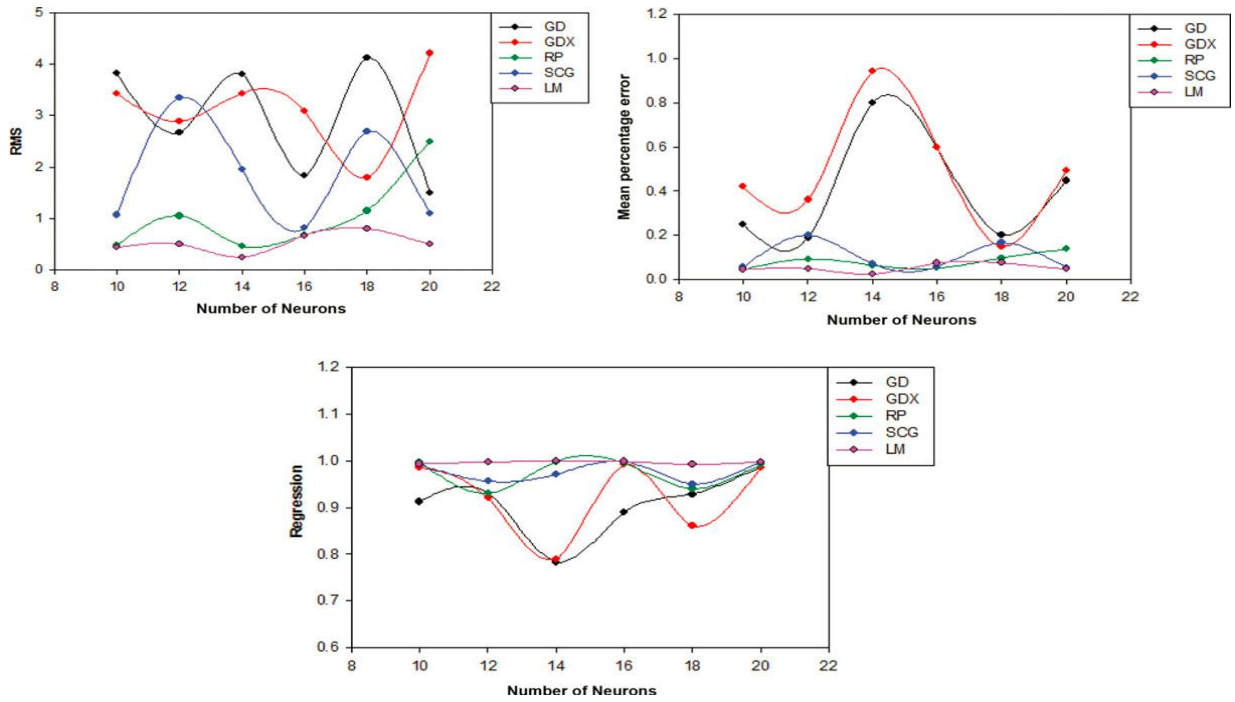

Figure 6.4. Comparison of (a) RMS, (b) mean percentage error, and (c) regression of different neural network algorithms

The purpose of applying the ANN was to demonstrate the feasibility of predicting the errors in tristimulus colour values L*, a* and b* so as to achieve colour values within the desired range. Comparison of the experimental and NN predicted outputs for training, testing and validation runs are shown graphically in **Figure 6.5** (and in **Figure A–1** and **Figure A–2** of Appendix A: Neural Network). The capital letters A, B, C, D, E and F in **Figure 6.5** each denote a different grade. It can be seen that the NN output values are in good agreement with the experimental output data for (L*, a*and b*) with 14 neurons. The ANN predictions for L*, a* and b* yield a mean relative error of 0.224%, a root mean square error of 0.242 and a regression correlation coefficient of 0.998. These values illustrate that the ANN predicts the polycarbonate colour values of six grades quite well despite the wide range of input conditions.

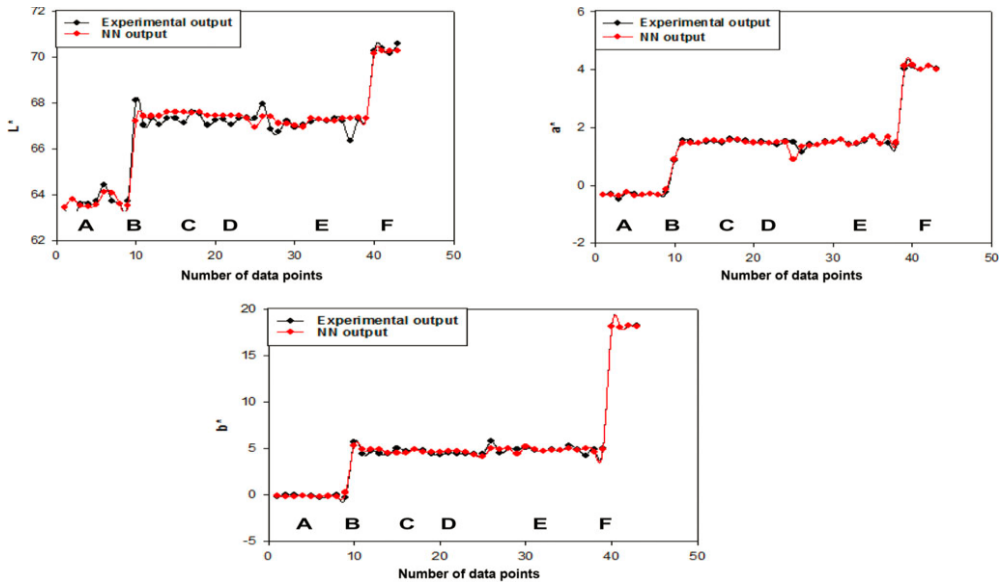

Figure 6.5. Comparison of NN output and experimental output for colour tristimulus values L*, a*, and b* of training data

It is clear that the performance of the ANN would have been even better, if data from a larger number of test runs had been available for the network training. By using **Equation (2.1)**, the DE value was computed from the output values from the experimental output data and LM algorithm of 14 neurons, it was found that the obtained DE from ANN was less than 1, with a maximum value of 0.869, when compared with the experimental DE having a maximum value of 4.2, as shown in **Figure 6.6**.

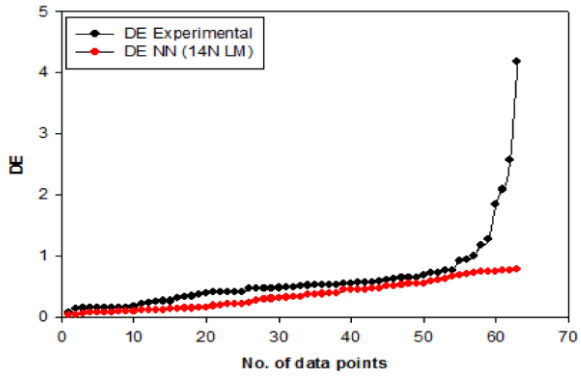

Figure 6.6. Comparison of experimental and neural network DE values in ascending order

ANN Applied to the Bulk Data. The processing and formulation data of 3,500 lots from the production records of SABIC IP was collected for developing ANN model for colour output prediction. The data set had 65 inputs, and three outputs – L* a* b* for each of

the 3500 lots. The inputs consist of various types of pigments and their concentration in parts per hundred gram of polycarbonate (pph), which varied from zero to a maximum value, which are presented in **Table A–3** (Appendix A: Neural Network). In the current analysis, the experimental results were used to train, validate, and test the designed ANN. The collected data were randomly subdivided into three sets: 75% of data was used for training, 12.5% for validation, and 12.5% for testing. The usual approach is to prepare a single data set and differentiate it by random selection. The learning algorithm called the feed forward backpropagation was employed for the single hidden layer. The gradient descent with momentum (GDM), resilient backpropagation (RP), scaled conjugate gradient (SCG), and LM algorithm were used for the variants. In the training stage, to study the output accuracy, the number of neurons was increased step by step (i.e., 15, 16, 17, 18, 19, and 20) in the hidden layer. The tan sigmoid (tan sig) transfer function was applied in the hidden layer, whereas the pure linear (purelin) transfer function was used in the output layer. After the successful training of the network, the network was tested applying the test data. Using the results produced by the network, colour difference was used to make comparisons by calculating the deviation or errors (DE) in colour values of test data points. [54]

The performance of GDM was not at an adequate level, and the statistical values in terms of regression and MSE were out of the desirable range, as shown in **Figure 6.7**. The GDM depends on two training parameters: the learning rate and momentum coefficient.

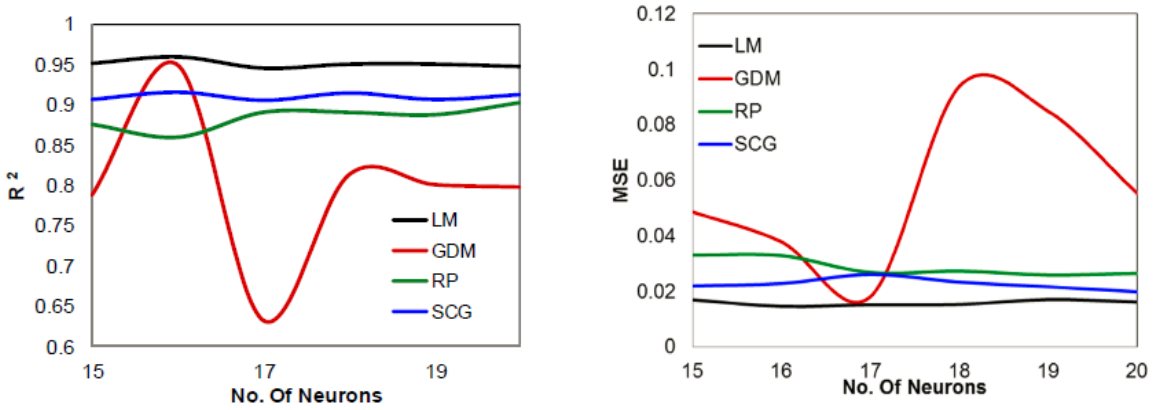

Figure 6.7. Comparison of (a) regression and (b) MSE for different algorithms cycle

The amount of momentum was set between 0 (no momentum) and 1 (large momentum). The accuracies of algorithms RP and SCG were satisfactory, but not consistent with hidden neurons. The LM algorithm showed good performance accuracy and consistency when changing the number of hidden neurons. The best network was the LM algorithm with 16 hidden neurons. When the number of hidden units (neurons) exceeded 16, the error increased and the overall efficiency of the model decreased. In LM, validation data were used for the early stoppage of training and to avoid overtraining. After 41 training cycles, the level of error was satisfactory and further cycles had no significant effect on error reduction, as is evidently shown in **Figure 6.8**. **Table 6.5** presents the regression and MSE with 16 neurons in the hidden layer and for training, validation, and testing. It is quite clear that the values are equal to zero for MSE and 1 for regression coefficient. For the given dataset, the training data indicated a better fit. The validation and test steps resulted in R-Squared values greater than 0.9. The correlation between the target and estimated values was 0.95 for the training data, and 0.93 for the test data. Training data provided better predictions (e.g., 0.95 for output variables than testing (e.g., 0.93) and validation (e.g., 0.938) data.

Table 6.5. R-Squared and Mean Square Error for 16 neurons in hidden layer

Sets	R-Squared	MSE
Training	0.96918	0.0147
Validation	0.96207	0.0149
Test	0.96101	0.0151

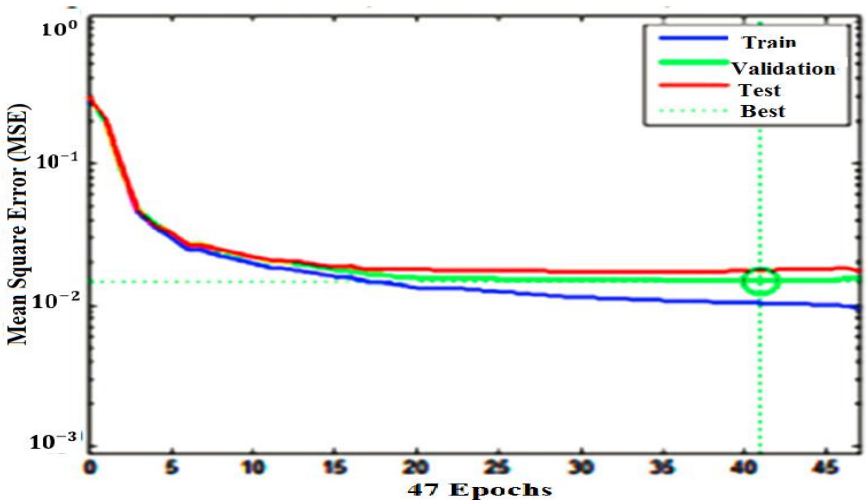

Figure 6.8. Network training cycle for LM algorithm

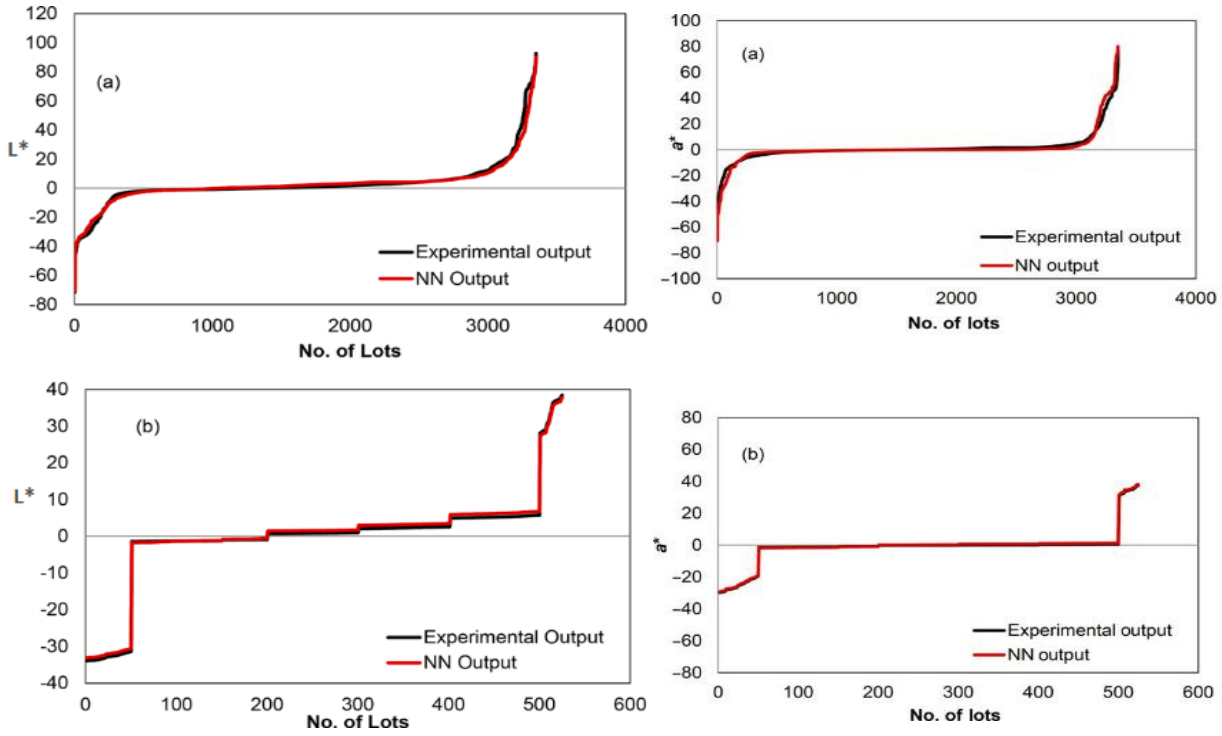

Figure 6.9. Comparison of experimental and neural network results for L*, a*: (a) training data and (b) test data

For graphical presentation of network quality, comparative graphs of predicted and experimental values are shown in **Figure 6.9**. The effect of colour values in terms of *L** *a** *b** are presented separately for the training data and test data. The graphs of a* revealed much smoother error curves in comparison to L*.

As an example of available data, **Table A–4** (Appendix A: Neural Network) presents the concentration of pigments (parts per hundred gram of polycarbonate resin) for a set of 40 lots, with corresponding *L** *a** *b** of the experimental and test data of the neural network. The *L***a***b** values of lots are concentration dependant. *L** values increase due to an increase in the concentration of white pigments, and decrease due to an increase in the concentration of black pigment. Similarly, *a** and *b** values vary due to the change in the concentration of red, green, blue, and yellow pigments. The results of the test data are in accordance with the experimental results with a slight variation. The variation in *L** values is slightly larger in comparison with those of *a** and *b**, due to a large change in the composition of white and black pigments. However, the trained neural network made it possible to analyze the pigments' influences. The results illustrate that the ANN predicts the polymer colour values

quite satisfactorily, despite a wide range of pigment composition. The data are reproducible with small variation. The deviation in colour values (DE) was calculated using experimental output (target) and test data of the neural network; the obtained DE values ranged from 0.04 to 0.99. The contours (**Figure 6.10a**) depict the contributions of DL* (deviation in the *L** value of the sample and standard) and Da* (deviation in a* value of the sample and standard). Similarly, **Figure 6.10b** presents the contribution of DL* and Db* (deviation in the *b** value of the sample and standard) in relation to DE. The contours show that DE is strongly affected by the contribution of DL* compared to Da* and Db*. The minimum value of DE was obtained with DL* = −0.02, Da* = −0.02, and Db* = 0.01, whereas the maximum value of DE was obtained with DL* = 0.973, Da* = 0.0013, and Db* = 0.024.

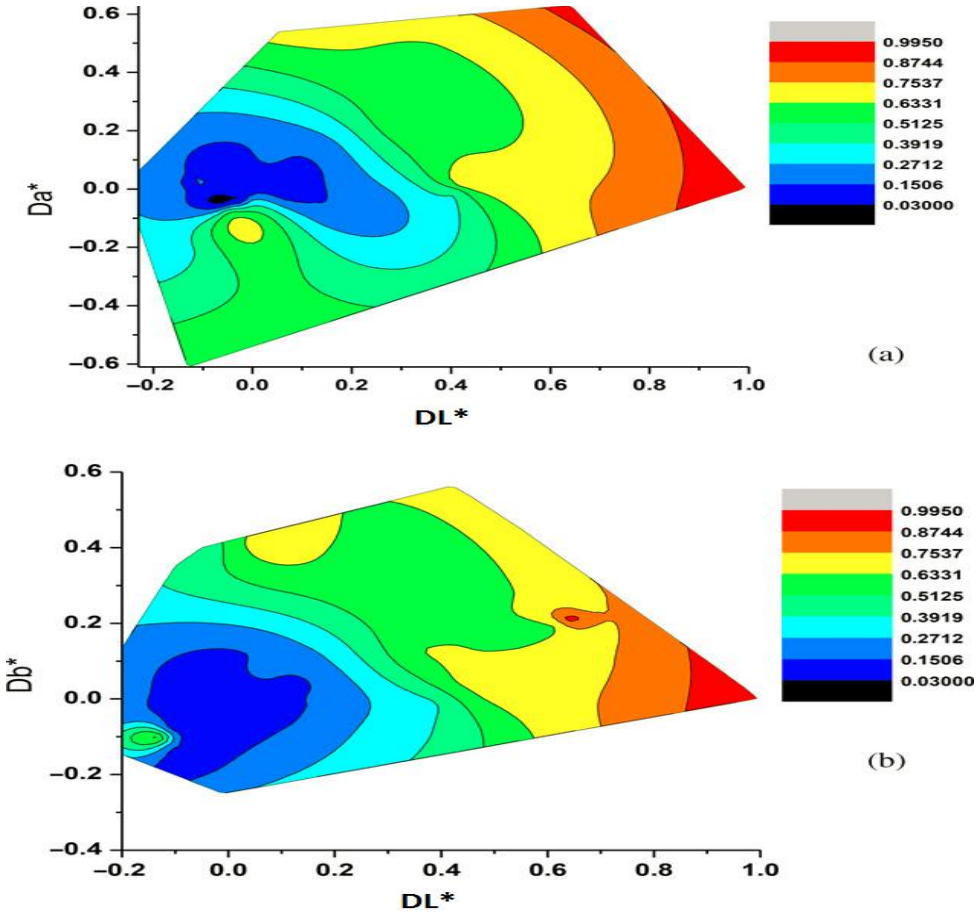

Figure 6.10. Contours of DE with respect to contribution of (a) D*L** and D*a** and (b) D*L** and D*b**

6.3 Effect of Processing Parameters on Colour – General Trends (GT)

Three polycarbonate grades were compounded under varying settings to evaluate the effects of processing parameters, namely temperature, feed rate, and screw speed. Experiments were carried out to monitor the general trend (GT) of each parameter while other parameters were kept constant. The extrusion lab line, Extruder 1 (see §4.2.1) was used at the SABIC IP Cobourg plant. The optimal set of processing parameters for consistent colour matching was determined.

6.3.1 Effects of processing parameters on three different grades

The effects of processing parameters on colour formulations for the three different grades associated with the same colour were analyzed. Stat-Ease Design-Expert® software was used for Analysis of Variance (ANOVA). The formulations of the three grades are given in **Table 6.6**, below.

Table 6.6. Colour formulation of the three grades

Resin/Colour	**Grade 1**		**Grade 2**		**Grade 3**	
Type	PPH	gm	PPH	Gm	PPH	gm
Resin 1	30	1800	30	1800	–	–
Resin 2	70	4200	70	4200	100	6000
Pigment A (White)	1.925	115.5	1.76	105.6	1.76	105.6
Pigment B (Black)	0.11	6.6	0.00968	0.5808	0.00968	0.58
Pigment C (Red)	0.1875	11.25	0.01602	0.9612	0.01602	0.96
Pigment D (Yellow)	0.1075	6.45	0.1084	6.504	0.1084	6.5

Figure 6.11 depicts the effect of feed rate (ranging from 20 to 30 kg/hr) on colour mismatch. It indicates that for all the three grades, the minimum deviation from the target colour output occurred at the lowest and highest selected feed rates. Lower deviation at the larger flow rate could be attributed to the higher shear rate, which promoted a better dispersion of pigments. On the other hand, at the lower feed rate, the twin-screw extruder showed the highest temperature at the starting mechanism of extrusion; this ultimately

promoted the flowability of the resin, and thus, dispersion of pigments in the compounding mixer.

Figure 6.12 indicates that the response of Grade 2 and 3 to the b* variation is quite similar. Both grades contain the same weight of pigment in their formulations. This identifies the importance of having the same pigment formulation, and stresses the accuracy of minute loading of pigments. It indicates how the minute changes in a formulation can cause a significant variation in colour output, leading to lot rejection.

Figure 6.13 depicts the effect of screw speed (ranging from 700 to 800 rpm) on colour mismatch. A decrease in the output colour difference (dE*) was observed at the centre level of speed.

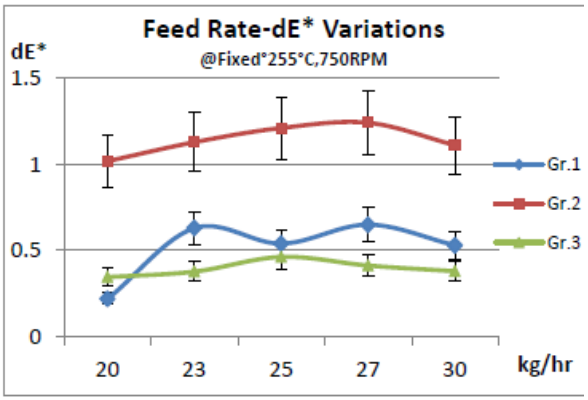

Figure 6.11. Effect of feed rate on dE*

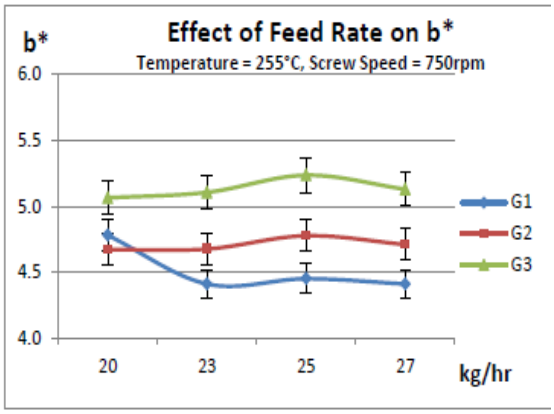

Figure 6.12. Effect of feed rate on b*

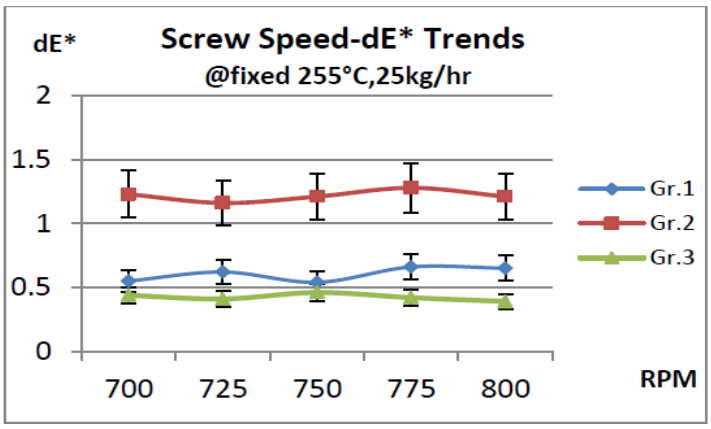

Figure 6.13. Effect of screw speed on dE*

Table 6.7 gives the Adequate Precision for dE* of 35.53. This is a signal-to-noise ratio; usually, a ratio greater than 4 is desirable. As shown in the table, the high R-Squared shows that the fitted model explains a large portion of the uncertainty observed in the data. This table also indicates that feed rate (C) and grade (D) have strong effects on dE*; their p-values (Prob > F) are less than 0.05 which indicates that they are statistically significant with a confidence level of 95%.

It is evident from **Figure 6.14** that dE* values remain higher for Grade 1 and Grade 2 than for Grade 3. This may be attributed to the lower amounts of the pigments used and better dispersion of these pigments in Grade 3. It is inferred from **Table 6.8** that there are slight variations in the colour values obtained by the optimization of experimental data, compared to the target values.

Table 6.7. ANOVA for each response (A=Temp, B=Speed, C=FeedRate, D=Grade)

Tristimulus values	Processing factors	F-statistic	Probability values	R^2	Adj-R^2	Pred-R^2	Adeq-precision
L*	Model	193.82	0.0001	0.94	0.94	0.93	34.082
	A	5.21	0.029				
	D	288.12	0.0001				
a*	Model	37.71	0.0001	0.90	0.87	0.83	20.8
	A	0.24	0.626				
	C	3.46	0.073				
	D	122.62	0.0001				
	CD	5.2	0.0117				
	A^2	3.32	0.079				
b*	Model	75.96	0.0001	0.92	0.91	0.85	23.8
	C	1.05	0.3126				
	D	185.69	0.0001				
	CD	2.98	0.0654				
dE*	Model	184.47	0.0001	0.97	0.96	0.95	35.53
	C	10.63	0.0028				
	D	538.19	0.0001				
	CD	3.13	0.0583				
	C^2	21.44	0.0001				

Table 6.8. Possible solutions for each grade

Grade	Parameters			Tristimulus Values			
	Temp	Speed	Feed Rate	L*	a*	b*	DE
	Deg. C	Rpm	Kg/hr	B/W	R/G	Y/B	
1	250.9	750	25.16	67.15	1.48	4.47	0.54
2	243.56	750	21.21	66.9	1.55	4.69	1.1
3	257.34	750	24.38	67.58	1.64	5.14	0.43

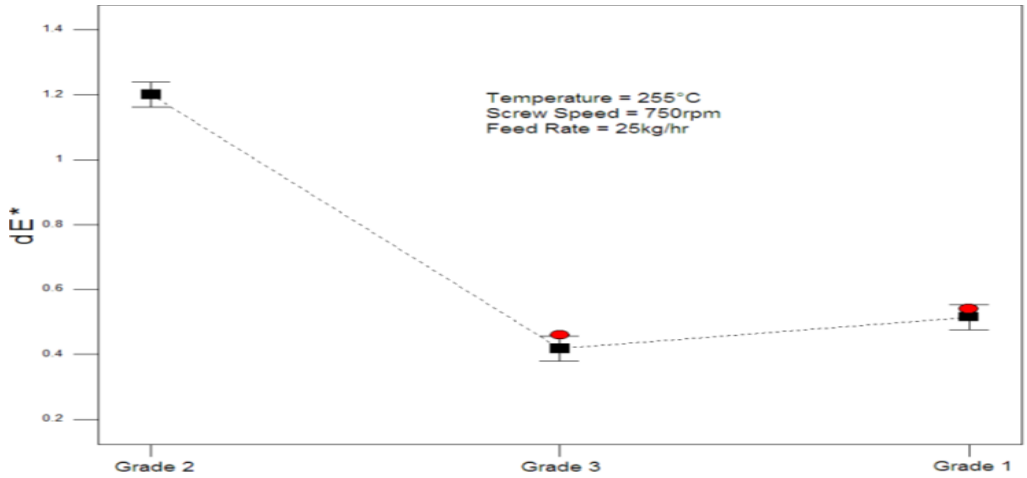

Figure 6.14. Effect of grades on dE*

The interaction and overlay plot, given in **Figure 6.15**, shows the area that satisfies the required target value, highlighted by yellow colour, while the area that does not meet the criteria is shaded gray. The single points represent the optimized values of L*, a*, b*, and dE* for the studied grades.

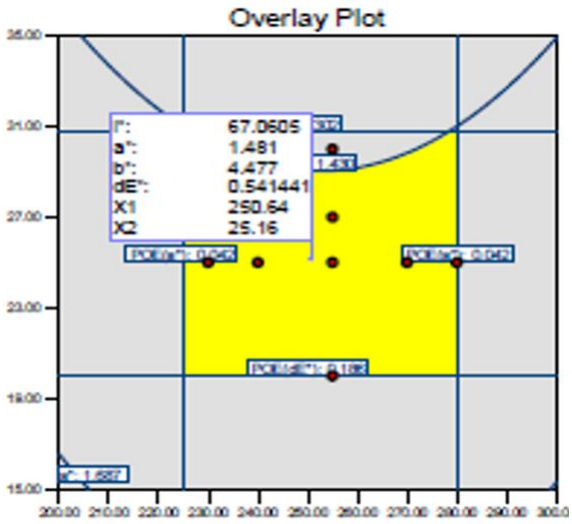

Figure 6.15. Interaction and overlay plot

6.3.2 Effect of Processing Parameters for Other Grades

An Opaque Grade. The three grades evaluated in the previous section were opaque; therefore, an opaque grade was also studied to evaluate its response to varying processing parameters. The formulation is indicated in **Table 6.9**.

Table 6.9. Compounding material for the opaque grade

S. No	Type	Grade A	
		PPH	gm
1	Resin -1	90	5400
2	Resin -2	10	600
3	Pigment-A (White)	1.40044	84.0264
4	Pigment-B (Black)	0.01051	0.6306
5	Pigment-C (Red)	0.03786	2.2716
6	Pigment-D (Yellow)	0.01525	0.915
7	Pigment-E (Blue)	0.03	1.8
8	Pigment-F (Yellow)	0.03231	1.9386

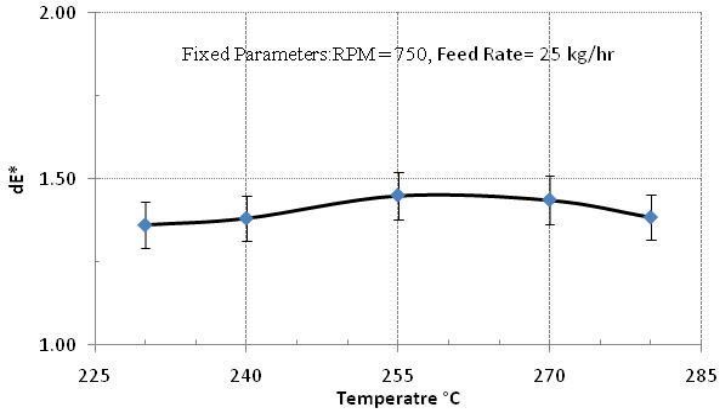

Figure 6.16. Effect of temperature on opaque colour (dE*)

The temperature variation curve shown in **Figure 6.16** reveals that the dE* values hardly change with increasing temperature, however, there is a slight decrease in dE* above 255°C (Level 3). At higher temperatures, the shear stress decreases due to a lower viscosity, which may mitigate this effect. **Figure 6.17** and **Figure 6.18** depict the effect of feed rate and screw speed on colour mismatch. A decrease in output colour difference (dE*) was observed at higher feed rates and at the centre level of speed.

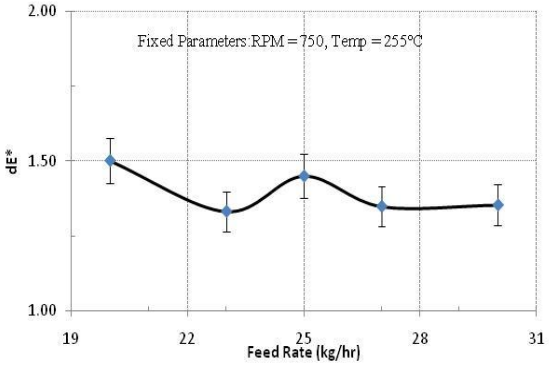

Figure 6.17. Effect of feed rate on opaque colour (dE*)

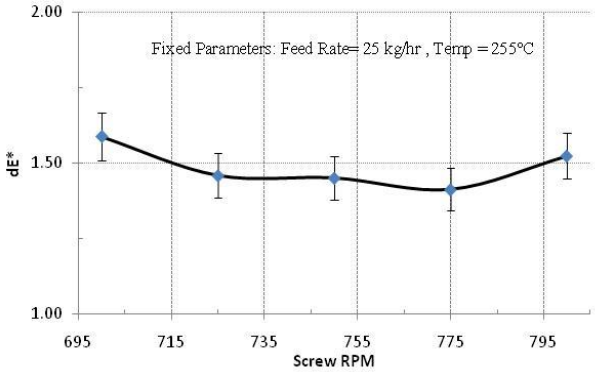

Figure 6.18. Effect of speed on opaque colour (dE*)

A Translucent Grade (g3). Figure 6.19 shows the effect of temperature on dE* for a translucent grade. **Table 4.1** describes the composition of the compounding material. A sharp decrease in the colour difference, dE*, is evident when increasing temperature from 230ºC to 240ºC, beyond which near constant colour values are observed up to 280ºC. This grade (g3 in **Table 6.4**) was selected for detailed study as discussed in the subsequent sections.

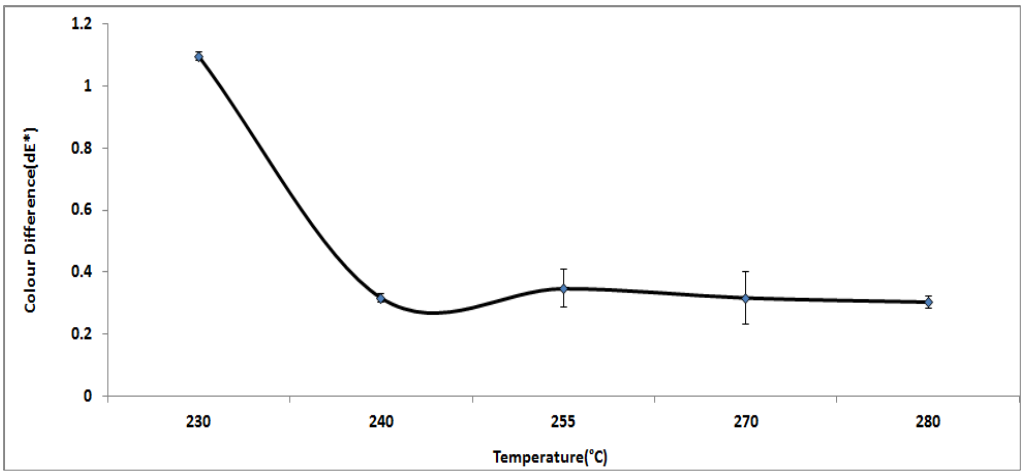

Figure 6.19. Effect of temperature on colour output (dE*)

6.4 Response Surface Methods

6.4.1 3-Level Factorial Design

Analysis of Variance. The quadratic model is the highest order model with the significant terms (Prob > F less than 0.05). Therefore, this model is appropriated for description of L* response. This was confirmed by the adjusted R-Squared value (78%) presented in **Table 6.10**, which summarises the ANOVA results.

Table 6.10. Analysis of variance for L*, a*, and b*

Response	Significant Terms	R^2	Pred. R^2	Adj. R^2	Adeq. Precision
L*	A, B, C, AB, AC, BC, A^2	0.78	0.46	0.683	9.2
a*	A, B, C, BC	0.78	0.45	0.69	6.65
b*	B, C	0.79	0.47	0.68	7.8

The R-Squared value indicates that the components usually would explain about 78% of the variability in the responses whereas about 22% of the variability in the responses remains unexplained. The "Pred R-Squared" of 0.46 is in reasonable agreement with the "Adj R-Squared" of 0.68. The signal-to-noise ratio, measured in Adeq Precision, is 9.2, which presents an adequate value indicating that the model can be used to navigate the design space.

Parameters Interaction. The analysis indicates that there are strong interactions between the three processing parameters. Strong interactions were observed between various processing parameters for L* and a*, while b* did not present any interaction between the investigated parameters. The contour graph for the most significant process parameter interactions are presented in **Figure 6.20**.

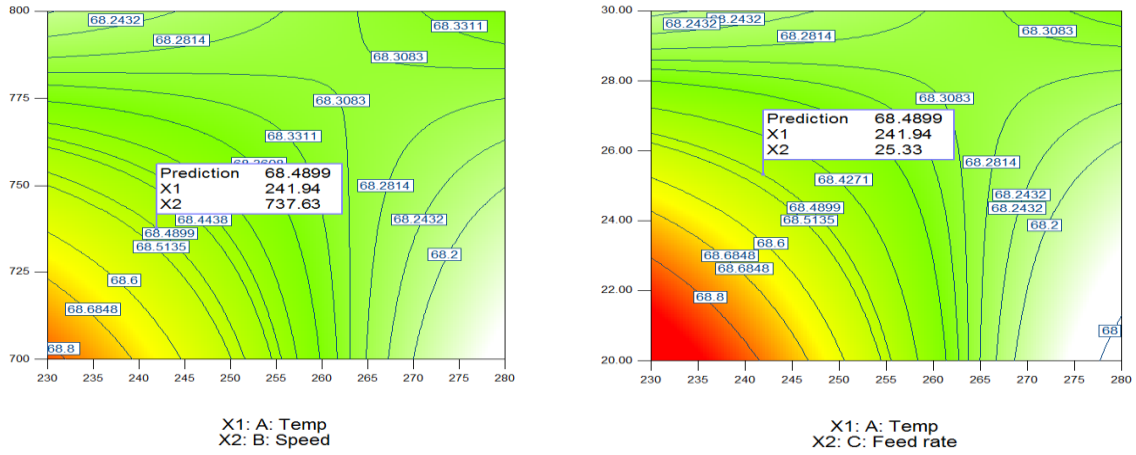

Figure 6.20. Contour plot for L*: (a) temperature vs. speed, and (b) temperature vs. feed rate

Figure 6.20a shows that the contour plot, created for the constant feed rate of 25.33 kg/hr, presents a non-linear relationship between temperature and speed. It indicates that the optimum value of L* is achieved at the region of lower temperature and speed – to be more exact, at about 241.94°C and 737.63 rpm.

Figure 6.20b presents contour plots drawn at a speed of 737.63 rpm. The plot indicates the non-linear relationship between temperature and feed rate with upward and downward segments. It also presents several combination of temperature and feed rate that will satisfy the objective. In general, the L* value increases with a decrease of temperature and feed rate; the optimum values can be achieved at a lower temperature and the medium feed rate: 241.94°C and 25.33 kg/hr.

Table 6.15 presents a comparison of the actual and predicted values, indicating a very good agreement.

Table 6.11. Comparison of experimental and predicted values

Run	Average Output Response					
	L*		a*		b*	
	Actual Value	Pred. Value	Actual Value	Pred. Value	Actual Value	Pred. Value
1	68.6	68.44	1.66	1.57	15.52	15.41
2	67.98	67.93	2.04	2.02	16	15.8
3	68.53	68.48	1.67	1.57	15.45	15.41
4	67.95	68.23	1.28	1.39	15.14	15.17
6	68.16	68.32	1.21	1.47	15.34	15.49
7	68.93	68.74	1.75	1.74	15.7	15.65
8	67.97	67.94	1.31	1.42	14.85	15.02
9	68.54	68.55	1.72	1.69	15.5	15.56
10	68.43	68.48	1.47	1.57	15.35	15.41
11	68.51	68.39	1.27	1.39	15.53	15.17
12	68.06	67.88	2.08	1.69	16.06	15.56
13	68.59	68.81	1.67	2.02	15.53	15.8
14	67.91	67.83	1.13	1.36	14.93	15.32
16	68.47	68.49	1.56	1.42	15.37	15.02
17	68.29	68.34	1.51	1.36	15.13	15.32
18	67.85	68.11	1.14	1.57	14.92	15.41
19	68.02	67.98	2.08	1.74	16.06	15.65
21	67.79	68.06	1.38	1.45	14.76	15.25
22	68.75	68.81	1.7	1.69	15.55	15.56
23	67.97	68.03	1.46	1.47	15.31	15.49
25	68.59	68.33	1.57	1.45	15.51	15.25
26	68.64	68.57	1.77	1.74	15.58	15.65
27	68.61	68.4	1.72	1.45	15.47	15.25
28	68.3	68.29	1.41	1.36	15.36	15.32

Desirability. A numerical optimizer was used for optimization in the feasible region. The response optimizer of Design-Expert® calculated a number of local points in the feasible area of the variable. The predicted values of L*, a*, and b* for the investigated grade are presented in the desirability curve shown in **Figure 6.21**. The maximum combined desirability of 73% in terms of L*=68.49, a*=1.57, b*=15.46 and dE*=0.25 was achieved at processing parameters of 241.96°C, 737.6 rpm and 25.32 kg/hr, which was in quite good agreement with the target values. From the contour graph, the increase of temperature over 241°C or decrease of temperature below 241°C caused desirability to decrease. The slight

variation of the optimized values with respect to the target values is in the range of experimental error. The model appears valid for the prediction of colour values.

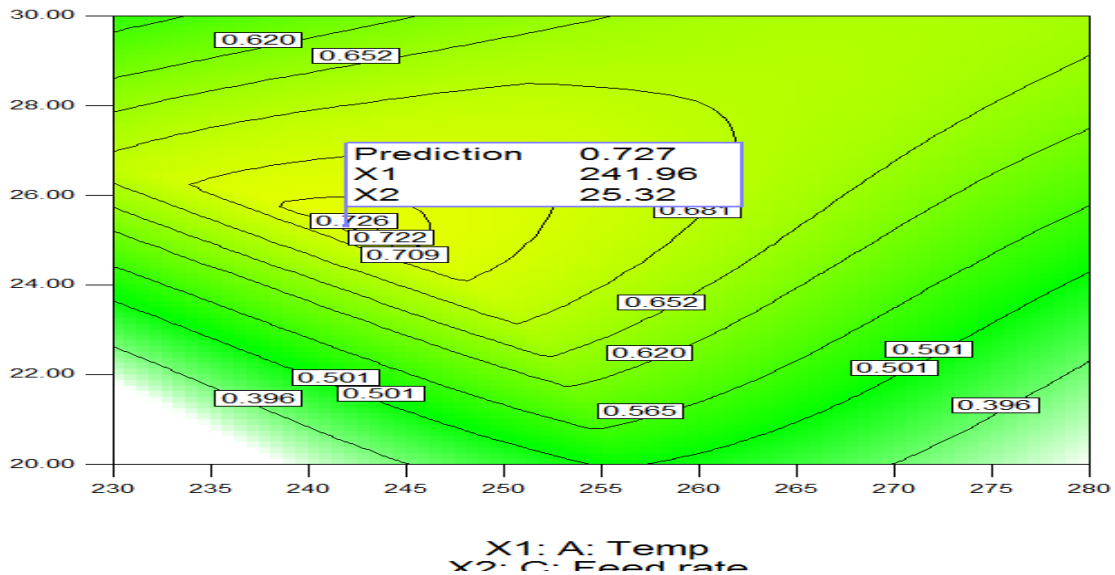

Figure 6.21. Desirability curve

Perturbation Plot. Figure 6.22 depicts the perturbation plot where the X-axis represents the coded unit of parameters and Y-axis represents the desirability. The plot demonstrates the effect of all factors at their respective center points in the design space. The comparatively less curvature of temperature (A) and speed (B) are indicative of their insignificance on the desirability in the design space considered. The strong curvature of curve C (feed rate) indicates that the feed rate has a strong impact on the desirability compared to temperature and speed.

Overlay Plot. Figure 6.23 shows the overlay plot of temperature (A) vs. speed (B), revealing a feasible region to achieve the target values. It is worth noting that this contour plot is derived from the model considering the main effects and interactions. The yellow region highlighted in this plot indicates the range of temperature (X1) and speed (X2) where requirement for the mean responses, i.e. L*, a* and b*, are satisfied. The best possible tristimulus values are L* = 68.49, a * = 1.59 and b* = 15.45.

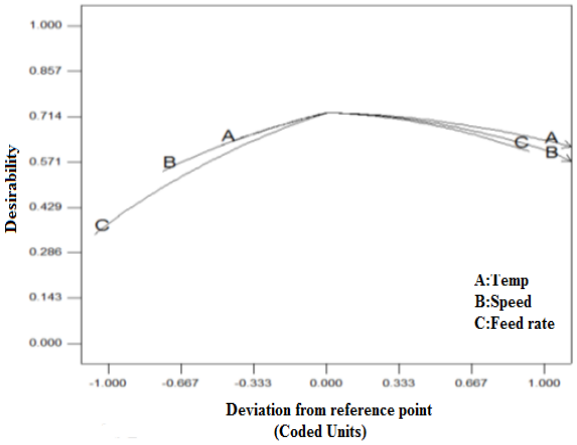

Figure 6.22. Perturbation plot

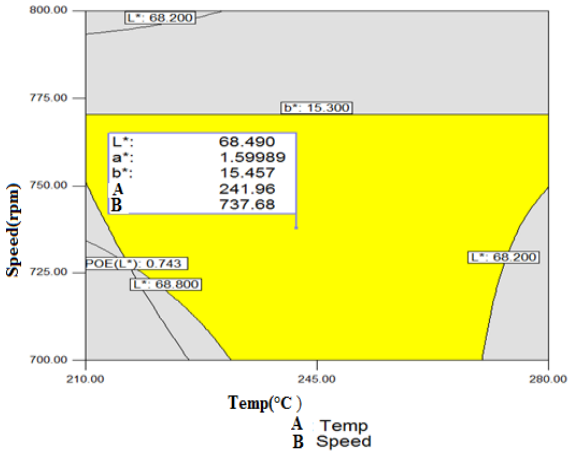

Figure 6.23. Overlay plot

6.4.2 Box-Behnken Design (BBD)

The BBD designed experiments were carried out by our group on grade g3. The results obtained are published in [127] and briefly discussed below.

Interactions and Contours Graphs. The interaction of the factors A and C affecting L*, a*, and b*. For brevity, only the L* contour plot is shown in **Figure 6.24**, which reflects the effect of temperature and feed rate on the output response, while the screw speed was maintained at its mid-level. It is evident from the L* graph that an increase in temperature induces a negative effect on L*, whereas the feed rate imposes a reverse effect on the response.

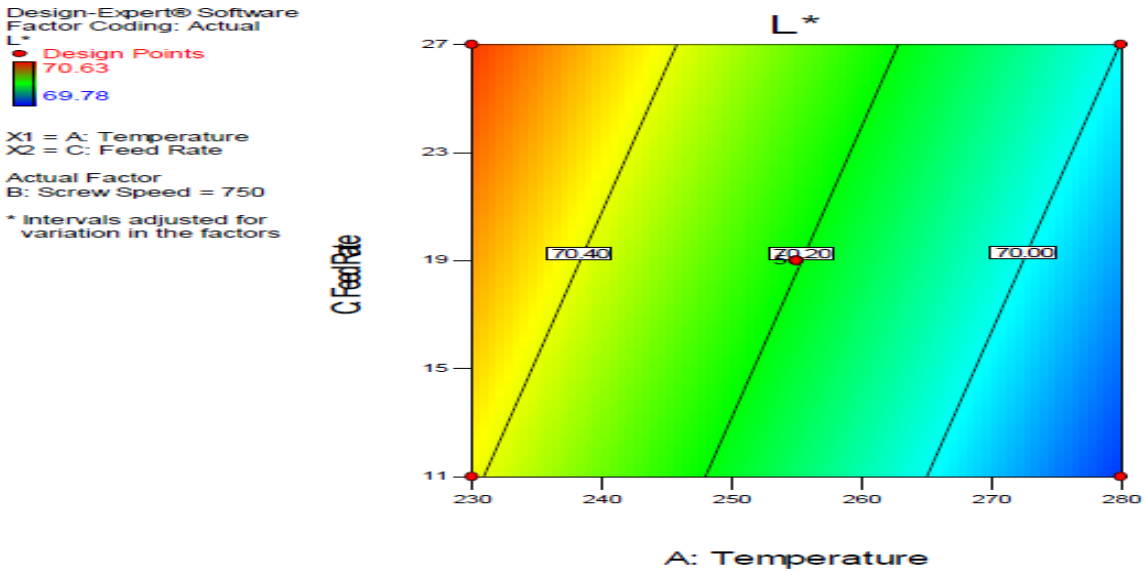

Figure 6.24. Contour plot for L* along temperature and feed rate

Desirability. Figure 6.25 shows a 3D graph of the combined desirability against the processing parameters. It displays a process window that is large enough to easily satisfy the optimization criterion. The contour graph shown in **Figure 6.26** reflects the same optimal solution with a desirability level of 0.866. A verification test for a significance level of 0.05 and 200 trials was carried out using the confirmation node of the software. It verifies the fitness of optimal solutions as the response mean values are within 95% CIs.

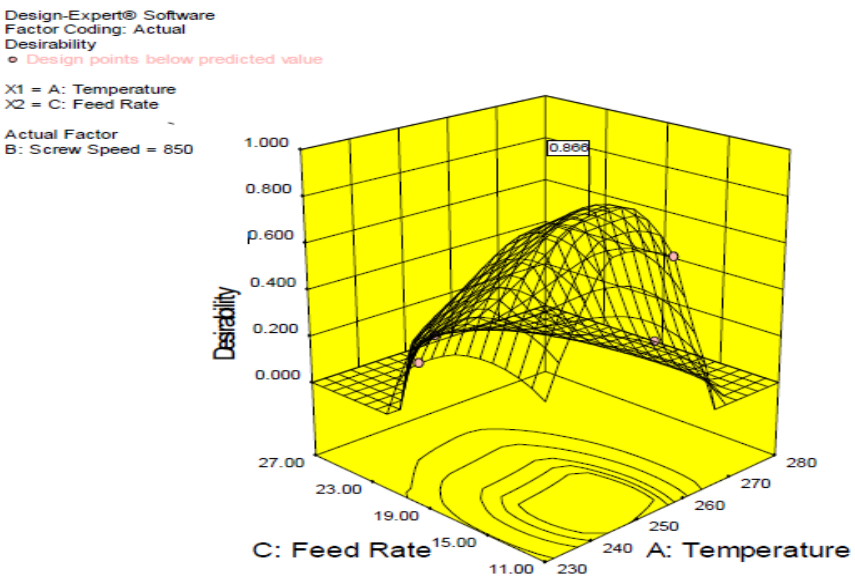

Figure 6.25. 3D surface graph flagged with optimal desirability

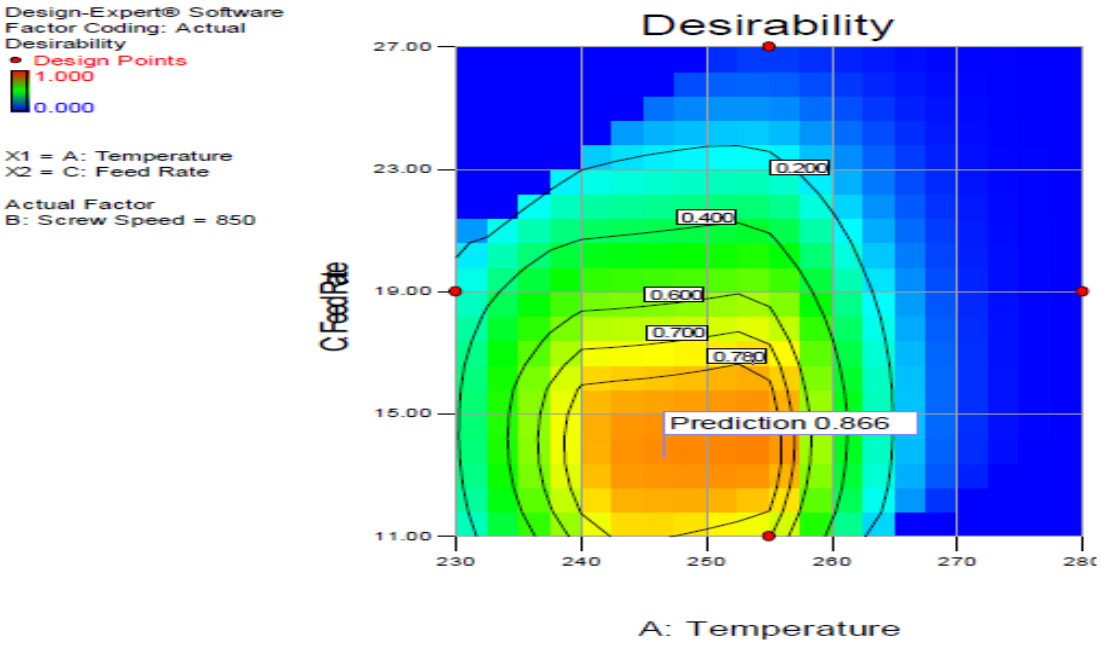

Figure 6.26. 2D contour graph flagged with optimal desirability

Graphical Optimization (Overlay plot). Solutions suggested by the numerical optimization are expected to be located in the 'sweet spot' (bright yellow) as shown in **Figure 6.27**. This is how graphical optimization helps numerical optimization to obtain a desired set of process conditions that truly satisfies all the constraints.

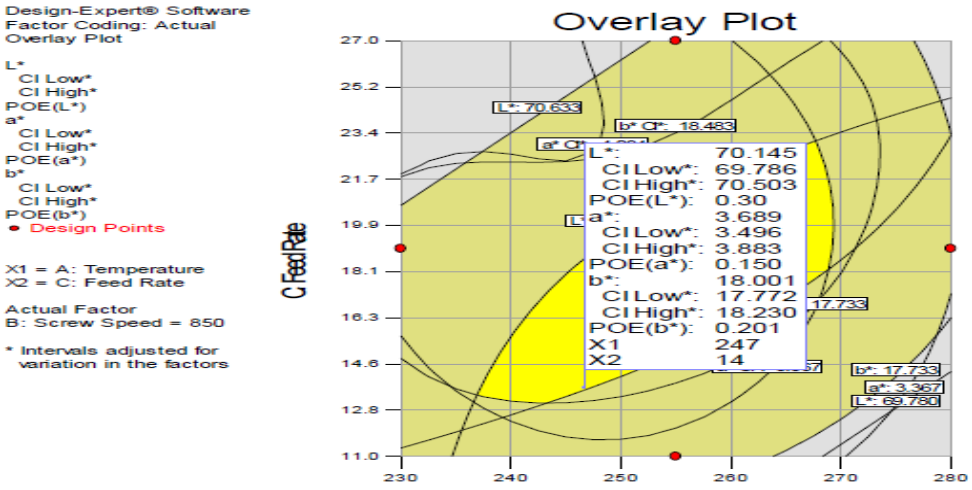

Figure 6.27. Graphical optimization and sweet spot flagged for a desired solution

The flagged point has a desirability level of 0.866 and predicts output response values of L*=70.15, a*=3.69 and b*=18.00, at 95% confidence intervals (CIs) and a minimum level

of POE for an optimal set of process variables (e.g. temperature of 247°C, screw speed of 850 rpm and feed rate of 14 kg/hr).

6.5 Characterization of a Selected Polymer Grade

The translucent grade g3 from the previous section was selected for further characterization studies. It was a blend of two resins, R1 and R2, with MFIs of 25 and 6.5 g/10min, respectively.

6.5.1 Rheological Behaviour of PC Blends Prepared on ML

The first study to be undertaken was to investigate the effects of blending ratios on the rheological properties of two polycarbonate resins (R1, R2) comprising the selected PC grade. To do this, blends were prepared in which the resin ratios were controlled in steps of 10%. This resulted in eleven batches were the percentage of each resin change from 100% to 0% in decrements of 10% for each subsequent batch.

Melt Flow and Delta Pressures. The blends were characterized using the MFI indexer at SABIC IP and the ML at U of T. **Figure 6.28a** presents the effect of Resin 2 amount on MFI of the blend. It shows that the melt flow index for R1 was 28.22 gm/10min and that of R2 was 8.10 gm/10min, against the nominal values of 25 and 6.5 published by the manufacturers. A reduction in MFI was expected given an increasing amount of R2.

Figure 6.28b presents the pressure differences in the blending process of polycarbonate on the ML, both with and without pigments. It clearly shows a linear correlation with increasing R2 amounts. The obtained data indicates that with inclusion of additives and pigments the pressure difference (ΔP) decreases. This indicates that the additives used provided lubricity, in addition to their intended stabilization functions. However, the increase in pressure difference from increasing the amount of R2 is proportional to the viscosity of the blends, where high viscosity corresponds to a low melt flow index.

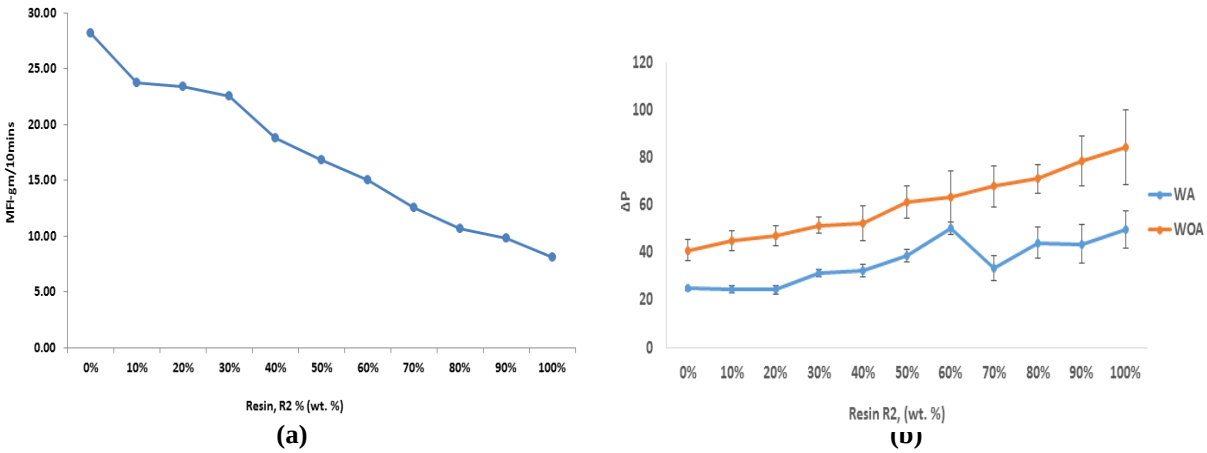

Figure 6.28. Variation in (a) melt flow index vs. polycarbonate resin R2, wt. %, and (b) pressure difference with respect to polycarbonate resin R2, wt. % with and without additives

Rheological Behaviour WOA and WA. The PC blends were rheologically characterized at 230, 255, and 280°C using the Ares rotational rheometer. The main focus was later extended to the polymer blend of 30/70 by weight (which is the ratio for the selected grade) to extract the impact of viscosity on colour output as measured by the deviation from the target values. The obtained viscosity data will allow developing a simulation scheme to predict wetting and stabilization of pigments, which have a direct impact on polymer colour changes. Polycarbonate composites were rheologically characterized in different dynamic phases as detailed in the following sections.

The presence of a consistent viscous region was confirmed via the strain sweep experiment. **Figure 6.29** illustrates the strain sweep test for a blend consisting of 50% R1 and 50% R2. The response from the strain sweep test revealed that all blends behaved linearly at strain magnitudes of greater than 10%, at various selected temperatures. Increasing the temperature causes reduction in viscosity.

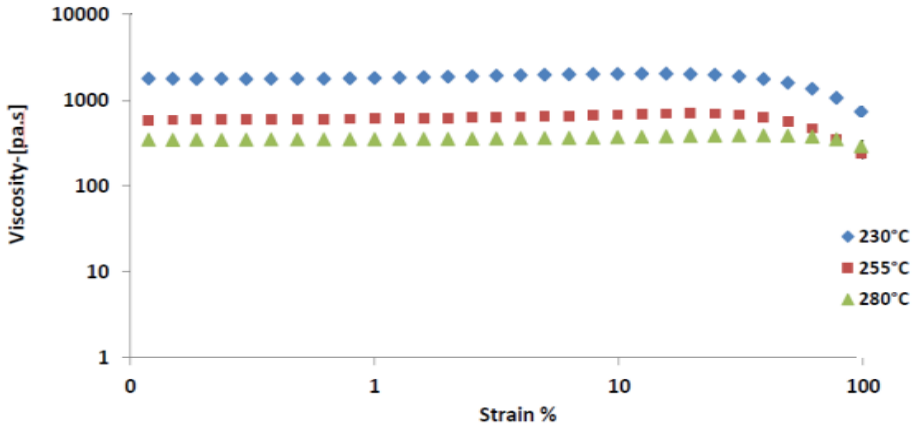

Figure 6.29. Strain sweep test for blend R1-R2 (50%-50%) at 10Hz

Figure 6.30a illustrates the storage modulus response at 255°C for the blends without additives (WOA) for three blends. It indicates that the lowest storage moduli appear at the low frequencies, but the separation then reduces at the higher frequencies. The 100% R2 blend showed the highest modulus at low frequencies indicating that this resin is capable of storing more energy than 100% R1, which also exhibits the pseudo-elastic behaviour at low frequencies. However, all of the examined blends showed wider gaps at low frequencies and fell into a narrow band at the higher frequencies.

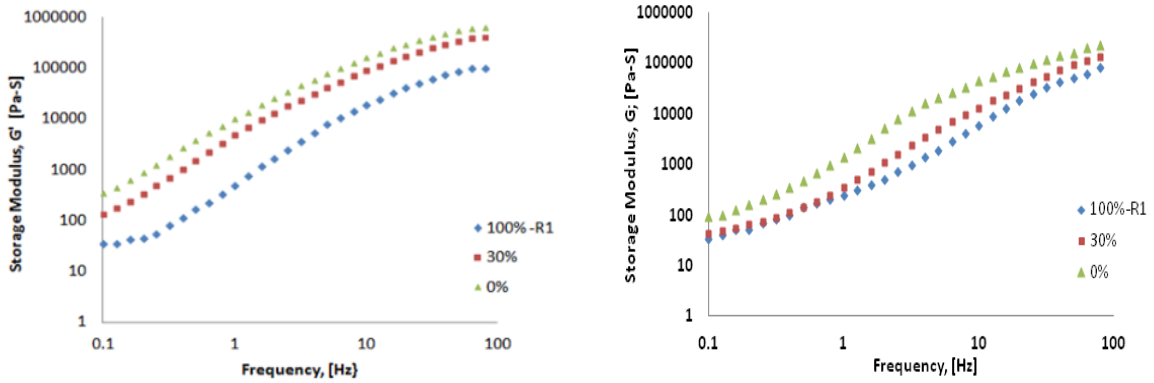

(a) **(b)**

Figure 6.30. Storage modulus of Blend 100%-R1, 30%, 0% at the temperature of 255°C: (a) without additives and pigments, and (b) with additives and pigments

Results of complex viscosity at 255°C vs. frequency for the blends without additives (WOA) are presented in **Figure 6.31a**. Blend 100% R1 exhibited the lowest viscosity with a

solid like behaviour at the low frequencies compared to blend 0% R2, while both presented shear thinning behaviour at the higher frequencies. With addition of R2 into the R1 resin, viscosity of the blends increased substantially. The dynamic responses of R1/R2 blends do not appear to follow the "rule of mixing" which expects variation of the parameter to be in proportion to the amounts of constituent elements of the blend. The increase in viscosity with addition of R2 may be due to solvation of the highly entangled structure of R2 molecules in R1 molecules. Similarly, **Figure 6.31b** presents viscosity of blends where the pigments and additives (WA) are added. Resin R2 (100%) shows a higher viscosity and exhibits a strong shear thinning effect while Resin R1 (100%) shows a lower viscosity in comparison to 100% R2 and the other blends. In general, viscosity of the blends decreased in the presence of pigments and additives by approximately 8-20%.

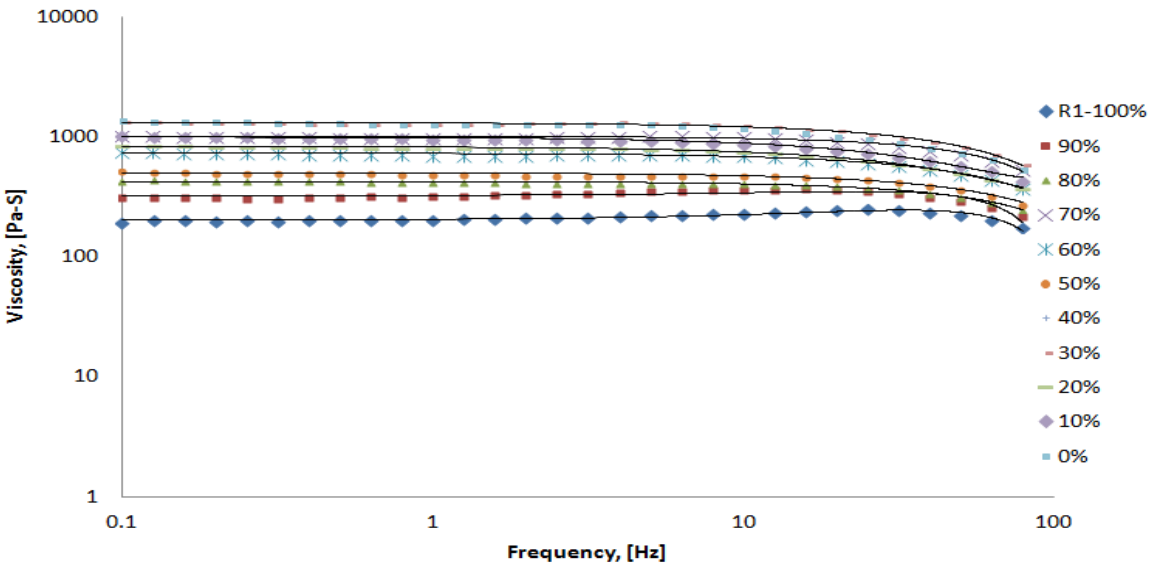

(a)

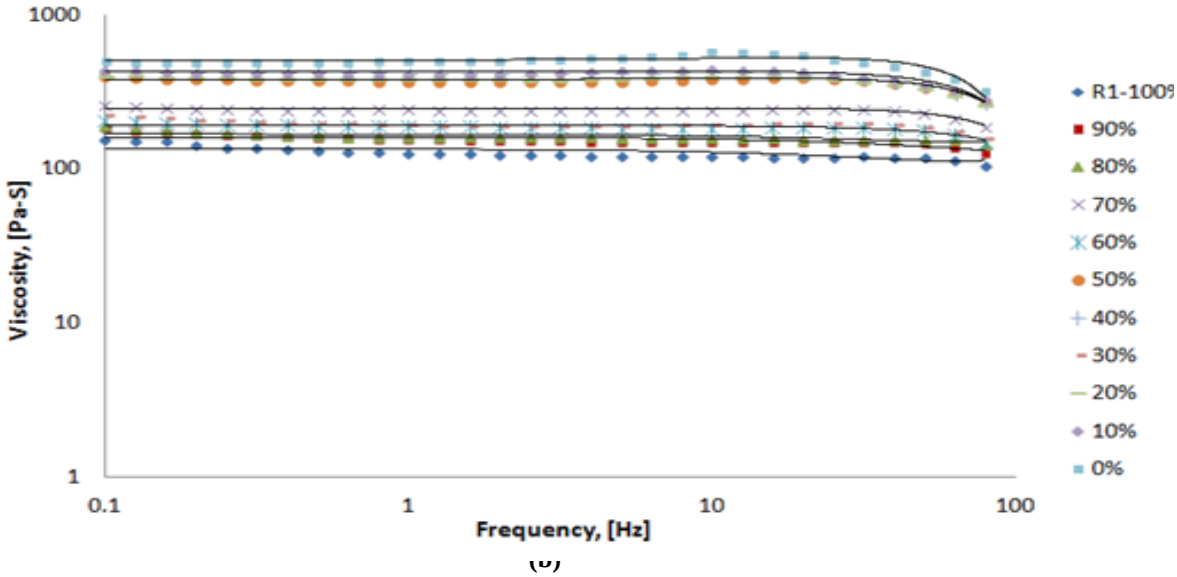

(b)

Figure 6.31. Complex viscosity at a temperature of 255°C: (a) without additives and pigments, and (b) with additives and pigments

The Carreau model was used to fit the viscosity data. **Figure 6.32** (extracted from **Figure 6.31**) compares the blend 30/70 R1/R2 with (WA) and without the addition of additives and pigments (WOA). With additives, the viscosity of the blend decreased by approximately 20%.

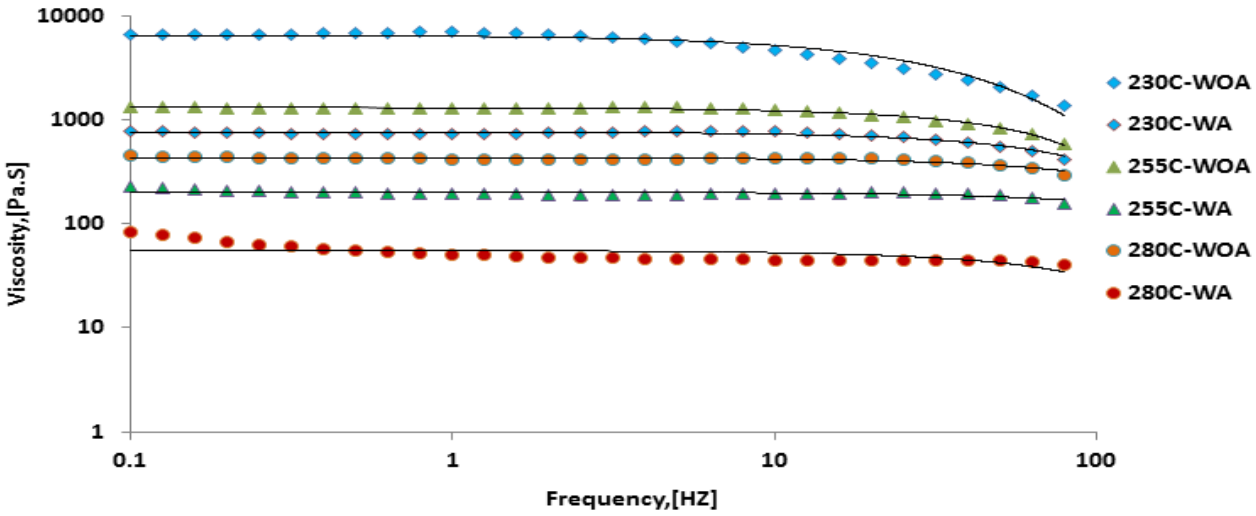

Figure 6.32. Complex viscosity behaviour vs. frequency for all blends of R1-30%: without and with addition of additives at investigated temperatures along with the corresponding Carreua models

The steady shear viscosity responses for blend with 30 wt. % of Resin R1 to various temperatures are depicted in **Figure 6.33**, without and with the addition of additives. The magnitude of shear viscosity is quite comparable to that of complex viscosity.

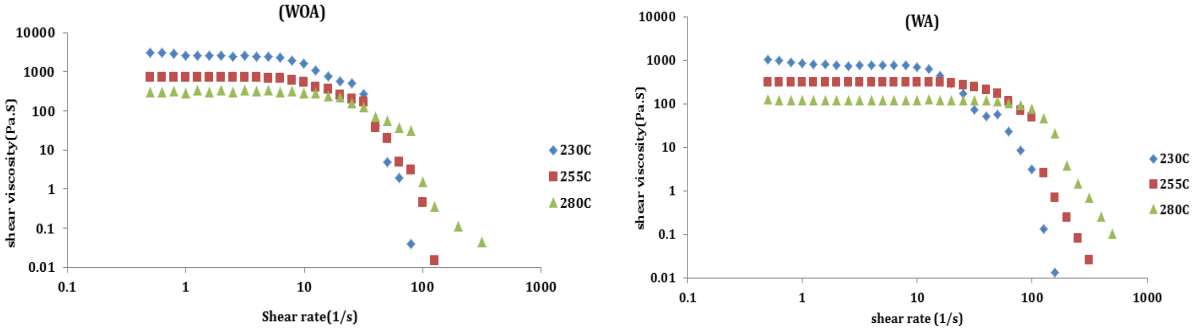

(a) **(b)**

Figure 6.33. Shear viscosity for Blend R1-30% at temperatures of 230, 255, and 280°C: (a) without additives, and (b) with additives

The change in viscosity at the higher end of the shear rate range occurred due to shear thinning – the slippage of chains over each other and molecular alignment. The increase in temperature led to a decrease in viscosity because the mobility of polymer molecular chains increases with temperature.

Figure 6.34 presents the results of complex shear viscosity measurement for blend R1-30% at temperatures of 230, 255, and 280°C. It shows that the linear regime of complex viscosity coincided with the linear regime of shear viscosity. Similar behaviour was observed in all of the blends.

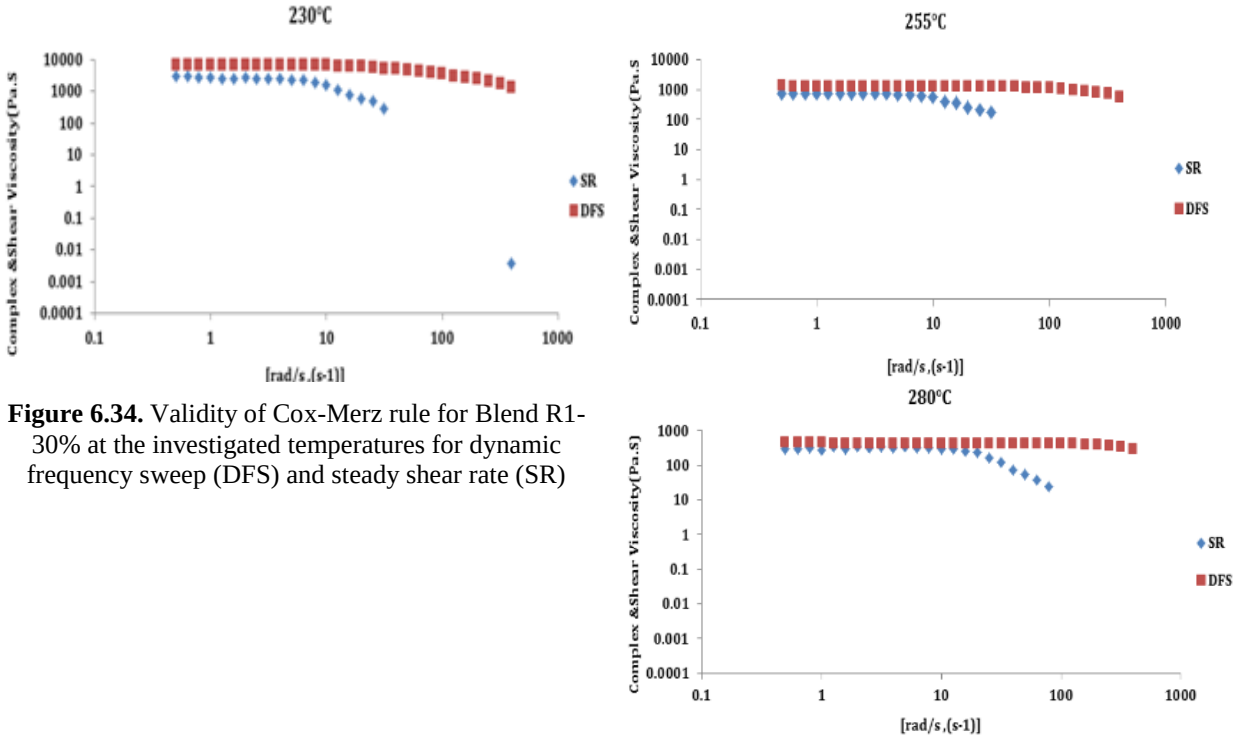

Figure 6.34. Validity of Cox-Merz rule for Blend R1-30% at the investigated temperatures for dynamic frequency sweep (DFS) and steady shear rate (SR)

6.5.2 Rheological Behaviour of the Blend Compounded at SABIC (SB)

Initially, the composites were rheologically characterized using an Ares-G2 rheometer, in three different dynamic modes at 230, 255, and 280°C: dynamic strain sweep (DSS), dynamic strain frequency sweep (DSFS), and Steady sweep-rate (SSR). **Figure 6.35** shows the complex viscosity behaviour vs. strain rate, measured at a frequency of 10Hz, and temperatures set at 230, 255 and 280°C. Complex viscosity exhibited mostly constant behaviour in the range from 0.1 up to a strain magnitude of 100%. As expected, complex viscosity decreased as the temperature increased. The relationship between viscosity and strain was constant at lower strains and at all temperatures, but started to show shear thinning behaviour at higher strains. Also, as the temperature increased, shear thinning began at the higher strains.

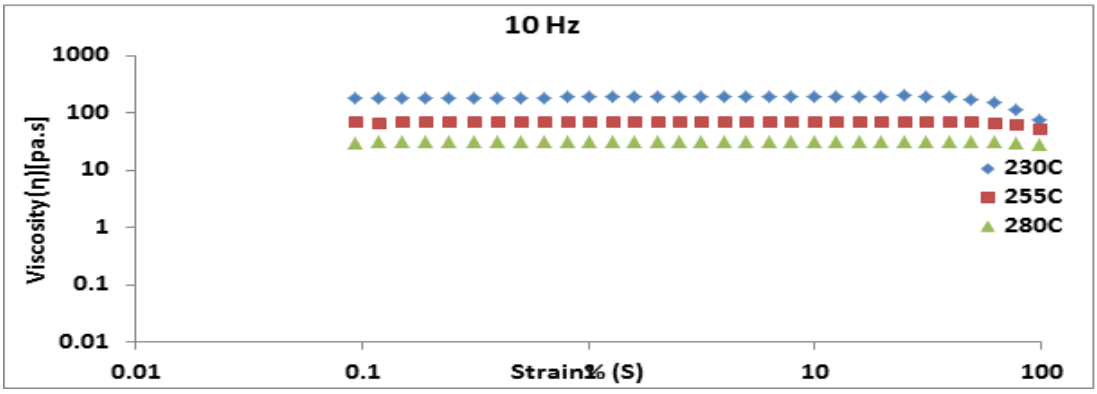

Figure 6.35. Strain sweep test for grade PC1 content of 30 wt. % at 10 Hz

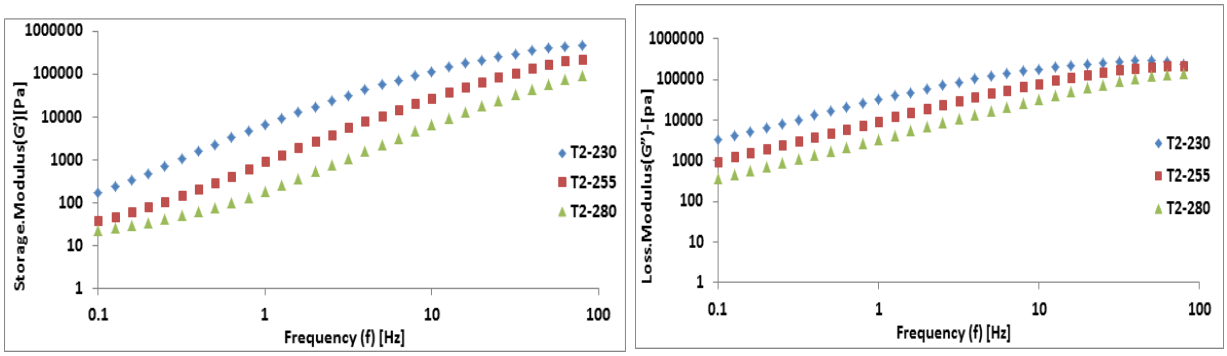

(a) **(b)**

Figure 6.36. Storage (a) and loss (b) modulus at 230, 255, and 280°C

The storage modulus refers to the ability of a material to store energy and is related to the stiffness of the material. The loss modulus represents the heat dissipated by the sample reflecting the damping characteristics of the material. Storage modulus (G′) decreased with increasing temperature and increased with increasing frequency. Similarly, loss modulus (G″) increased with increasing temperature and increased with increasing frequency as shown in **Figure 6.36**.

Dynamic Frequency Sweep – Complex Viscosity (η*). Complex viscosity (η*) decreased with increasing temperature and the onset of shear thinning occurred at a higher frequency. Upon an increase in frequency, a drop in the melt viscosity (shear thinning) was observed.

Steady Shear Rate Sweep – Shear Viscosity (η). Similarly, as temperature increased, shear viscosity (η) decreased. When shear rate increased, the polymer melt began

to exhibit shear thinning. As temperature increased, the onset of shear thinning occurred at a higher shear rate.

The Cox-Merz Rule. The Cox-Merz rule states that the steady shear rate viscosity vs. shear rate curve is virtually identical to the complex viscosity vs. dynamic sweep frequency curve. It is also interesting to note that the shear viscosity showed similar results to the corresponding complex viscosity; it decreased with increasing shear rate/frequency (at the examined temperatures of 230, 255, and 280°C), as shown in **Figure 6.37**.

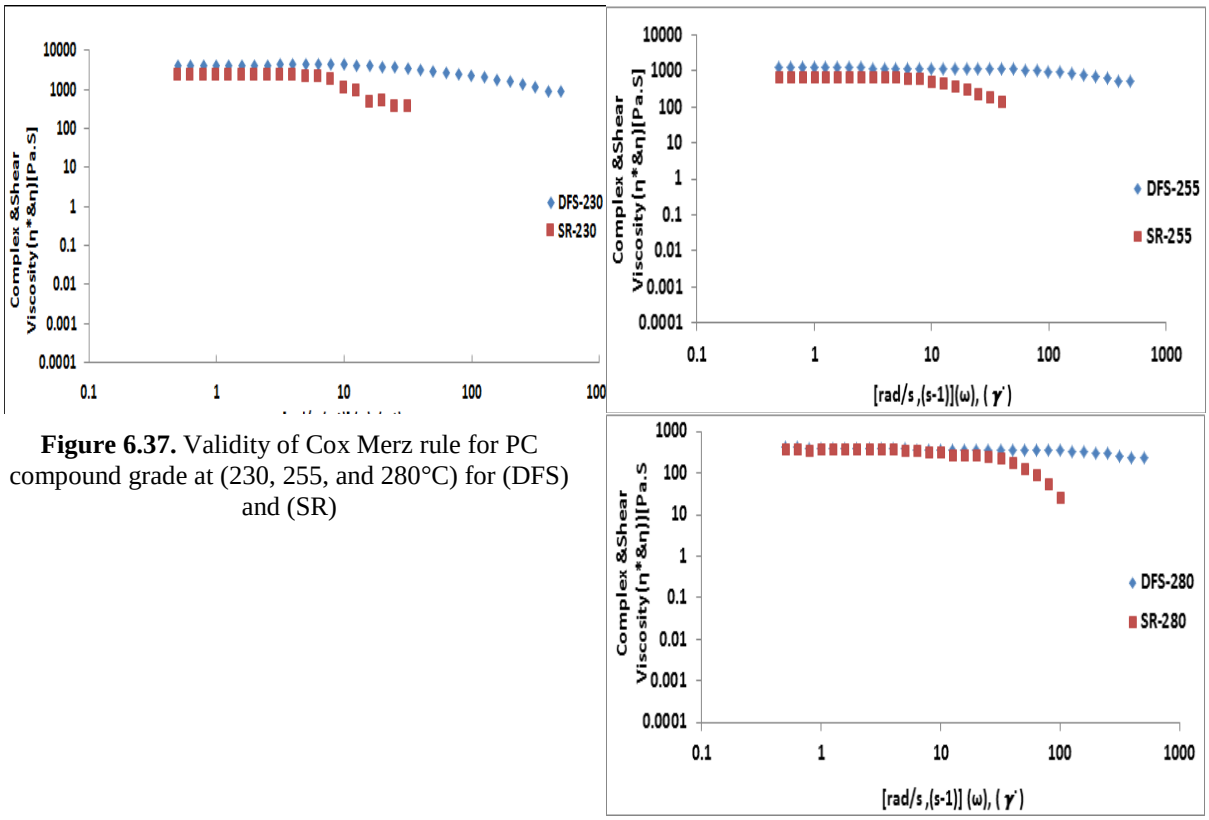

Figure 6.37. Validity of Cox Merz rule for PC compound grade at (230, 255, and 280°C) for (DFS) and (SR)

Rheological Characteristics at 230, 255, and 280°C. The rheological results measured at temperatures of 230, 255 and 280°C display a shear thinning effect as frequency/shear rate and temperatures increased. The crossover point occurred at 230ºC (26.32Hz, 2.36E5 Pa) and at 255ºC (72.6 Hz, 1.82E5 Pa) but did not occur at 280ºC. At higher frequency ranges, tanδ decreased as frequency increased. Therefore, as presented in **Figure 6.38**, the crossover point moved to a lower frequency as the temperature decreased to 230°C. The effect of shear thinning was more significant at a higher frequency and at a lower

tanδ. Therefore, at 230, 255 and 280ºC, the general trend is a steady decrease in the tanδ (G″/G′) values with increasing frequency.

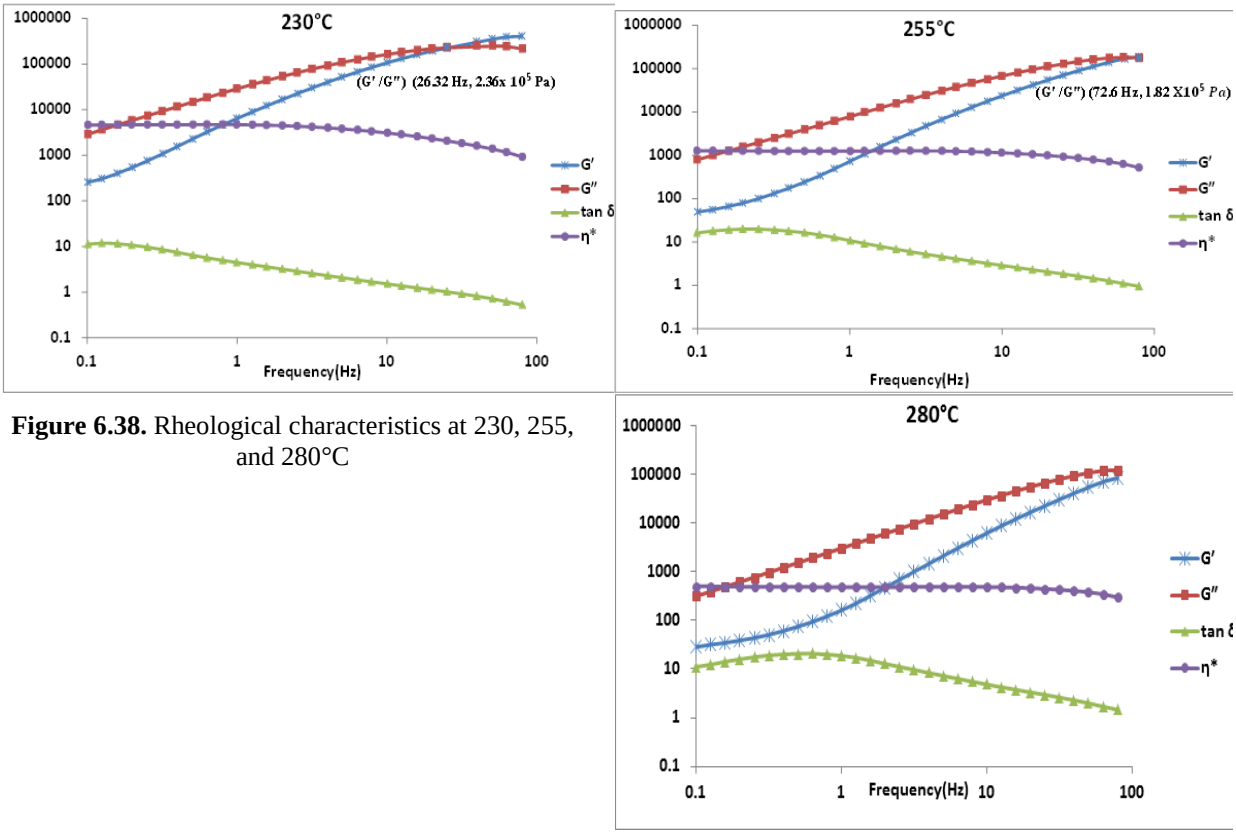

Figure 6.38. Rheological characteristics at 230, 255, and 280°C

Figure 6.38 presents the results of complex shear viscosity and tanδ at 230, 255, and 280°C. The increase in temperature and frequency shows a proportional relation: decreasing tanδ increases shear thinning. Loss modulus was greater than storage modulus (G′) before the crossover point and the material's viscous behaviour dominates the flow properties. The crossover point indicates a physical gel formation caused by a combination of entanglement of chains and other interactions. After the crossover point and at a temperature of 230ºC, G′ surpassed G″ and thus material elastic behaviour became dominant (behaved more like a solid). In general, as frequency increases, the storage and loss modulus increase, while tanδ and viscosity decrease, which indicates shear thinning as shown in **Figure 6.39** and **Figure 6.40**.

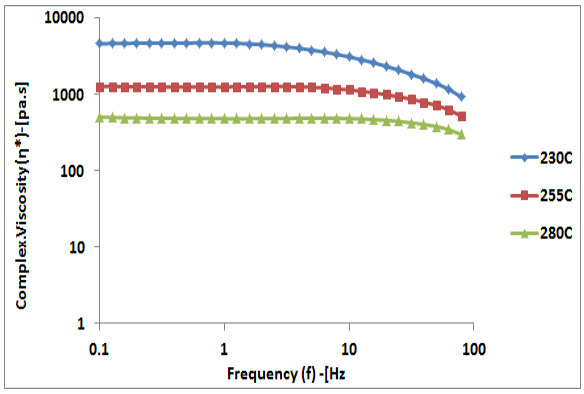

Figure 6.39. Complex viscosity for R1 30% blends at 255°C

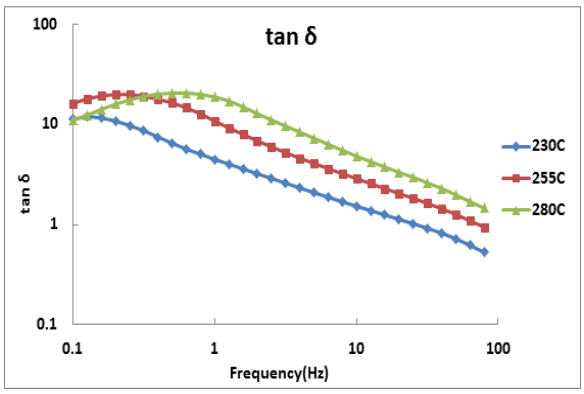

Figure 6.40. Tan δ for R1 30% blends at 255°C

The two figures, above, indicate that as temperature was increased, the material showed a decrease in the complex viscosities, |η*|, leading to shear thinning. However, the ratio G''/G'= tan δ did not change at a low frequency, indicating that the internal friction was independent of low frequency.

In this thesis, the same methodology and the same technique was used in order to determine the degree of dispersion of PC compounds at temperatures of 230, 255, and 280°C. **Figure 6.41** illustrates the effect of temperature on colour difference (dE*) at temperatures of 230, 255, and 280°C. It reveals a reduced value of colour difference when increasing the temperature at a fixed feed rate and speed. However, the most favourable colour difference value (dE*) was obtained at the higher temperatures namely 255ºC and 280ºC with dE*=0.3.

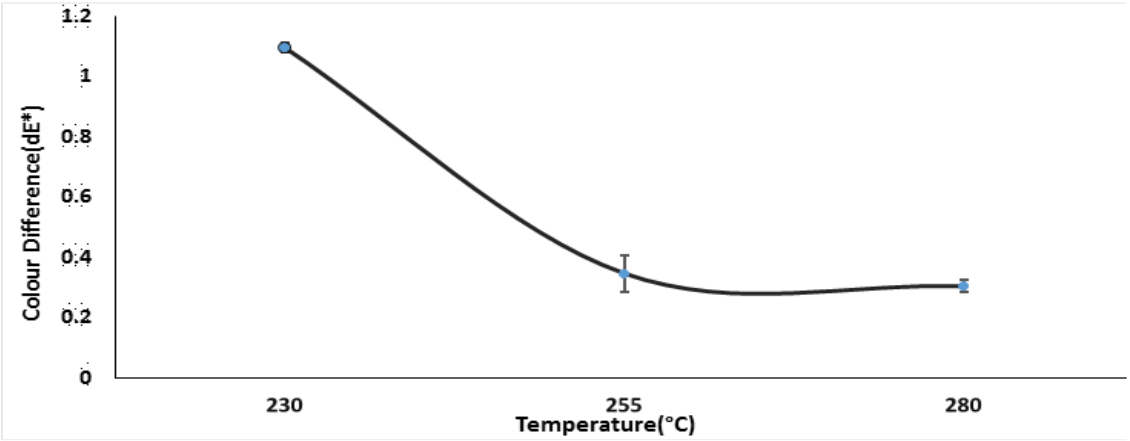

Figure 6.41. Effect of temperature on colour output with respect to dE* (DE)

Figure 6.41 shows the effect of temperature on colour difference (dE*) for the R1 30% sample that was processed at varying temperatures. It shows a steady reduction in value (dE*=0.3) at and beyond 255°C. According to **Figure 6.38**, the tanδ value is less than unity at temperatures of 255°C and higher, indicative of lower viscosity values and greater wettability. Thus, the reduced viscosity seems to exhibit a correlation with greater pigment dispersion leading to reduced colour deviation. As presented in **Figure 6.41**, the greatest effect of shear thinning was observed at a higher frequency and temperature. In general, as frequency increased, the storage and loss modulus increased, and tanδ and viscosity decreased.

Wetting enables the shear forces produced during extrusion to be transferred onto the pigments in order to de-agglomerate particles, which reduces average pigment size and increases the number of particles (frequency) dispersed, ultimately reducing the colour shift (dE*).

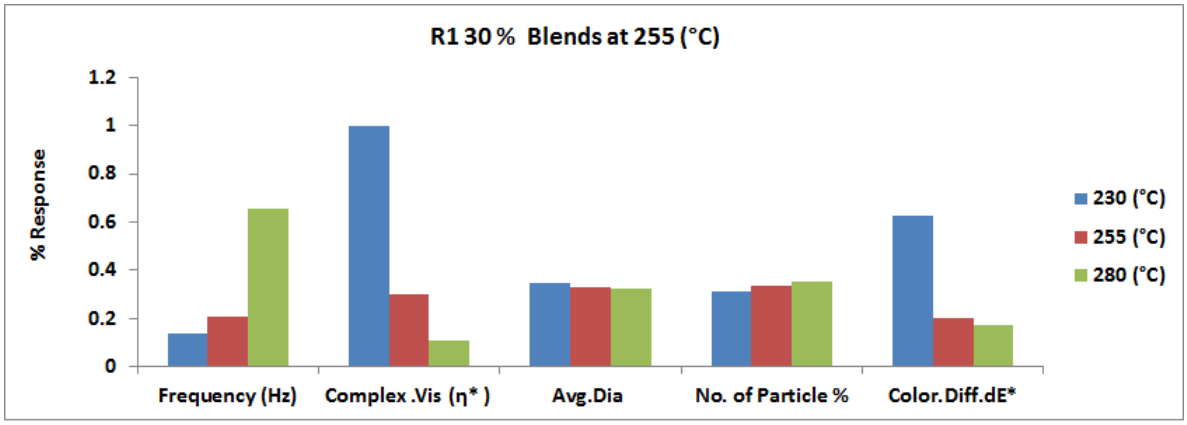

Figure 6.42. Effect of rheological parameters at temperature 230, 255, and 280°C on colour

Figure 6.38 and **Figure 6.42** indicate the significant relationships between tanδ, frequencies, number of particles, average particle size and colour differences at 230, 255 and 280ºC. It suggests that pigment dispersion is efficient at a temperature of 255ºC or higher.

6.5.3 Modelling and Experimental Simulation of Viscosity

There are several generalized non-Newtonian models for viscosity η=f ($\dot{\gamma}$) for higher shear rates. Among them is the Carreau model. C1 presents the absolute viscosity while C2,

C3, and C4 are the fitting parameters. **Table 6.12** gives the results of the Carreau model fitting and presents the parameters for blend 30/70 R1/R2. It shows that the Carreau model exhibited good agreement with the observed behaviour of the blends.

6.5.3.1 Compounded Plastic Grade (SB & ML) at 230, 255, and 280°C

Figure 6.38 shows the fitting parameters of the Carreau model for the blend at temperatures of 230, 255, and 280°C. These simulated parameters for certain polymer blends according to **Equation (5.17)** are given in **Table 6.12** and **Table 6.13**. Note, C_1 indicates the absolute viscosity.

Table 6.12. Carreau model parameters for SB at 230, 255, and 280°C

	Processing Parameters			
Temp	**C1**	**C2**	**C3**	**C4**
230ºC	4752.8	0.08	1.13	0.17
255ºC	1264.6	0.02	1.35	0.07
280ºC	447.2	-2.548x1019	-1.61x1018	1.11

Table 6.13. Fitting parameters of Carreau model, PC blend (ML) with pigment and additives (WA), and without pigment and additives (WOA)

Temp	**Parameters (WA)**				**Parameters (WOA)**			
°C	**C1**	**C2**	**C3**	**C4**	**C1**	**C2**	**C3**	**C4**
230	1796.2	0.0724	2.8261	0.3169	6796.9	0.0848	1.3201	0.2096
255	452.79	0.0209	16.12	0.3232	1299.1	0.0223	1.6618	-0.002
280	191.87	0.0899	1.4858	1.0199	378.1	271.28	-18.67	0.9955

6.5.3.2 Master Curves at Reference Temperature of 255°C

Master curves are normally extracted for extending material functions. A master curve is of great value since it covers times or frequencies outside the range easily accessible via experimentation. Fitting the experimentally determined shift factors to a mathematical model permits the master curve to be shifted to any desired temperature and offer information about short- and long-term behaviour of the materials. The fitting parameters of the Carreau model for the master curve at the reference temperature of 255°C are given in **Table 6.14** and illustrated in **Figure 6.41**.

Table 6.14. Carreau model parameters at reference temperature of 255°C

	Processing Parameters			
Grade(g3)	**C1**	**C2**	**C3**	**C4**
143-M3	1283.1	0.037	1.34	0.34

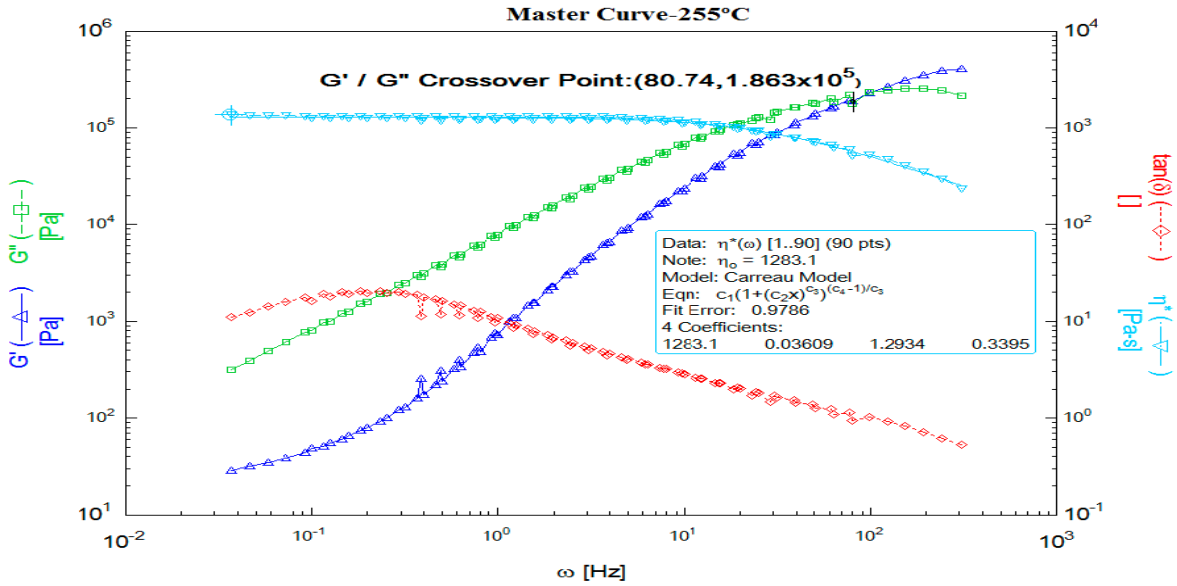

Figure 6.43. Master curve at reference 255°C w.r.t Hz

6.6 Effect of Processing Parameters on Dispersion

The objective here was to evaluate the influence of processing parameters on the dispersion quality of polycarbonate compounds. This information can be used to obtain a set of optimum processing conditions at which an extensive range of particles may be dispersed in the composition.

The information on pigment dispersion was obtained using digital optical microscopy (DOM). The purpose was to evaluate pigment dispersion in PC compositions by understanding the relation between processing conditions, particle size distribution, and the colour difference output. This will help in understanding dispersion issues that have bearing on colour variations for different PC compound grades.

Compounding pigments. Producing coloured compounds or masterbatches from pigments requires a good dispersion by wetting the pigment surface with the polymer, breaking up agglomerates, and separating pigment particles. The better the dispersion of pigment particles, the stronger the colour. To obtain good dispersion, compounders typically use twin-screw extruders, additives, and maintain the designated processing conditions.

The effect of processing parameters on dispersion of pigment in plastic was investigated. This study evaluates particle size distribution (PSD), and analyzes its relationship to processing parameters. To attain accurate results, various morphological techniques were used to evaluate the effects of processing parameters. The objective was to observe the existence of the agglomeration, and the shape and size of the particles in the specimen. The main focus was extended to establish a quantitative methodology that was developed through a combination of PSA, SEM, MCT scanner, and DOM observations to describe pigment dispersion in polycarbonate composites. This method included the evaluation of rheological properties and its effects on dispersion of pigments, which helps in reducing the colour differences and thus in reduced wastage. For each processing parameter, three samples were produced at three levels (GT) and moulded in to colour chips for the microscopy dispersion test. Colour chips were measured for their colour output properties and particle size distributions.

6.6.1 Effect of Temperature

6.6.1.1 Effect of Temperature on Colour Values

Figure 6.44, below, illustrates the effect of temperature on the colour difference (dE*) at 230, 255, and 280ºC, for the samples produced at 750 rpm and a feed rate of 25 kg/hr. It indicates a reduced value of colour difference as temperature increased. The best colour difference value (dE*) occurred at the higher temperatures (255 and 280ºC, with dE*=0.3). The target values (standard value) according to CIE (L*, a*, b*) were 68.5, 1.43, 15.7, respectively. The data at 230ºC presents the highest colour difference dE*. The negative colour values of dC*, da*, dl* and db* indicate that the green-blue hue originates from the incomplete dispersion of the pigments. At the highest examined temperature

(280ºC), dL* and da* were positive for a lighter and more red colour, respectively and db* was negative for a bluer hue. Note that dC* was always negative at the three examined temperatures, which is an indication for low chromaticity. The negative values of dC* and db* indicate that the chromaticity of the bluer hue originated from incomplete dispersion. In general, the total colour difference variation was decreased when temperature increased. According to these results, samples processed at 280ºC had better pigment dispersion than at 255ºC; both had better dispersion than those processed at 230ºC.

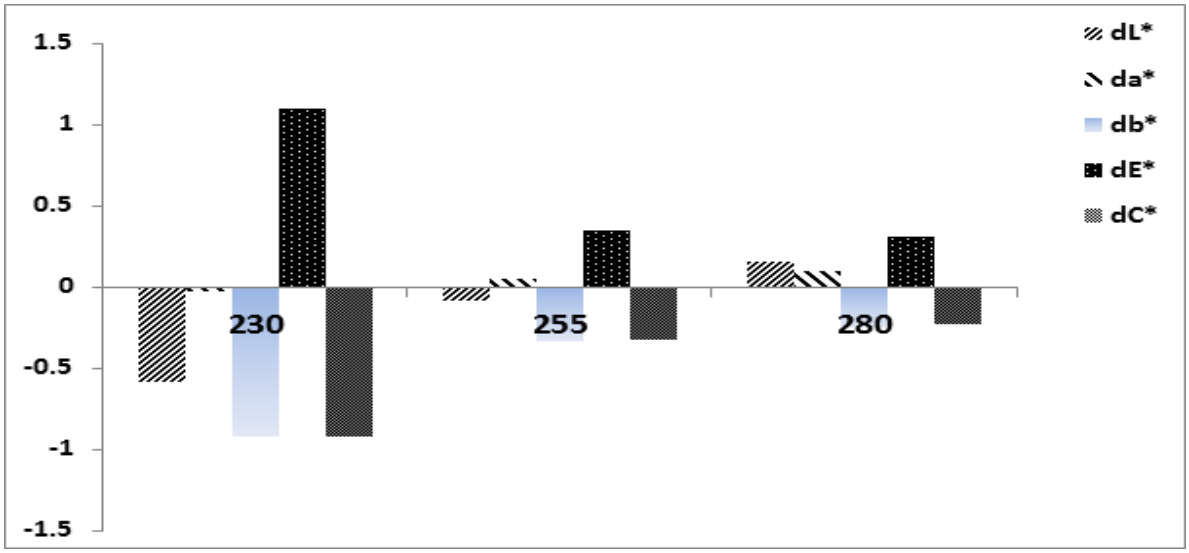

Figure 6.44. CIELAB colour differences for the samples produced at temperatures of 230, 255, and 280°C

6.6.1.2 Effect of Temperature on Pigment Size Distribution

Figure 6.45 illustrates the pigment size distribution at the three temperatures. In order to represent the pigment size distribution, a frequency histogram, wherein the x-axis represents the particle diameter size and the y-axis represents the relative amount of particles or the frequency. The data analysis showed that at the highest selected temperature of 280ºC, 55.3% of the particles were approximately 0.84 micron in size in comparison with 52.4% of particles having a size of 0.79 micron at 255°C, and 48.9% of particles having a size of 0.78 at 230°C. Again, differences in colour measurement in **Figure 6.44** are in good agreement with the particle size distribution in **Figure 6.45**. The results are shown at a higher peaks reveals the lowest colour difference.

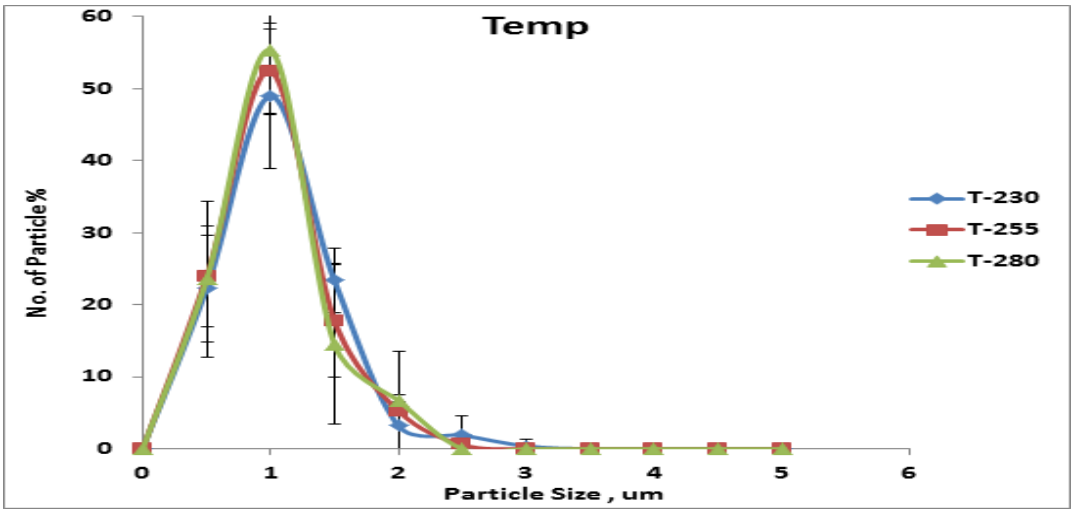

Figure 6.45. Pigment size distribution in the blends produced at the examined temperatures

Figure 6.44 illustrates the colour output in terms of DE (deviation from target) at the investigated temperatures. The DE was 0.3 at 280°C and 0.35 at 255°C, in comparison to 1.1 at 230°C. The results agree with **Figure 6.45**, which clearly shows a narrow peak in size distribution at 280°C, which drove the reduction in deviation from target due to better pigment dispersion.

6.6.2 Effect of Feed Rate

6.6.2.1 Effect of Feed Rate on Colour Values

Figure 6.46 illustrates the effect of feed rate on the colour values at a fixed speed of 750 rpm and temperature of 255°C. The colour values of dL* and db* showed minimum values at the central points, but da* increased with an increase in feed rate. The data represented at 20 kg/hr showed the highest colour difference in terms of dE*, db*, dl* and dC*. The higher dC* was due to the positive colour values of dl* and db*, which indicates that the light-yellow colour value was positive. Pigment particles in this sample showed incomplete dispersion and higher agglomerations than the other two samples. At a feed rate of 25 kg/hr, a positive value of da* was obtained. Increasing the feed rate to 30 kg/hr, resulted in a positive value for da* and dl*. This caused a slight reduction in the colour difference.

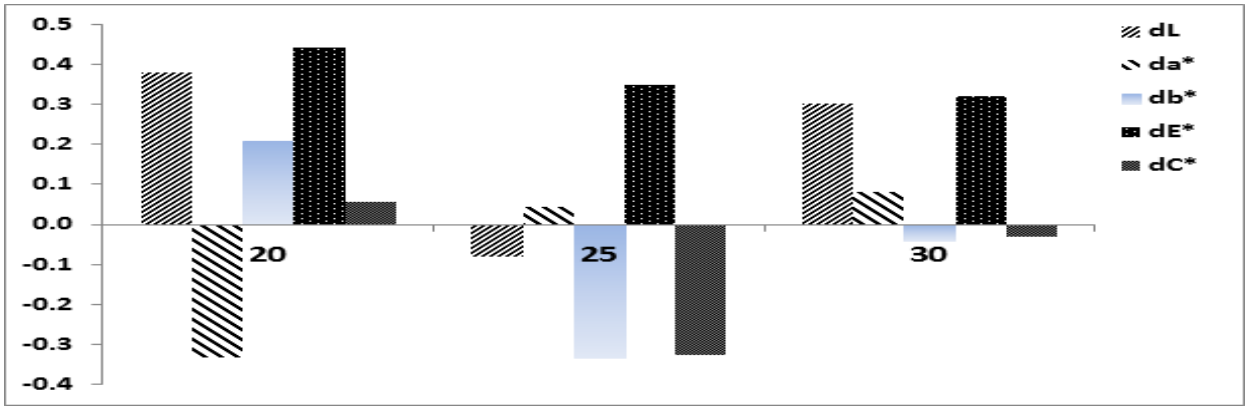

Figure 6.46. CIELAB Colour differences at various feed rates: 20, 25, and 30 kg/hr parameter samples

6.6.2.2 Effect of feed rate on Pigment size distribution

In general, the total colour differences decreased when the feed rate increased. The sample produced at a feed rate of 30 kg/hr revealed a better dispersion of pigments than the one produce with a feed rate of 25 kg/hr, which in turn showed a better dispersion than that produced with a feed rate of 20 kg/hr. **Figure 6.47** shows the pigment size distribution at the three feed rates. Data analysis showed that at the highest selected feed rate of 30 kg/hr, 53.8% of the particles were approximately 0.8 micron in size in comparison with 52.4% of particles having a size of 0.8 micron at 25 kg/hr, and 47.8% of particles having a size of 0.78 at 20 kg/hr. **Figure 6.46** illustrates the colour output in terms of DE (deviation from target) at the investigated feed rates. The DE is 0.32 at 30 kg/hr and 0.3466 at 25 kg/hr, in comparison to 0.44 at 20 kg/hr. The results agree with **Figure 6.47**, which clearly shows a narrow peak in size distribution at 30 kg/hr, which leads to a reduction in the deviation from target colour values.

Again, differences in colour measurement in **Figure 6.46** are in good agreement with the particle size distribution in **Figure 6.47**. The results shown at higher peaks reveal the lowest colour difference and the highest number of particles.

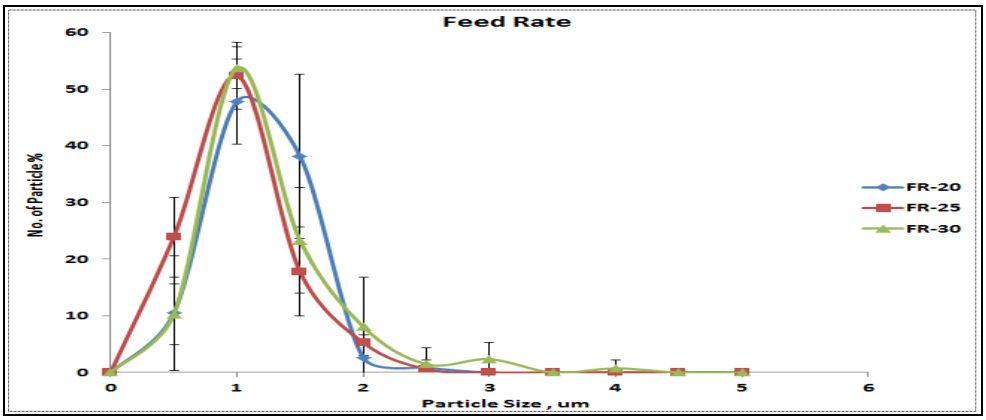

Figure 6.47. Pigment size distribution at the examined feed rates

6.6.3 Effect of Speed

6.6.3.1 Effect of Speed on Colour

Figure 6.48 illustrates the effect of screw speed (rpm) on colour values at a fixed feed rate of 25 kg/hr and a temperature of 255°C. Speed was increased from 700 rpm to 800 rpm. It was found that the colour values of dL* and db* were lower than the target values at the three levels except for da*, which was slightly positive at 750 rpm. Basically**,** this indicates that the red inorganic pigment was better dispersed at the middle speed level (750 rpm). The total colour difference dE* was the lowest at 750 rpm. The negative dC* and db* values indicate the chromaticity of a bluer hue originated from incomplete dispersion. Transparent polycarbonate plastics do not scatter light. In order to achieve a certain level of opacity, white pigment is normally added to create scattering; consequently, it affects the apparent colour strength. [36-38]

At the lowest speed of 700 rpm, the material was exposed to a lower shear heating or a lower shear rate. Agglomeration can, in principle, take place in the zones with a low shear. With increasing the speed to 750 rpm, deagglomeration was promoted in the zones with a high shear. Higher screw speeds can generate large shear forces and frictional heat states may arise and affect the heat stability of the pigment as well as damage other components of the polymer matrix; agglomeration of the broken particles is possible. High velocities raise material temperature; as a result, failures in colour appearance, physical properties, and degradation are possible.

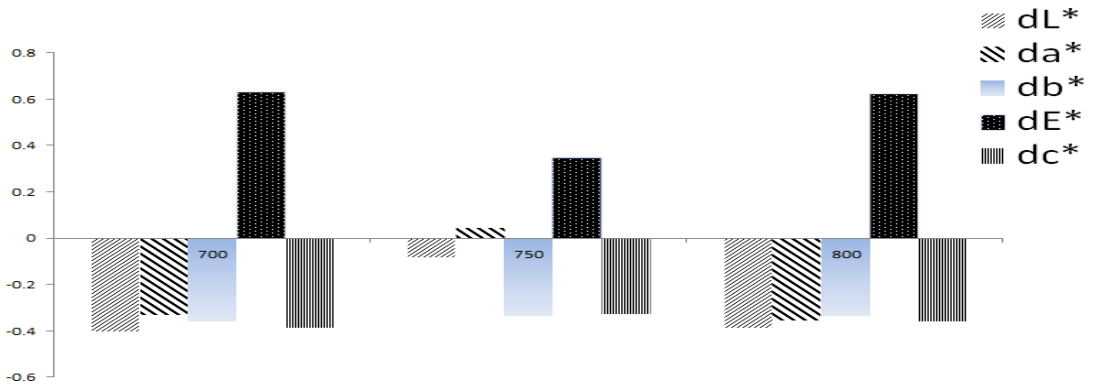

Figure 6.48. CIELAB colour differences for the samples processed at 700, 750, and 800 rpm

6.6.3.2 Effect of Speed on Pigment Size Distribution

As mentioned earlier, the lowest colour difference was obtained at the middle screw speed of 750 rpm. To correlate this with the pigment distribution, particle size and dispersion analysis were carried out as shown in **Figure 6.49**. The dispersions were characterized with DOM analysis in combination with images from SEM and the Micro-CT scanner. The analysis showed that at the middle speed of 750 rpm, 52.43% of the particles were approximately 0.79 micron in size in comparison with 42.8 % of particles having a size of 0.96 micron at 700 rpm, and 44.98% of particles having a size of 0.88 at 800 rpm. Again, differences in colour measurement in **Figure 6.48** are in good agreement with the particle size distribution in **Figure 6.49**. The results show higher peaks at 750 rpm, which is the level that yields the lowest colour difference. **Figure 6.48** illustrates the colour output in terms of DE (deviation from target) at the investigated screw speed. The DE is 0.62 at 800 rpm and 0.35 at 750 rpm, in comparison to 0.63 at 700 rpm. The results agree with **Figure 6.49**, which clearly shows a narrow peak in size distribution at 750 rpm, which leads to a decrease in deviation from target colour values.

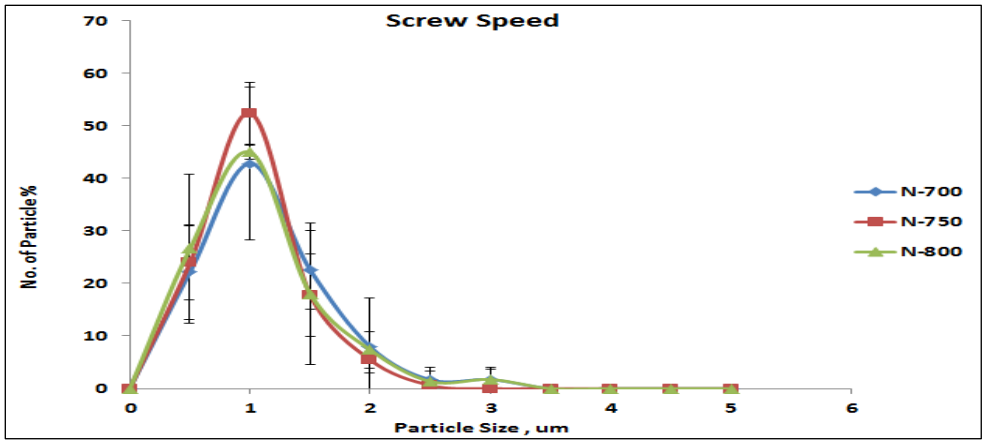

Figure 6.49. Pigment size distribution at the examined screw speeds

6.7 Morphological Dispersion Analysis

One of the objectives of this thesis work was to evaluate the pigment dispersion in the compounded plastics and to examine the relationship between the processing conditions, particle size distribution, morphology and the colour difference output.

6.7.1 Pigment size

A particle size analyzer was used to determine pigment size distribution. The results presented here show how to improve dispersion, reduce agglomerates, and thus, the size of pigment particles by increasing ultrasonic power and ultrasound time, and thereby the input energy. The particle sizes of the pigments were measured. The effect of ultrasound exposure time on particle size is illustrated in **Figure 6.50**. The time had a strong effect on particle size determination. By increasing time, the detected particle sizes were reduced. Although the effects vary for different pigments, given sufficient exposure, all pigment particle sizes approached the same size.

Figure 6.50 illustrates the average diameters of four "as received pigments" with the variation in ultrasound time. The average diameter of particles decreased to a value of 0.1 μm at 150 seconds except for black pigments, which decreased to a diameter of 4μm. The increase in ultrasound time increases the dwell time and induces more energy to de-agglomerate the particles.

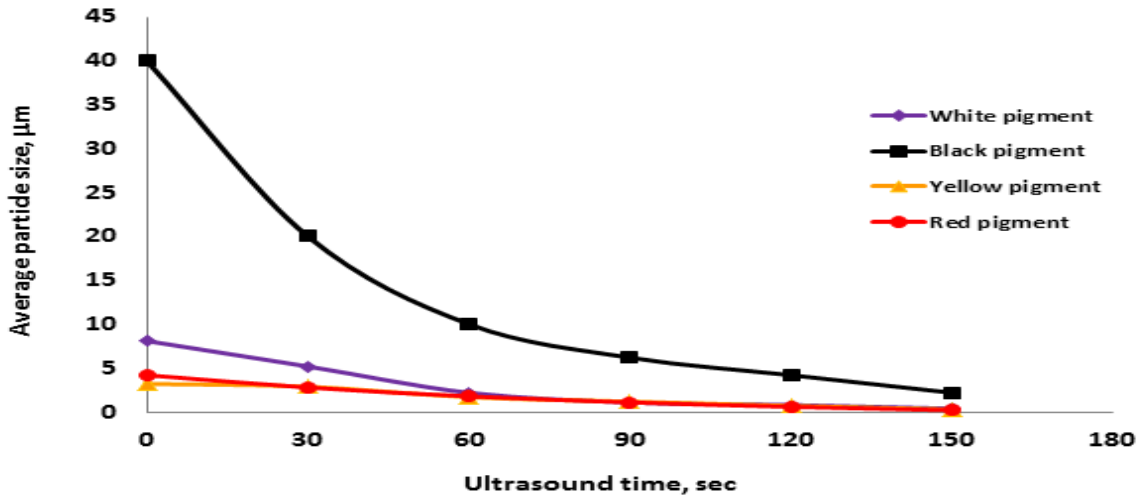

Figure 6.50. Average particle size for four pigments using wet analysis with varying ultrasound time at 30W

6.7.2 SEM Characterization

The results obtained from the particle analyzer (**Figure 6.50**) are quite comparable with the results of the SEM presented in **Figure 6.51** with respect to the primary particle size. The average particle diameter was between 100-200 nm.

The SEM micrograph, **Figure 6.51a**, depicts the presence of agglomerates in white pigments. It reveals the existence of primary particles that had a spherical shape in the vicinity of 0.1 µm in size. **Figure 6.51b** shows SEM pictures of yellow pigments. The figure shows agglomerates consisting of primary particles of elliptical or cylindrical shapes that had a diameter of approximately 0.1 µm. Similarly, agglomerates were found in black and red pigments (c, d) having primary particles in spherical shape with diameters of 10 µm and 0.1 µm.

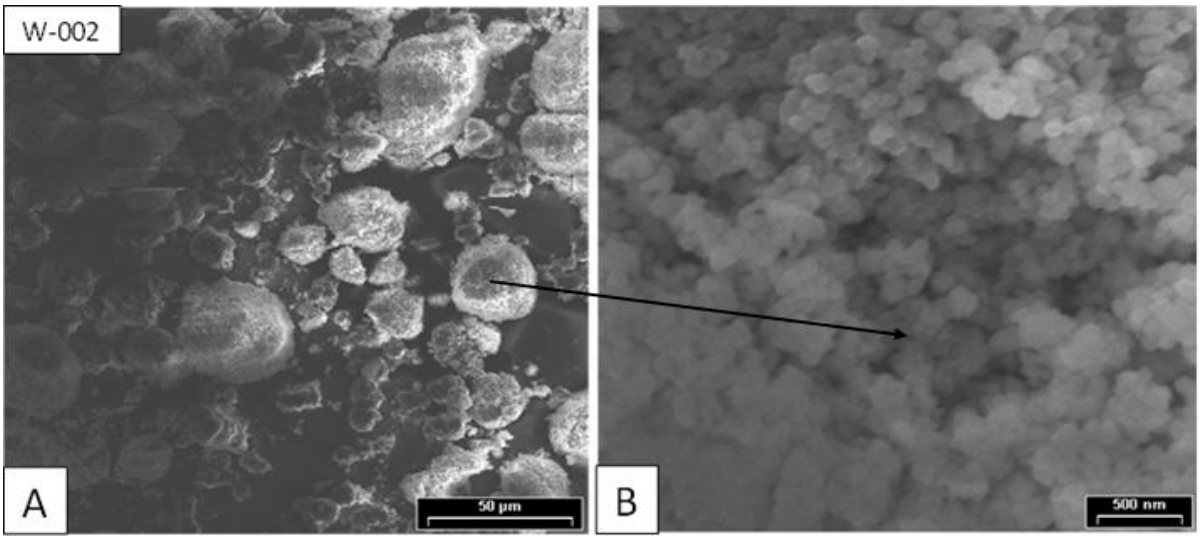

(a)

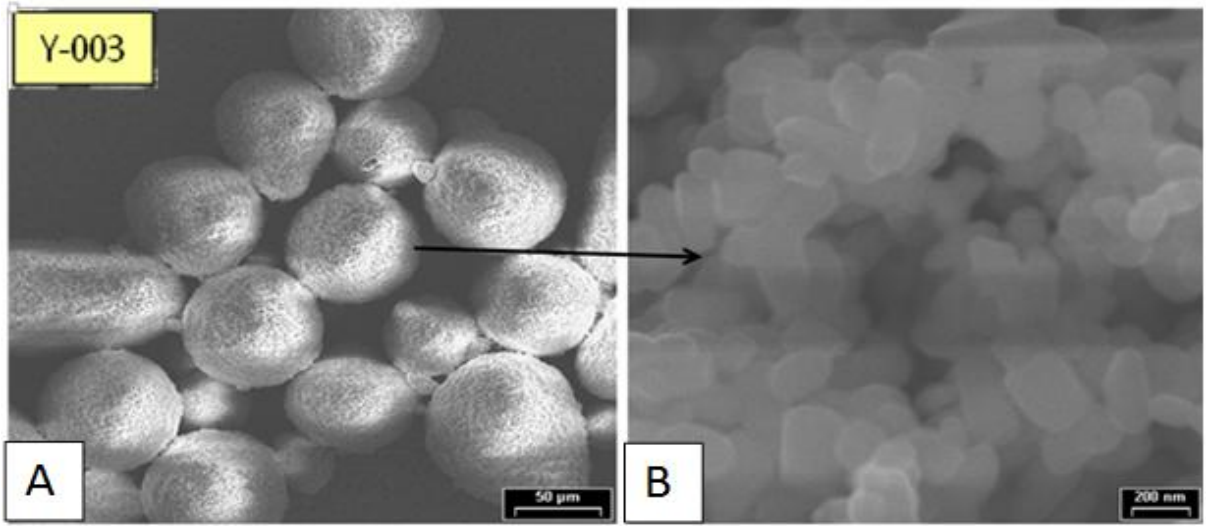

(b)

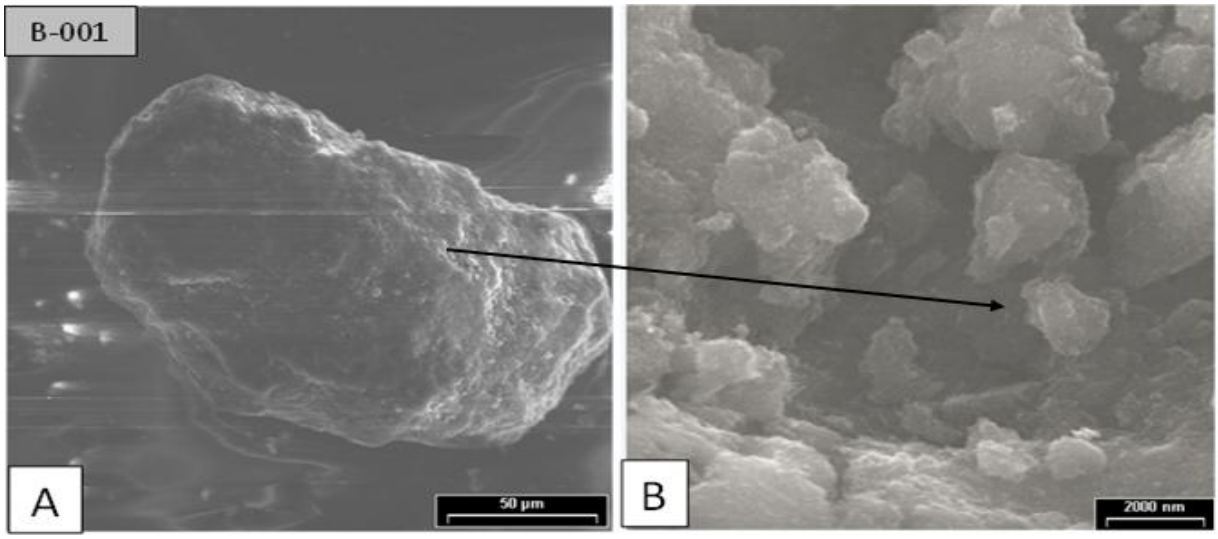

(c)

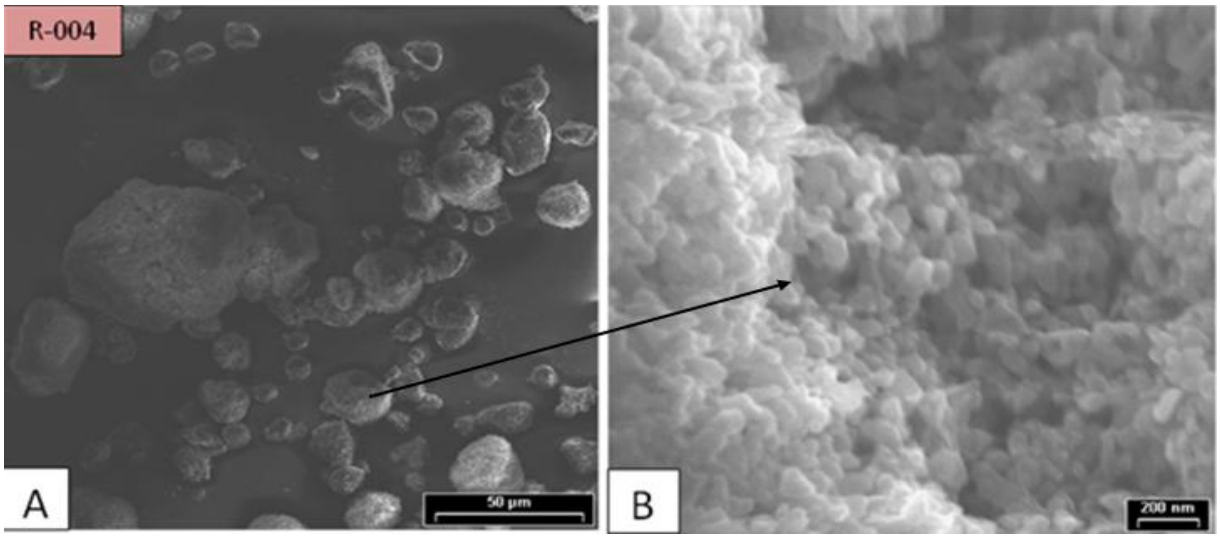

(d)

Figure 6.51. SEM micrograph of black (a), white (b), yellow (c), and red (d) pigments

6.7.3 Influence of Viscosity on Pigment Dispersion

One of the major parameters influencing the pigment dispersion is the viscosity of the (blend) matrix. For rapid pigment wetting, the viscosity should be low, whereas for rapid de-agglomeration the viscosity should be high. This indicates that, for optimum dispersion, there should be an intermediate and sufficient viscosity to promote both desired outcomes: dispersion and de-agglomeration. **Figure 6.52a** illustrates the micrograph of the blend (30/70 R1/R2) at 230°C (magnification of 1000X and 4000X), while **Figure 6.52b** presents the effect of temperature on the size distribution of pigments. Evaluation was based on the

degree of pigment dispersion in a hot pressing sample. With the increase of temperature, the peak of the distribution curve became narrower in terms of particle size, indicating that 50% of particles had a size of 0.8 microns at 280°C in comparison to 38% at 230°C.

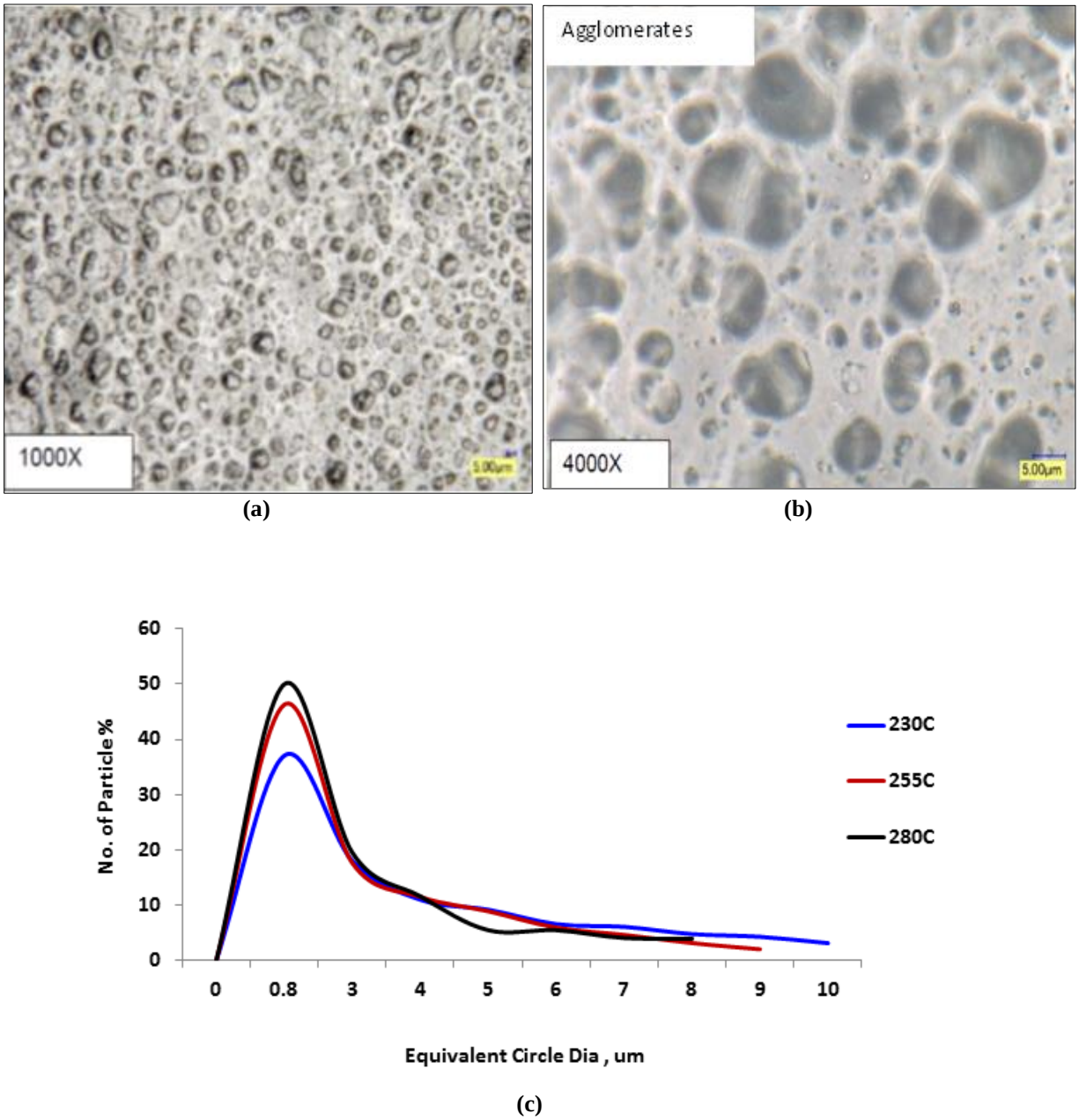

Figure 6.52. (a) Micrograph of the blend containing 30% by wt. of Resin R1, processed at 230°C (1000X and 4000X): agglomerates; (b) particle size distribution at the examined processing temperatures of 230, 255, and 280°C: hot pressed samples

Figure 6.41 (§6.5.2) illustrates the colour output in terms of DE (deviation from the target) at the investigated temperatures. The DE is 0.30 at 280°C and 0.34 at 255°C, in comparison to 1.1 at 230°C. It illustrates that the viscosity at 280°C and 230°C is quite adequate for wetting the particles. The reduction in viscosity and surface tension at the higher temperatures of 255°C and 280°C leads to enhanced wetting of pigments as compared to the wetting prevalent at 230°C, causing more de-agglomeration. This phenomenon can be explained by the Washburn Equation given by **Equation (6.1)**, below. [133]

$$\mathrm{I(t)} = \sqrt{\frac{\mathrm{C} \cdot \bar{r} \cdot \gamma_{\mathrm{L}} \cdot \cos\theta}{2 \cdot \eta}} \qquad \textbf{(6.1)}$$

$I(t)$, C, $\bar{r}$, γ_L, η, and θ represent the flow of the liquid, the pigment specific constant, the average pore radius of the agglomerate, the surface tension of the fluid, the dynamic viscosity of the fluid, and the contact angle between pigment and fluid, respectively.

The equation shows that the rate of pigment wetting depends on the viscosity and surface tension of the fluid. It also indicates that if the dwell time is too short, the pigment will not be sufficiently dispersed and if the dwell time is too long the material can be over-dispersed which results in decreasing gloss and increasing haze. The dispersion process requires an energy input and this energy is proportional to the surface tension. Due to the smaller surface tension, there will be a greater change in surface area for a given amount of dispersion energy. Lesser dispersion energy is needed for a lower surface tension and this is also beneficial for overcoming the cohesive forces between the primary particles of agglomerates. This means that, at 280°C and 255°C, the rotation speed rate (rpm) and the residence time in the extruder were enough to allow the shear forces to overcome the cohesive forces in order to break agglomerates to smaller particles. These results are also supported by **Figure 6.52**, which clearly shows that the highest peak of size distribution belonged to the blend processed at 280°C, which in turn led to a decrease in deviation from the target colour values, i.e. lower DE, as presented in **Figure 6.41** (§6.5). Moreover, the comparison of the peak height of the blends processed at the two temperatures of 255°C and 280°C reveals that a decrease in the particles size distribution peak by 4% changed the DE

value from 0.30 to 0.34. However, with respect to the re-agglomeration of particles, two phenomena are playing key roles: (1) the nature of the polymeric chain, namely that, if the chains are not sufficiently solvated, then they will collapse onto the pigment surface, and (2) the higher the interfacial tension the greater is the driving force for the solid to reduce its interfacial area. These two phenomena can promote re-agglomeration of particles to form flocculate. [134, 135] Nevertheless, incorporating additives plays a substantial role in stabilizing the particles in order to avoid flocculation as the size of particle decreases. Using additives can reduce the dispersion time by reducing the contact angle, as indicated in the Washburn Equation **(6.1)**, reduce the necessary energy input and prevent re-agglomeration during dispersion. The lower viscosity at 280°C improved the dispersion process by increasing wetting properties but also enhanced the stability of the pigment concentrate in the presence of stabilizer.

6.7.4 Effect of Processing Conditions on the Dispersion and Morphology of Pigments

Digital optical microscope (DOM) is the most common quick method used for measuring dispersion. The advantages are: an object can be observed from any angle, the operations are adaptable with the free angle and observation system, and it can support magnification up to 0.X to 5000X with a single unit.

A DOM was used to characterize the blends manufactured in this study. The processing parameters used for preparing the samples to scan the agglomerations were temperatures of 230, 255, 280°C; speeds of 700, 750, 800 rpm; and feed rates of 20, 25, 30 kg/min. When one processing parameter was being studied, the others were fixed at their midpoint level. A magnification of 5000X was used to detect particles. Evaluation was based on the degree of pigment dispersion in colour chip samples.

Figure 6.53 shows the pigment agglomerations for the blend processed at the following conditions: temperature of 230°C, feed rate of 20 kg/hr, screw speeds of 700 rpm, and 800 rpm (at the lowest levels of temperature and feed rate, and at the lowest and the highest screw speeds). The peak of the size distribution curve becomes narrow approximately

at the condition where lower output colour differences were observed. The approach shows a relationship between the number of particles and the colour difference at various temperatures, feed rates and screw speed.

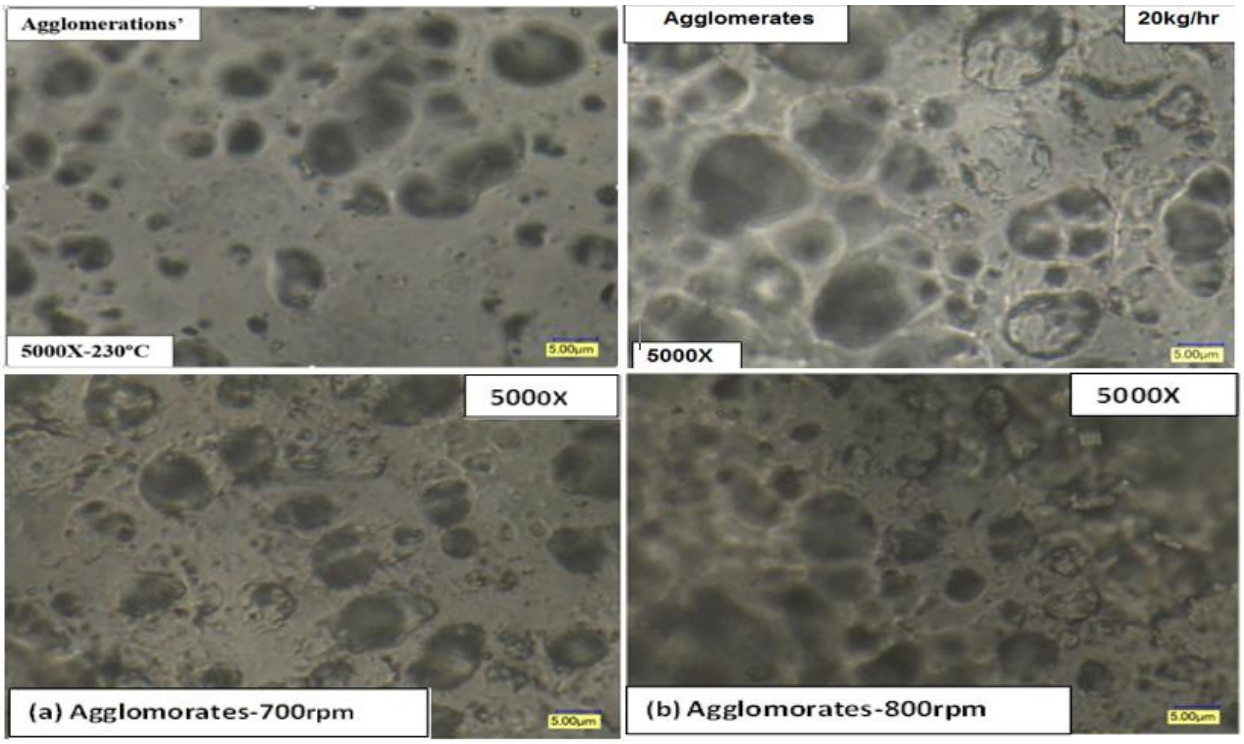

Figure 6.53. *(Clockwise from top left)* Micrograph at 5000X of the blend R1-30% at 230°C, 20 kg/hr, 700 rpm, and 800 rpm (colour chips)

As observed in the morphological micrographs, agglomeration of the pigment clearly occurred at a lower processing parameter, e.g. 230°C, 20kg/hr. Therefore, higher processing temperatures, e.g. 255 and 280°C, are employed to reduce the colour differences at a constant rate (0.3), increase pigment wetting, reduce or prevent pigment agglomeration, improve pigment dispersion, and reduce colour shifts. The pigment distribution and agglomeration are shown in morphological micrographs captured using different techniques. The morphology was examined by digital optical microscopy (DOM) and scanning electron microscopy (SEM). The optical microscopic graphs for the processing parameter samples are shown in **Figure 6.53** through **Figure 6.59**.

The degree of dispersion was enhanced at higher temperatures. For instance, dispersion at 255°C seemed to be somewhat better than that at 230°C. The micrographs in

Figure 6.54 show that at higher temperatures there is the less the evidence of agglomeration. **Figure 6.54** shows uniform particle dispersion by using a chip sample processed at 750 rpm and a microtome sample processed at 280ºC. **Figure 6.55** shows the agglomerations for the samples processed at (a) 700 rpm, (b) 800 rpm, (c) 230ºC, and (d) 30 kg/hr by using 50-micron chip samples, cut by a microtome.

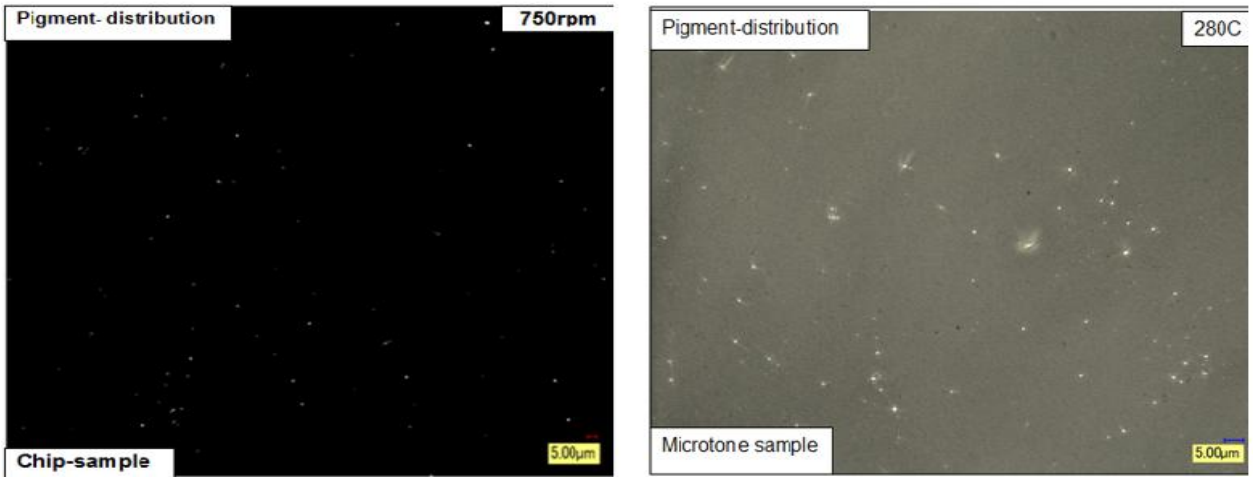

Figure 6.54. DOM-Particle distribution for chip sample processed at 750rpm *(left)*, and microtome sample processed at 280ºC *(right)*

The SEM and DOM micrographs show that more agglomerated pigments could be mostly observed at the lower range of processing parameters. A higher degree of dispersion is obtained at the higher levels of processing parameters, e.g. temperatures, and feed rate. The results also reveal that samples of the same grade that were processed differently exhibit different rates of dispersion under the same or different operating conditions (see **Figure 6.53** through **Figure 6.59**).

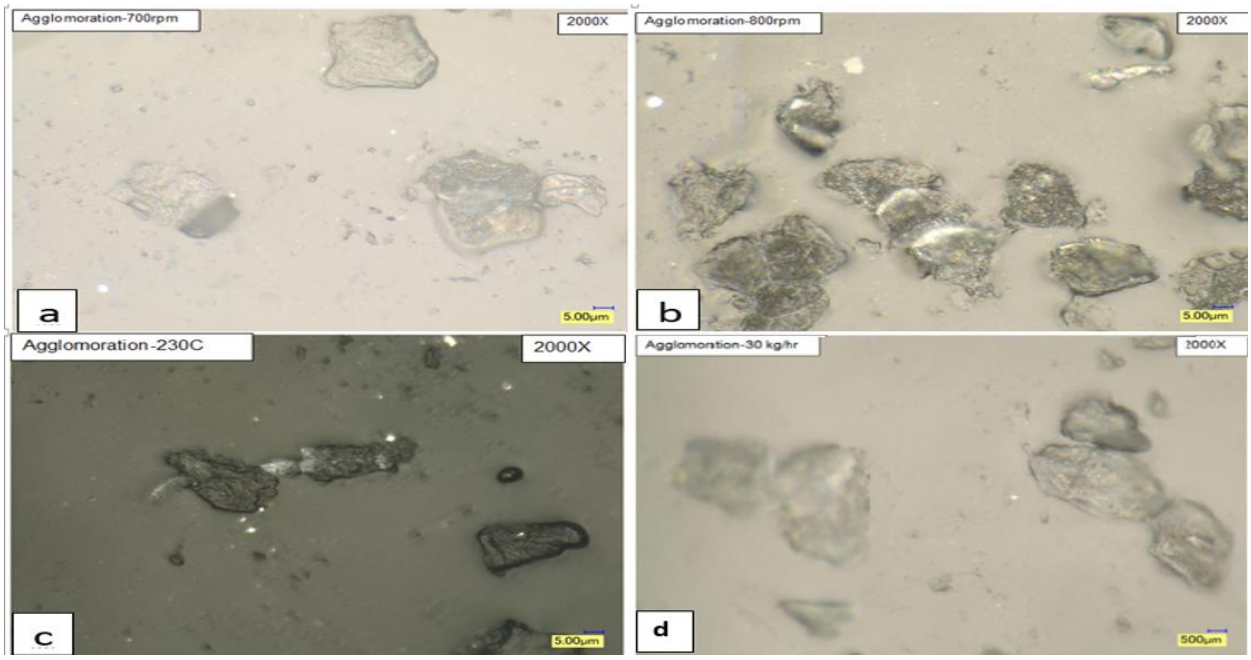

Figure 6.55. DOM-agglomerations for (a) 700rpm, (b) 800 rpm, (c) 230ºC, and (d) 30 kg/hr; samples magnified to 2000X, measured by 50-micron chip, and cut by microtome

Figure 6.56, **Figure 6.57**, and **Figure 6.58** illustrate the SEM micrograph of the compounded grade at varying temperature, feed rate, and speed processing parameters at a magnification range of 500X-3000X. The specimens used were from the 30%-R1 sample. Agglomeration of the pigment clearly occurred at lower processing parameters, e.g. 230°C. The total colour difference, dE*, increased at lower processing parameters and higher agglomerations than that of the sample, produced at higher parameters.

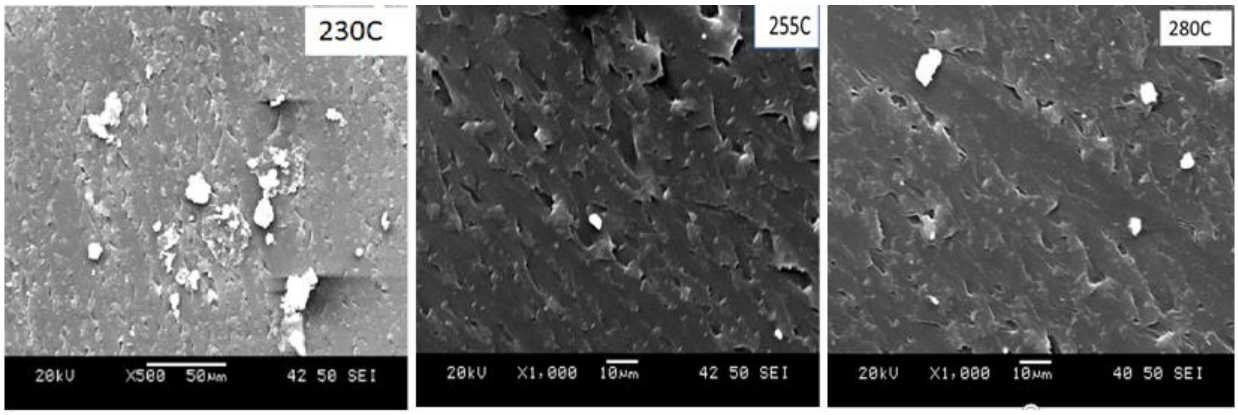

Figure 6.56. SEM micrograph of polycarbonate grade compound at 230, 255, and 280°C

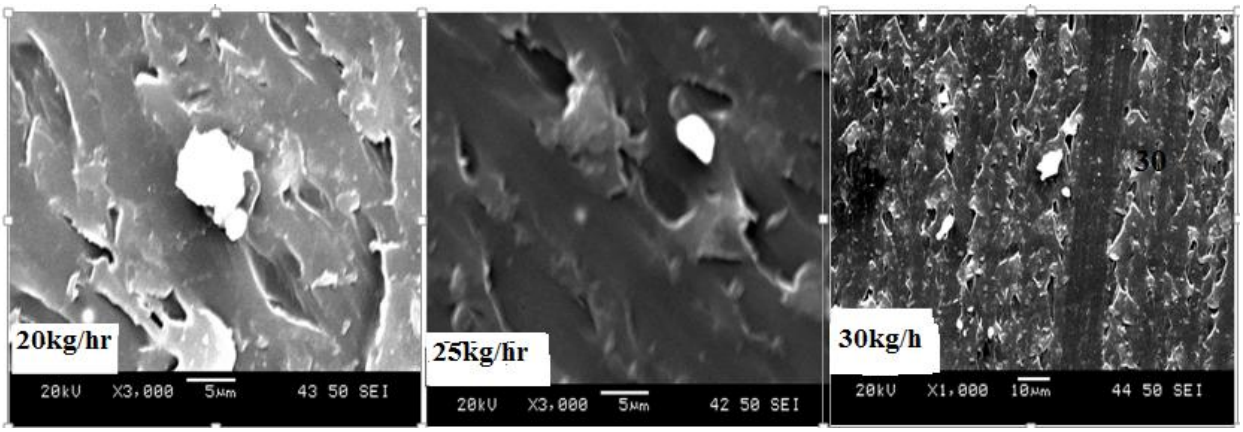

Figure 6.57. SEM micrograph of polycarbonate grade compound at 20, 25, and 30 kg/hr

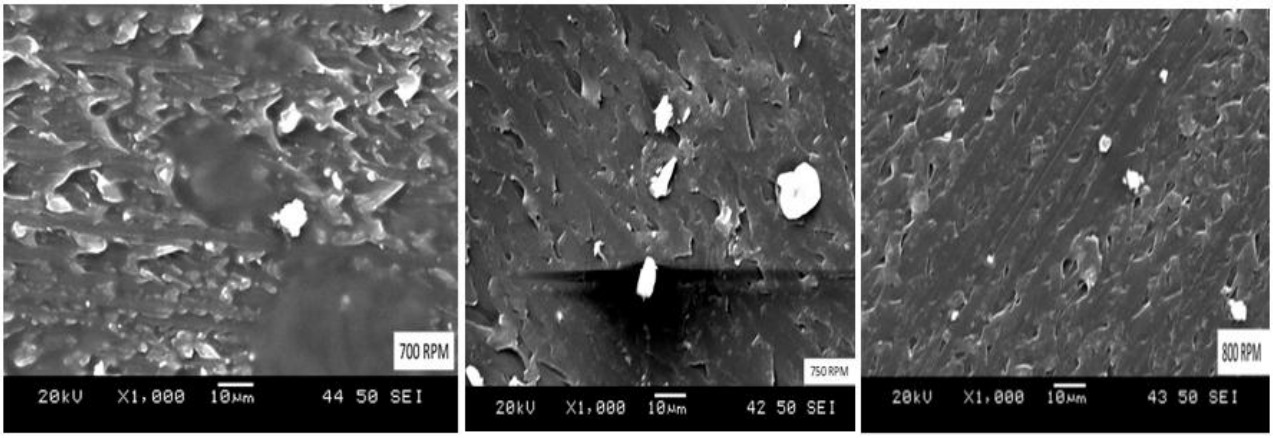

Figure 6.58. SEM micrograph of polycarbonate grade compound at 700, 750, and 800 rpm

Figure 6.59 shows the Micro CT scan of the pigment distribution in the blend processed at 750 rpm, 255°C and 25 kg/hr. **Figure 6.59a** and **Figure 6.59b** show agglomeration, a spherical particle shape, and **Figure 6.59c** and **Figure 6.59d** reveal a uniform pigment distribution. No significant changes were observed in dispersion, while a particular number of agglomerates existed at the various temperatures.

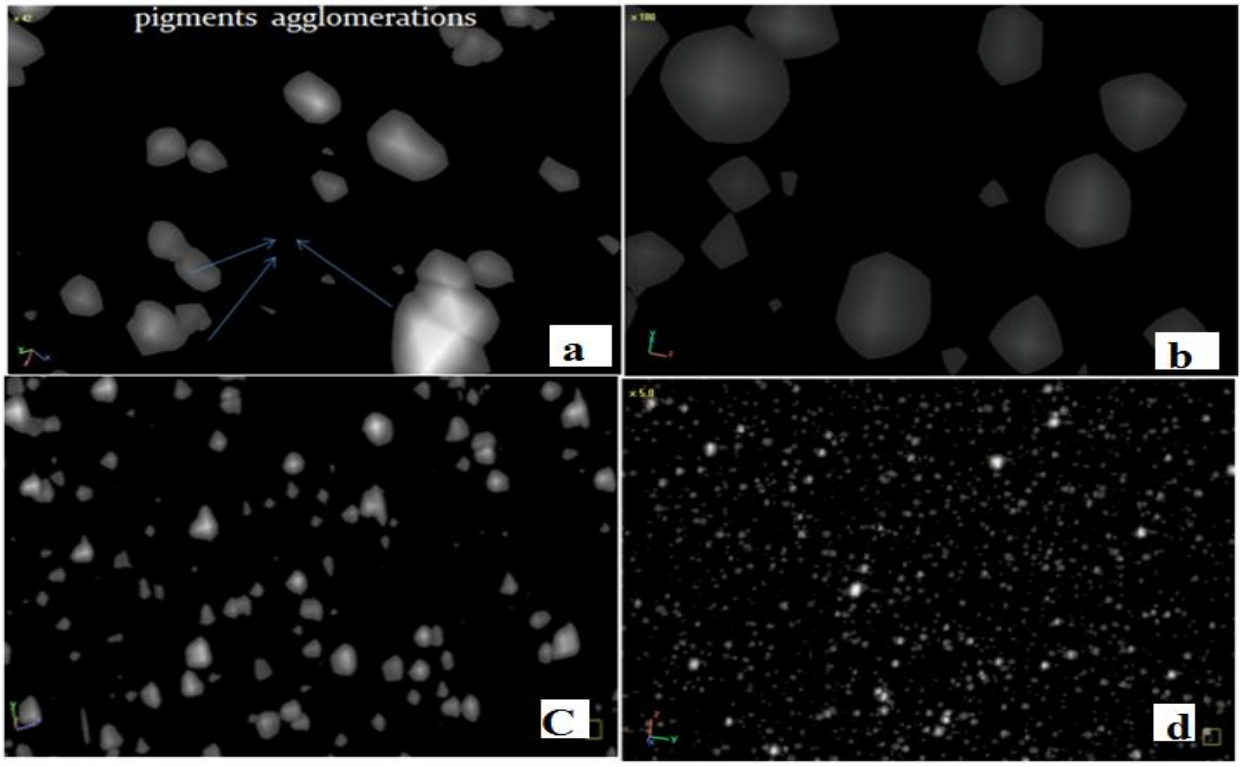

Figure 6.59. Micro CT scanner micrographs of the blend processed at 750 rpm, 255°C, and 25 kg/hr: (a) agglomerations, (b) particle shape, and (c, d) pigment distribution

6.8 Experimental Characterization of the Blends

Rheological properties are paramount to the development of screw configuration designs of extruders for the purpose of proper compounding of plastics. The objective of this part of the study was to investigate the rheological behaviour of the compounds. The blends were processed in two different co-rotating twin-screw extruders. The first was a twin thermo Haake Mini Lab II screw micro compounder (ML), and the second was a Coperion twin intermeshing co-rotating extruder (SB).

6.8.1 Complex viscosity

Comparison of rheological properties and thermal behaviours of the compounded PC formulation that contained 30 wt. % of resin R1 and 70 wt. % of resin R2 is shown in **Figure 6.60**, below. **Figure 6.60a** compares the blend compounded with and without additives and pigments, while **Figure 6.60b** compares the blends compounded by the two TSE types, ML

and SB. This would lead to understanding additional dispersion issues that have bearing on colour variations in different compounding processes.

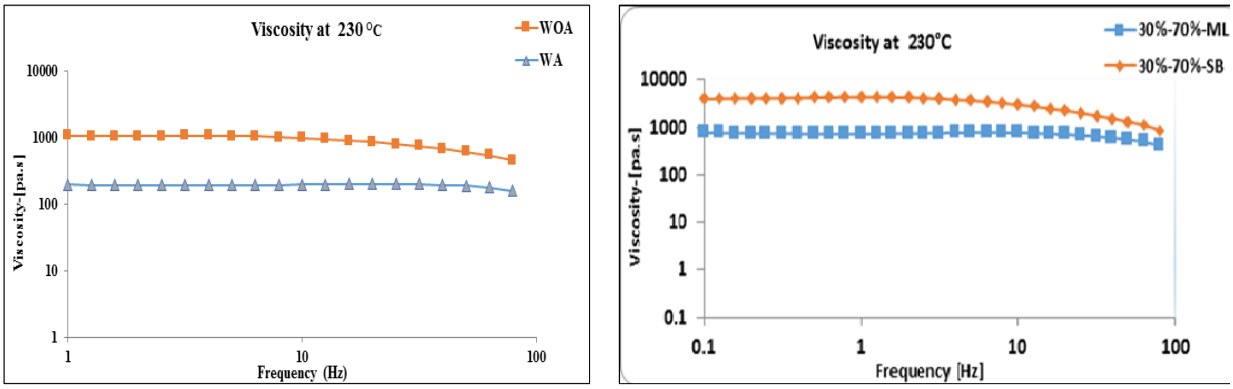

(a) **(b)**

Figure 6.60. Complex viscosity for the blends measured at a temperature of 230°C: (a) WOA vs. WA, and (b) ML vs. SB

Figure 6.60 shows the results of complex viscosity measurements at the above mentioned conditions. **Figure 6.60a** indicates that the compounded plastic with additives (WA) exhibited a lower viscosity than the compound without them (WOA). This is likely due to the material being blended with additives and pigments. It would explain how different additives could be used to alter materials processing properties, such as colourants, stabilizers, and flame retardants. The sum of the effect of the additives and pigments is that they can react and soften the polymer, thereby reducing viscosity, accelerating pigment wetting, and improving the colour of polymer blends.

From earlier studies, there are many variables that can affect the viscosity in plastic parts: base material type, colourant type, particle size, material thickness, and more importantly, processing conditions of extruders as have been shown in **Figure 6.60b**. The materials processed on the SB extruder showed a higher viscosity than the one processed by the ML extruder. This could be due to the configuration and design of the SB extruder, which had a higher L/D ratio, higher speed, higher feed rate, and higher delta pressure. In addition, the SB blending was processed with a super floater blender, and premixing was conducted with the twin co-rotating extruder and the pressing process of the hydraulic clamps of the injection-molding machine. Therefore, there are more parameters that may have contributed

to the higher viscosity output of SB because of the small size and spherical shape of pigments observed in the samples it produced.

Screw design represents an important factor in the compounding stage of colouring plastics in extrusion and molding machines. It governs the quality of mixing, creating pressure differences, generates frictional heat to melt plastic resin, and conveys the molten material through the die channels. The use of intermeshing screws besides the L/D ratio, is an important practice in mixing a composite, where a high ratio of L/D means a good mixing and ability of the screw to melt the resin in a high shear rate field. The depth of screw flight impacts the experienced shear rates by the blend. In the dispersion process, it is necessary to de-aggregate and de-agglomerate the pigment particles. In this stage, the cohesive forces inside the agglomerates have to be overcome and achieve a homogenous pigment distribution and dispersion. One of the major parameters influencing pigment dispersion is the viscosity of the blend. For rapid pigment wetting, the viscosity should be low, whereas for rapid de-agglomeration the viscosity should be high; thus, a trade-off is inevitable.

6.8.2 Viscosity and Particle Size Distribution

Figure 6.61 shows the viscosity and particle size distribution PSD measurements for the blends processed in Minilab (ML) and SABIC (SB). The blend processed in ML show a lower viscosity than the one processed in SB. For the ML blend, a larger number of particles (69%) had a small particle size, compared to 50% for SB. This could be attributed to the lower viscosity of the melt, which caused greater wetting, leading to the molecular bonds to break to produce a larger number of particles. Presence of additives, blending, extrusion and injection molding, high pressure, shear rate and shear heat could also cause the particles to break into smaller sizes. The compounds produced with SB showed a higher viscosity, which could be due to the smaller particle size distributed in the resin matrix. The most favourable result in terms of colour was achieved when the blend exhibited a higher viscous behaviour. Smaller particle sizes present a higher total surface area and thus give rise to a higher viscosity; therefore, a higher shear heating would not affect the colour mismatch and degradation.

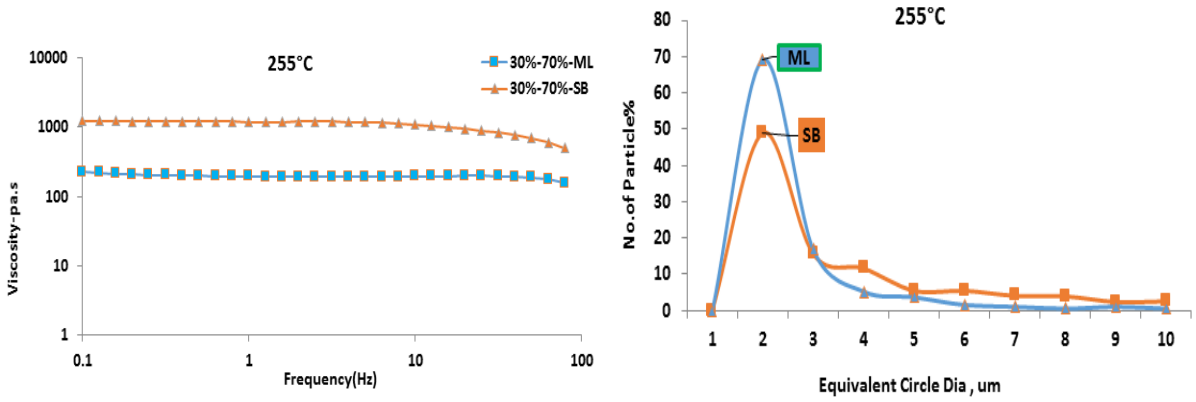

(a) **(b)**

Figure 6.61. Viscosity (a) and particle size distribution (b) for the blends processed in two different extruders (ML and SB) at a temperature of 255°C

6.8.3 Experimental Viscosity Models: Effect of Process

Figure 6.62 shows that those blends which include additives (WA) showed lower viscosity than those without additives (WOA). It also indicates that the blends processed with ML show a lower viscosity than those processed in SB. According to the empirical Cox-Merz rule, ($\eta(\dot{\gamma}) = \eta^*(\omega)$), for polymer melts, the absolute value of the complex viscosity, $\eta^*(\omega)$, at an angular frequency, ω, matches the shear viscosity, $\eta(\dot{\gamma})$, at the same value of shear rate, $\dot{\gamma}$.

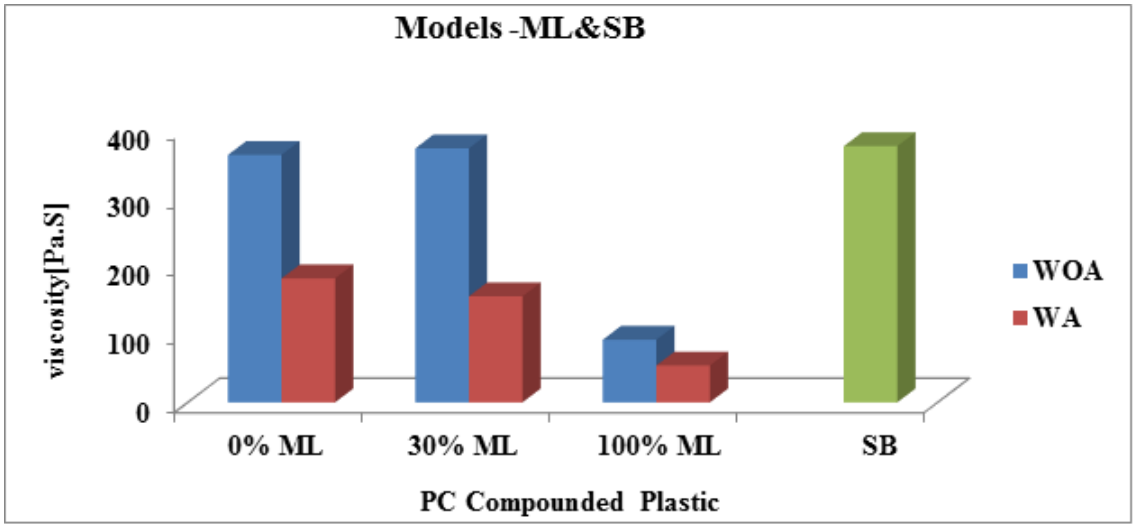

Figure 6.62. Experimental viscosity models WOA (ML) and WA (SB)

The agreement between the steady viscosity and complex viscosity was shown to be very good for each extrusion process. **Figure 6.63** presents the results for the blends containing 30 wt. % of resin R1 processed at temperatures of 230, 255, and 280°C. The constant regime of complex viscosity coincided with that of shear viscosity.

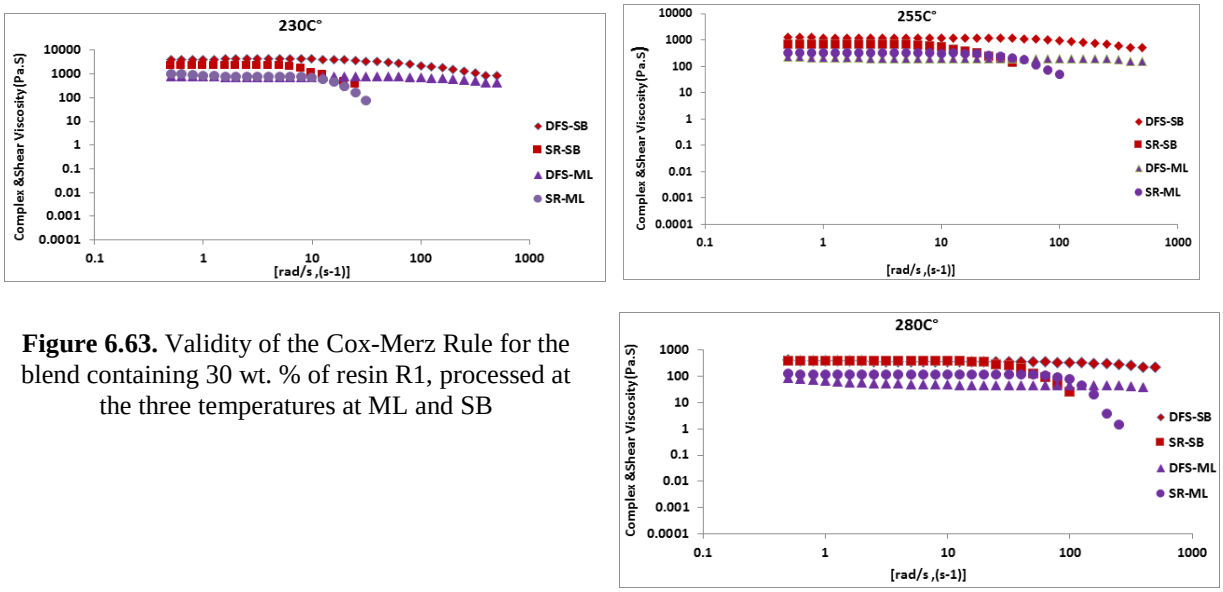

Figure 6.63. Validity of the Cox-Merz Rule for the blend containing 30 wt. % of resin R1, processed at the three temperatures at ML and SB

Note that, in **Figure 6.63**, DFS stands for Dynamic Frequency Sweep and SR stands for Steady Shear Rate.

6.8.4 Evaluation of Pigment Dispersion

Table 6.15 shows output colour results of grade g3 when compounded with different processing parameters. The optimal processing temperature to minimize the colour deviation was 280°C when speed and feed rate were fixed at their midpoint levels. Similarly, feed rate was 30 kg/hr, with a constant speed (750 rpm) and temperature (255°C). Lastly, the focus extended to the recommended processing speeds of 750 rpm with a constant feed rate (25 kg/hr) and temperature (255°C).

Table 6.15. Effect of processing parameters on colour in terms of tristimulus values

	Parameter Levels						
Parameter not held constant	**°C**	**kg/hr**	**rpm**	**L***	**a***	**b***	**dE***
Temperature (°C)	230	25	750	67.913	1.396	14.763	1.096
	255	25	750	68.423	1.473	15.353	0.346
	280	25	750	68.655	1.523	15.443	0.303
Feed Rate (kg/hr)	255	20	750	68.886	1.396	15.90	0.44
	255	25	750	68.423	1.473	15.353	0.346
	255	30	750	68.803	1.51	15.64	0.320
Screw Speed (rpm)	255	25	700	68.096	1.1	15.32	0.633
	255	25	750	68.423	1.473	15.35	0.347
	255	25	800	68.116	1.073	15.35	0.623

Particle size of pigments is significantly important in determining the minimum deviation from the target colour value due to its scattering efficiency, and other optical properties. **Figure 6.64a-c** show the particle size distribution studied using DOM from the specimens of plastic that were microtomed. The thin slices were characterized at the three processing parameters discussed earlier. Scattering efficiency increased rapidly as the average particle size decreased to approximately 0.2 micron and the optimal number of particles was increased at higher processing conditions. The percent of particles of optimal size at the optimum temperature was 35.75933%.

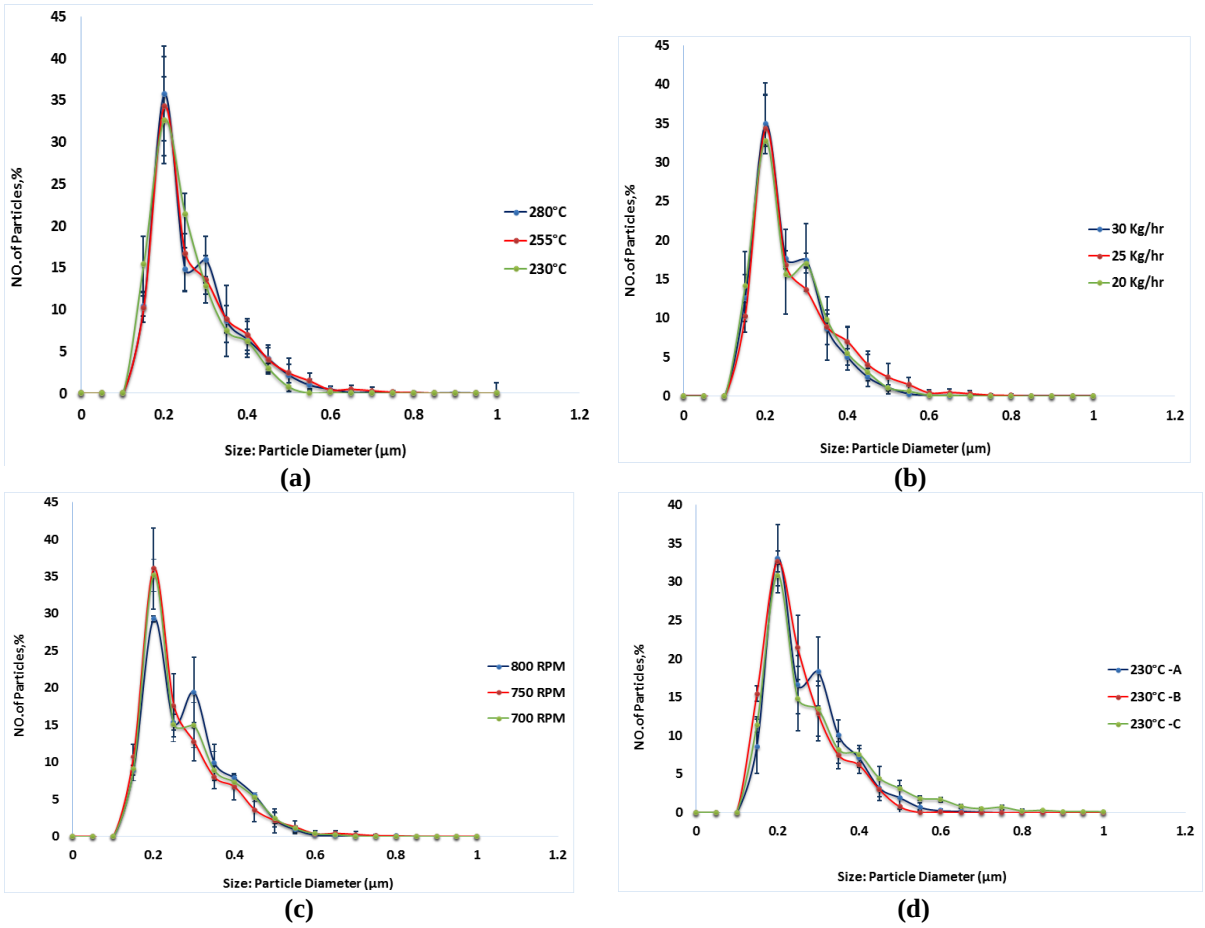

Figure 6.64. Particle diameter distribution for (a) temperature, (b) feed rate, (c) speed, and (d) for 230°C temperature layers at thickness A (90 µm), B (70 µm), and C (50 µm)

The narrower distribution of the particle sizes around 0.2 um at higher temperatures (**Figure 6.64a**) and feed rates (**Figure 6.64b**) can be explained by the lower viscosity of the compound at the conditions of 280°C and 30 kg/hr, which led to a lowered viscosity. A lower viscosity of the compound would facilitate greater ingress of the polycarbonate melt through capillary-like passages in between the particles forming the agglomerates, by virtue of the phenomenon described by the Washburn equation, thereby promoting agglomerate breakup and particle dispersion. In contrast, higher screw speeds (**Figure 6.64c**) resulted in greater average particle size and a broader particle distribution, with the greatest effects observed at the highest screw speeds of 800 rpm. Polycarbonate, being susceptible to the phenomena of shear-thinning, can undergo a rapid decrease in viscosity with increasing shear rates. A drastic reduction is viscosity would reduce the generated shear stress and the associated

frictional forces at the particle-polymer interface that are required for particle agglomeration break-up. Thus, the observed effect would be larger particle sizes as well as broader distributions as the agglomerate breakup is not optimal.

Chapter 7: Conclusions and Recommendations

Plastic systems offer a promising alternative to traditional material systems. This research offers essential insights into compounded plastics and provides a more realistic approach for colour matching.

A number of experiments and approaches have been presented. All, however, centre on the effect of processing conditions during the plastic compounding process on colour output. The following sections highlight key findings, recommendations, and contributions.

7.1 Key Findings

7.1.1 Data Mining

It has been demonstrated that data mining can be affectively used for identifying many problems that lead to colour deviations. These can include problems with formulation, material and processing parameters, the equipment being used, and the personnel handling the various aspects of production. Although an enormous amount of data was available, some of it was not reliable such as most of the processing pressure gages were out of calibration and the pressure data was useless. Similarly, there was no mechanism for inspecting incoming pigment batches or keeping track of their usage in individual products. The key aspect in using data mining for colour management is collecting and maintaining an efficient production data base system. The more detailed and reliable the database, the more robust the problem identification process will be. With the limited data made available, we were able to successfully identify many issues.

7.1.2 Use of Artificial Neural Network for Prediction of Colour Outputs

This study demonstrates that artificial neural network modeling can be applied to obtain models that can be used to predict the performance of the plastic compounding process. The output parameters L*, a*, and b* were determined through the use of an ANN

with more than 60 inputs. The neural network model predicts the performance to within an RMSE value smaller than 0.225, a regression coefficient value under 1, and a mean error smaller than 0.25%.

The obtained results confirmed the accuracy of the ANN procedure as a powerful tool that can be used to both predict and optimize colour properties. Furthermore, the large amount of available information of polymers colours can be effectively used for improving the compounding process.

7.1.3 Effect of Processing Parameters on Colour

The effects of processing parameters on the colour outputs of different grades were studied and statistical analysis was performed to determine the correlations between the inputs and the outputs. These included experiments for determining general trends (GT) and response surface methods (RSM) based on design of experiments (DOE). Within DOE, 3-level full factorial designs and the Box-Behnken design (BBD) were used.

In all cases, predictive models were developed for colour outcomes and optimum processing conditions/windows were determined. It was found that different grades responded differently in terms of the desired colour output under same or similar operating conditions. SABIC IP deals with a very large number of products; in fact, the majority of their products are produced only once, and hence, this methodology is of limited use.

Therefore, focus was shifted to understanding the fundamental factors that result in colour deviations. Due to the large number of products, this is an extremely challenging task. For this thesis, one specific grade was selected for investigation. A number of such studies focused on widely differing grades can potentially lead to a sufficient understanding that can lead to the development of comprehensive predictive models.

7.1.4 Rheological Studies

Rheological behaviour of the selected grade was studied in detail. The grade is a blend of two different resins; therefore, it was also decided to study the changes in its

behaviour with changing proportions of the resins in the blend. For this, 11 batches were prepared in which the proportion of one resin was increased in steps of 10%.

The material was shown to follow the Cox-Merz rule. This study also generated parameters that could be used with the Carreau model for predicting the viscosity of the blend. This enabled us to understand the dependence of wetting, de-agglomeration, dispersion, and the consequential colour shifts of polymer blends on viscosity.

7.1.5 Dispersion of Colour Pigments

Dispersion and distribution of pigments are essential for obtaining a stable and uniform colour. These are dependent on material properties and processing conditions. The specimens from the experiments were subjected to morphological studies and analysis to observe pigment dispersion and correlate it with colour outcomes. These studies were carried out using DOM and SEM.

Key findings from these studies are summarised below.

- It was found that at higher feed rates, higher temperatures, and at the centre level of speed, smaller sized particles with better dispersion were observed.
- Scattering efficiency increased rapidly as the average particle size decreased to approximately 0.2 µm and the optimal number of particles increased. It was also observed that agglomeration occurred in zones of large pigment size.

7.1.6 Particle Size Distribution

The particle size of pigments was important in determining the minimum deviation from the target colour due to scattering efficiency and other optical properties. The particle size analyzer (PSA) was used in the wet test to study pigment dispersion after application of ultrasonic power. It was found that raw pigment sizes were broken into smaller sizes, and were reduced to 0.1-0.2 µm (particle diameter) depending upon the power and the duration of its application. Thin slices of injection-molded chips were also imaged with SEM. These also

recorded an average particle size of 0.2 μm. The obtained measurements were from specimens that exhibited the minimum colour difference.

7.2 Recommendations

Based on the results of the studies carried out in this project, further research is recommended to improve understanding of the scientific and engineering characteristics of compounding plastic and to help develop various aspects relating to the characteristics and appearance of colours. These are summarized below.

1. It is recommended to perform experimentation on additional materials, e.g. different brands of SABIC polycarbonate such as Bayer and Makrolon, and colourants with designed processing parameters to explore more possible colour mismatch trends. The compounding processing conditions for these polycarbonate brands may differ from those of standard Lexan polycarbonate brands.

2. It is not trivial for a commercial compounder to carry out research work as it takes a lot of resources out from the regular production process. Therefore, for a future experimental design (DOE), it is suggested to reduce the number of runs. An eight-run selection is the most practical and generally applicable instead of the 17 runs of the general factorial design, thereby reducing experimental cost and operating time.

3. Possible processing factors that were not included but may have an impact should be studied, e.g. residence time, screw configuration, load, and cooling temperature.

4. The conducted research tools of the translucent grade (g3) can be applied as an advanced grade colour model tool to develop other compounded grades based on the results of rheological behaviour and the correlation of viscosity data with colour. Additional experiments and simulations can help improve our understanding of colour compounding. The Carreau viscosity model results for (WOA and WA) ML and SB) can be applied for further investigation of other grade grades. The subsequent viscosity models could be used to predict an optimal set of processing parameters specific to the plastic grade.

5. The crossover point indicates a physical gel formation caused by a combination of entanglement and interactions. Further investigation into the physical gel formation may provide an alternative way to determine the degree of dispersion of the pigments in the polycarbonate blend composition. In addition, further investigation into the significance of the crossover point as an indication of dispersion can be performed, particularly by selecting different ranges of temperatures used in the compounding of materials.

7.3 Contributions

The key contributions of this research were presented at conferences. Approximately 21 articles, mainly related to plastics colouration, were published in international journals and conference proceedings, including:

- Three papers on the initial phase of data mining and statistical analysis were published in IEEE, SPE-Antec, and Journal of Information Technology. The analysis identified batches that had colour mismatches and formed the basis for much of the remainder of the research in this thesis. [28-30]

- On the specific topic of artificial neural network (ANN), two journal papers were published in the journal Advanced Polymer Technology, and one conference paper was published in annual international conference, PPS-29. The degree of accuracy of the artificial neural network (ANN) was plausible and showed promise for use in prediction modelling. [33, 54, 136]

- Over 15 articles, mainly related to plastics colouration, were published in international journals and conference proceedings: Advanced Polymer Technology [33, 54], Quality Engineering [127, 137], Polymer Engineering of Science (PES) [84], and conferences SPE-Antec [123, 124, 126, 137-141], International Conference of the Polymer Processing Society (PPS) [142, 143], the Annual Technical Conference of the Society of Plastics Engineers (ANTEC), Dubai, UAE, and the UOIT 3rd Annual Graduate Student Research Conference. [144, 145] These papers covered a wide range of experimental design

techniques to investigate the effect of process parameters on the colour deviation from the target colour output (dE*).

- A journal paper was published in Polymer Engineering of Science. This paper focused on the rheological characterization of polycarbonate blends. Two different twin-screw extruders were used on various polycarbonate blends, both with and without additives and pigments. The effect on the polycarbonate's viscosity as well as the colour output was measured under a number of conditions using a rheometer. [84]

- The above paper also centred on understanding pigment dispersion in polycarbonates as well as polycarbonate morphology. The paper leveraged work from some of the aforementioned papers in that the same compounding process parameters were controlled. Information about pigment dispersion was gathered from a number of sources, including PSA, DOM, and SEM. [84]

References

1. Henderson, J., Ball, A. and Zhang, J., *Cycle Time Reduction for Optimization Of Injection Molding Machine Parameters for Process Improvement.* in Western Carolina University, Cullowhee, North Carolina, 28723 Proceedings IJME – Intertech Conference., 2006.

2. Lewis, P.A., *Organic Colorants*, in *Coloring of Plastics, Fundamentals*, R. Charvat, Editor. 2004.

3. Markarian, J., *North American compounders seek growth in innovation ,Plastics Additives & Compounding,VOL(8),PAGE (42-45),2006.*

4. Markarian, J., *US compounding industry faces challenging times.* Plastics Additives & Compounding,10(6): p. 38-41, 2008.

5. Billmeyer.F , S.M., *Principles of color Technology*. 2nd Edition ed. 1981.

6. *Coloring of Plastics*. edited by charvat,Robert ed. Color as a Science. New jersey, 2004.

7. SABIC. *Scattering, Absorption/Opacity, Transparency and Translucency*. Internal Scattering [cited 2014 March 19]; Available from: https://**WWW.SABIC-IP.COM/STATICCXP/USER/IMAGES/LEARNABOUTCOLOR/TRANSPARENCY_AND_TRANSLUCENCY_1.JPG**.

8. Charvat, R.A., *Coloring of Plastics, 2nd edition*. Wiley 2004.

9. Callister , W.D., Jr., *Materials Science and Engineering: An Introduction*. 7th ed ed. The spectrum of electromagnetic radiation,, ed. I. Copyright © 2007 John Wiley & Sons. USA: John Wiley & Sons. Page 116, 2007.

10. Mathew, W.H., .J, *Color as a Science*, in *Coloring of Plastics*, R. Charvat, Editor. 2004.

11. Mulholland , B., *Color and appearance* Color and appearance **24**(2): p. 4-5, 1993.

12. Chong.T.F. *reproducibility of Color difference Measurements on Textile samples*. in *American Association of Textile Chemist&Colorists&Colorists International Conference,Page.323-332*. Montreal,Canada, 1993.

13. Rich, D.C., *Colorimetry, Color Specifications and Production Tolerances by Visual and instrumental Means; Coloring of Plastics, Fundamentals*. 2 ed, ed. R. Charvat. Cleveland, Ohio: john Wiley,2004.

14. Hunterlab. *Observer* The basics of Color perception and measuremnt 2001 [cited 17 Feb ,2015; Available from: https://**WWW.GOOGLE.CA/?GWS_RD=SSL#Q=HUNTERLAB+2001**.

15. Judd, D.B., and Wyszeki, G., *Color in Business, Science and Industry*. 2nd ed.: Wiley, 1975.

16. McCarty, W.H., *Process and Apparatus for Producing Colored Chemical Coatings*. US patent # 3,601,589 ,USA,1971.

17. Olmsted, R., *Advanced Color Formulation Technology, in Coloring of Plastics, Fundamentals, 2nd ed.* edited by Robert Charvat, 2004.

18. TriboCoating. *Testing processes*. Hue judgment 2014 [cited 2015 27 April]; Available from: HTTP://WWW.TRIBOCOATING.DE/INDEX.PHP?ID=100&L=2.

19. Rauwendaal, C., *Polymer Mixing, A Self-Study Guide.* Hanser Publishers, Munich., 1998.

20. Giles, H.F., Wagner, J.R., Mount, E.M., *Extrusion: the definitive processing guide and handbook*. Vol. 1. Plastic design library and its logo are owned by William Andrew,ISBN-0-8155-1473-5 ,2007.

21. Cameron, J.M., *Compounding Equipment Dry Color Concentrate Manufacture; Coloring of Plastics, Fundamentals, 2nd ed*. 2004.

22. Russel, S., *The Color Compounding Process in Coloring of Plastics, Fundamentals, 2nd ed.* edited by Robert Charvat 2004.

23. Rwei, S.P., *Distributive Mixing in a Single-Screw Extruder – Evaluation in the Flow Direction.* Polymer Engineering and Science, 2001.

24. Wang, W., and Manas-Zloczower, I., *Dispersive and Distributive Mixing Characterization in Extrusion Equipment*, in *SPE ANTEC*. Department of Macromolecular Science, Case Western Reserve University: Dallas, Texas ,2001.

25. Wong, A.Y., *Screw Configuration Effects on The Colour Mixing Characteristics Of Polymer In Single-Screw Extrusion.* The University of Hong Kong, China Tinhua Liu, Sichuan Union University, China., 1998.

26. Mudalamene R.., N., M., and Sedar Jr. W.T., *Impact of Titanium Dioxide Surface Characteristics on Extrusion Processing*, in *SPE ANTEC*. DuPont Titanium Technologies, Wilmington, DE, USA ,2005.

27. Mulholland, B.M., *Effect of Additives on the Color & Appearance of Plastics.* SPE ANTEC. **Ticona, Ticona Engineering Polymers ,2007**.

28. Bourennani, F., **Alsadi, J**. , Rizvi, G. M. and Ross, D., *Manufacturing Processing Improvements Using Business Intelligence.* Journal of Information Technology Review. **2**(3): p. 125-131, 2011.

29. Bourennani, F., **Alsadi, J**. , Rizvi, G. M., and Ross, D. , *Decision Tree Classifier for Analysis of Parameters Association Causing Polymer Color Mismatch*, in *Annual Technical conference of the Society of Plastics Engineers (ANTEC)*. Orlando, Florida, USA. p. 1-5,2012.

30. Bourennani, F., Rizvi, G. M. , Ross, D. , *Plastic color mismatch causes identification using OLAP and data mining*, in *ICDIM 2010*. Thunday-Bay, Canada. p. 69-74 , 2010.

31. Braha, D.a.S., A., *Data mining for improving a cleaning process in the semiconductor industry,.* IEEE Transactions on Semiconductor Manufacturing. **15**(1): p. 91-101, 2002.

32. Kuo CF J., H.Y., Su TL and Shih CY *Computerized Color Distinguishing System for Color Printed Fabric by Using the Approach of Probabilistic Neural Network.* Polymer-Plastics Technology and Engineering. **47**(3): p. 264-272, 2008.

33. Saeed, U., **Alsadi, J.** , Ahmad, S., *Neural Network: a potential approach for error reduction in color values of polycarbonate.* Journal Advance polymer technology. **DOI 10.1002/adv.21402** (©2013 Wiley Periodicals, Inc,2013).

34. Xi, L., *In Developing a Neural Network for Prediction Applied in Materials Science and Engineering.* EPD Congress 1992.

35. Smets, H.a.B., WFL, Mater Select Des **64**(149 , 1992).

36. Joseph, B., Hanratty, F.W. , Kardos, J., Journal of Composite Materials **29**(100 , 1995).

37. May, G.S., IEEE Spectrum. **5**(47, 1994).

38. Fei-Long Chen, F.L. and S.F. Liu, IEEE Transaction,. **3**(13): p. 366, 2000.

39. Chitra, S.P., AI Expert **6**(20 , 1992).

40. Chitra, S.P., Chemical Engineering Progress. **89**(44 ,1993).

41. Hunt, K.J., Sbarbaro, D. , Zbikowski, R. and Gawthop, P., Journal of Automatica. **28,1083, 1992**.

42. Fukuda, T.a.S., T., IEEE Transactions on Industrial Electronics, (Vol 39 , issue 472 , 1992).

43. Thibault, J.a.G., B. P. A., IFAC Symposium Series **Vol 8**(issue 251 , 1991).

44. Huang, S.H.a.Z., H. C. , IEEE Components Packaging and Manufacturing Technology, Part A, (Vol 17 , issue, 212 ,1994).

45. Bulsari, A.B., Journal of Systems Engineering **Vol 4**(issue 131 , 1994).

46. Widrow, B.a.S., SD, *Adaptive Signal Processing.* Prentice-Hall: Englewood Cliffs, NJ, 1985.

47. Widrow, B., *Proceedings of the Second IFAC Workshop on Adaptive Systems in Control and Signal Processing.* Lund Institute of Technology, Lund, Sweden, 1986.

48. Psaltis, D., Sideris, A. and Yamamura, A. A. , IEEE Control Systems Magazine **Vol 8**(issue 17 ,1988).

49. Dirion, J.L., Cabassud, M. , Lann, M. V. L. and Casamatta, G. , Computers & Chemical Engineering. **Vol 19**(S797 , 1995).

50. Savkovic-Stevanovic, J., Computers & Chemical Engineering. **Vol 18**(1149, 1994).

51. Hornik, K., Neural Networks. **Vol 6**(1069 ,1993).

52. Muller, D.a.R., J. , *Neural Networks: An Introduction.* Springer-Verlag: New York, USA, 1990.

53. Rumelhart, D.E.a.M., J. L., *Parallel Distributed Processing.* Explorations in the Microstructure of Cognition, Foundations; MIT Press: Cambridge, MA, Vol 1,1986.

54. Saeed, U., **Alsadi, J.** , Ahmad, S. and Rizvi, G. M., *Polymer Color Properties: Neural Network Modeling.* Journal Advance Polymer Technology. **DOI 10.1002/adv.21402** (©2013 Wiley Periodicals, Inc,2014).

55. Effertz, K., *Understanding the Effects of a Compounding Process on the Production of Co-Extruded Vinyl Sheet through the Utilization of Design of Experiments (part II).* ANTEC-Conference Proceedings: p. 3574-3578 ,2004.

56. *HTTP://ITL.NIST.GOV/DIV898/HANDBOOK.* [Online] available **accessed in 2013**.

57. Bender, T.M., *Characterization of Apparent Viscosity with respect to a PVC-Wood Fiber Extrusion Process.* ANTEC-Conference Proceedings, 2002.

58. Borror, C.N., Montgomery, D. C. and Myers, R. H., *Evaluation of Statistical Designs for Experiments Involving Noise Variables.* Journal of Quality Technology. **Vol 34**(1): p. 54-70 , 2002.

59. Anderson, M.J., and Whitcomb, P. J., *RSM Simplified: Optimizing Processes using Response Surface Methods for Design of Experiments.* New York, NY: CRC Press. , 2005.

60. Montogomery, D.J., *Design and Analysis of Experiments, 6th ed.* New York, NY. John Wiley & Sons, 2005.

61. DeRudder, J.L., *Handbook of Polycarbonate Science and Technology Chap. 14.* D. G. LeGrand and J. T. Bendler, eds., Marcel Dekker,. **New York** p. 303-316 , 2000.

62. Wong, A.a.L., Y. , Journal of Polymer Research. **15**: p. 11–19 ,2008.

63. HorTokita, N., Pliskin, I. , Rubber Chemistry and Technology. **Vol 46**(1166 ,1973).

64. Pliskin, I., Rubber Chemistry and Technology. **46**(1218 , 1973).

65. Russel, W.B., Saville, D. A. and Schowalter, W. R., *Colloidal Dispersions.* Cambridge University Press, Cambridge., 1989.

66. Vincent, B., Advances in Colloid and Interface Science. **4**(19 , 1974).

67. Meade, D.I., *Introduction to colorant selection and Application Technology.* In Coloring of Plastics, Fundamentals, 2nd ed., 2004.

68. Mishra, A., K. , Scientific Journal & Industrial Research **Vol 67 ,2008**

69. Dealy, J.a.W., K. F. , *In Melt Rheology and its Role in Plastics Processing: Theory and Applications.* Van Nostrand Reinhold. New York: Kluwer Academic Publishers., 1990.

70. Abdel-Goad, M.a.P., P. , Journal of Non-Newtonian Fluid Mechanics: p. page 2-6, 2005.

71. Mange Sana, N., Chi kuku, R. S, and Mainza, A. N. , Journal of the South African Institute of Mining & Metallurgy / Saimm. **Vol 108**(issue 4): p. 237-243 ,2008.

72. Zaeh, M.a.H., R. , *Impact of stabilizers on the color of pigmented polymer articles Geneva.* Geneva, Switzerland, Clariant Business Unit Additives 2002.

73. Sanchez, P., Remiro, P. M. , Nazabal, J., Journal Applied Polymer Science. **Vol 50**: p. 995-1005 , 1998.

74. Liang, R.F.a.G., R. K., *Society of Plastic Engineering.* ANTEC: p. 2903-2907 , 2000.

75. Khan, M.M.K., *Rheological and mechanical properties of ABS/PC blends.* Korea-Australia Rheology Journal. **17**(1): p. 1-7, 2005.

76. Lee, S.a.M., P., *Pearson DMMK.* Journal of applied polymer science **59**: p. 243-250 , 1996.

77. Fatoni, R., *Product Design of Wheat Straw Polypropylene Composite.* Waterloo: University of Waterloo, 2012.

78. Cox, W.P., Merz, E. H., *Correlation of dynamic and steady flow viscosities.* Journal of Polymer Science. **28**: p. 619-622 , 1958.

79. Knavery, M., Gundea, Marta Klanjšek, Mozetičb, Miran, and Hrovatc, Anton, Dyes and Pigments. **57**(3): p. 235-243 ,2003.

80. Russell, S., *Color Compounding & Appearance of Plastics.* ANTEC, Ticona Engineering Polymers., 2007.

81. Talimi, M., *Characterization of natural fibre reinforced biodegradable composities*. University of Ontario Institute of Technology , 2011.

82. Shenoy , A.V., *Rheology of filled polymer systems*. Boston: Kluwer Academic Publishers , 1999.

83. Verhoyen, O.a.D., F., *A simplified method for introducing the Cross viscosity law in the numerical simulation.* Journal of Non-Newtonian Fluid Mechanics **74**: p. 25-46 , 1998.

84. **AlSadi, J.,** U. , Saeed, S.Ahmad, U. , Rizvi, G. , Ross, D. , Clarke, R. and Price, J. , *Processing Issues of Color Mismatch: Rheological Characterization of Polycarbonate Blends.* Journal of Polymer Engineering and Science. **John Wiley & Sons, Inc**(10.1002/pen.24041 , 2014).

85. Macosko, C.W., *Rheology: Principles, Measurement and Applications*. VCH Publishers: New York , 1994.

86. *Rheometric Scientific Applications Brief, Measuring normal forces*

87. Weissenberg, K., Nature. **159**(310, 1947).

88. Hong, B.K., Kim, H. S. and Chung, C. I. , SPE ANTEC Technical Paper. **47**(272 ,2001).

89. Hogan, T.A., Spalding, M. A. , Cho K.S. and Chung, C. I. , in *SPE ANTEC Technical Papers*. 2002.

90. Mount, E.M.a.C., C. I. , Polymer Engineering & Science **Vol 18**(711 , 1978).

91. Matthews, G., Vinyl and allied polymers. **2**(Iliffe, London 1972).

92. Abbasi, S., Leelapornpisit, W. , Derdouri, A. and Carreau, P. J. , *Morphology and Properties of Microinjected Polycarbonate/MWCNT Nanocomposites*, in *66th Annual Technical Conference of the Society of Plastics Engineers*. Plastics Encounter at ANTEC. p. 1513-1517 ,2008.

93. Su-Dong Park, D.-H.H., *Phase Transition of Multi-Walled Carbon Nanotube/Polystyrene Composites.* Journal of the Korean Physical Society. **Vol. 48, No. 3**: p. pp. 476-479 ,March 2006.

94. Vemardalds, T.G., *Improving Dispersion Of Organic Pigments.* Modern Paint and Coatings, 1985.

95. Smith, R.F., *Microscopy and Photomicrography 2 nd ed*. CRC Press, Boca Raton , 1994.

96. McCrone, W.C.a.D., J. G. , *The Particle Atlas 2 nd ed*. Vol. Vol 187. Ann Arbor Science Publishers , 1973.

97. Sommer, A.J., *Infrared spectra, Molecular Microspectroscopy Laboratory*, in *Dept. of Chemistry & Biochemistry*. Miami University: Oxford, OH ,1998.

98. Stoiber, R.E.a.M., S. A., *Crystal Identification with the Polarizing Microscope*. Chapman& Hall, New York , 1994.

99. Watt, I.M., *The Principles and Practice of Electron Microscopy*. 10 ed.: Cambridge University Press , 1985.

100. Thompson, B., *Printing Materials: Science and Technology.* PIRA: p. 329-330 ,1998.

101. Frimova, A., Pekarovicova, A. , Fleming, P. D. and Pekarovic, A. , *Ink Stability During Printing.* TAGA J. **Vol 2 ,2005**.

102. Sharma, M.K.a.M., F. J. , *Surface Phenomena and Fine Particles in Water-based Coating and Printing Technology*. New York : Plenum Press , 1991.

103. Sharma, M.K., *Surface Phenomena and Additives in Water-Based Coating and Printing Technology*. New York: Plenum Press, 1995.

104. Nobuoka, S., *The Relation between Particle Size and Shape of the Pigments and Optical Properties.* Color Mater. **55**(10): p. 758-765 , 1982.

105. Honigman, B., *The Crystal Properties of Organic Pigments.* Journal of Paint Technology. **Vol 38**(issue 493 , 1966).

106. Heitzman, S., *Special Effects pigments for plastic*, in *Annual Technical Conference of the Society of Plastic Engineer(SPE)*. Cincinnati, Ohio ,2007.

107. Lewis, P.A., *Pigment Handbook*. 2 ed. Vol. 1. New York: Wiley, 1988.

108. Herbst, W., Hunger, K. , *Industrial Organic Pigments, Production, Properties, Applications*. NewYork: publisher VCH , 1993.

109. Vermogen, A., Masenelli, K. , Séguéla, R. , *Macromolecules*. **Vol 38**(issue 9661, page 9, 2005).

110. Rajeev, R., Harkin-Jones, E. , Soon, K. , McNally, T. , Menary, G. , Armstrong, CG. and Martin PJ., *European Polymer Journal* **Vol 45**(issue 332 , page 40, 2009).

111. Callioster Jr. , W.D.a.R., D. J. , *Materials Science and Engineering - An Introduction, 6th ed.* New York, NY: John Wiley & Sons, 2011.

112. Zink, M.O., *The Value of Transparent and Opaque Pigments in Plastics Coloration.* CAD RETEC-Conference Proceedings: p. 319-328 , 2004.

113. Kosarzycki, M.a.K., L., *A Technique Comparison for the Quantification of Color Concentrate in a Polyacetal Component*. 3200 South 166th Street, New Berlin ,: publisher :Element New Berlin , pages WI 53151-2701, 2008.

114. Plantz, P.E., *SL-AN-30 Revision A.* Pigment Particle Size Using Microtrac Laser Technolog. WWW.MICROTRAC.COM **(accessed 2013)**.

115. Jährling, M.a.F., A., *HAAKE Minilab -Compounder and Reactor.* Thermo Scientific, 2005.

116. ARES, G. *TA Instruments-Rheometer*. [cited 2015 june 20; Available from: https://WWW.NDSU.EDU/CNSE/MCAL/EQUIPMENT/RHMTR.HTML.

117. Olsen, T.; MP600M Et:[ASTM D1238]. Available from: sop+extrusion+plastometler+[Updated May 11, 2015].

118. X-Rite. © 2007, X-Rite, Incorporated 2015; Available from: L10-328_color-Eye_7000A_en.

119. Keyence-Digital-Microscope. *VHX-1000* Available from: KEYENCE_vhx_1000_ku,2015 June 4.

120. JEOL USA, I. *(SEM)- Joel 5500*. [cited 2015 June 12; Available from: HTTP://WWW.PHOTONICS.COM/PRODUCT.ASPX?PRID=30250.

121. Plantz, P.E., *Pigment Particle Size Using Microtrac Laser Technology.* SL-AN-30 Revision A, 2009. **[online].Avaialable;www:Microtrac.com.[Accessed 2013].**

122. SkyScan. *Instruction Manual: Desktop X-ray micro tomography*. Bruker Corporation 2005; Available from: https://WWW.MICROPHOTONICS.COM/SKYSCAN1172.

123. **AlSadi, J.,** Rabbani, M. , Ahmed, S. , Rizvi, G. , Clarke , R. and Ross, D., *Effect of Processing Parameters on Colour During Compounding.* Annual Technical Conference of the Society of Plastics Engineers (ANTEC), Boston, USA: p. 1-4, 2011.

124. Rabbani, M., **AlSadi , J**. , Rizvi , G. , Ahmed S. and Ross , D., *Study on Effects of various Parameters on Colours During Compounding of Plastics*, in *Annual Technical Conference of the Society of Plastics Engineers (ANTEC)*. Boston, USA , 2011.

125. **AlSadi**, J., Ahmad, S. , Saeed, U. , Rizvi, G. , Ross, D. , Clarke, R. and Price, J., *Effects of Processing Parameters on Color Mismatch During Compounding.* Annual Technical conference of the Society of Plastics Engineers (ANTEC), Orlando, Florida, USA, 2012: p. 1-5.

126. **AlSadi, J.,** Ahmad, S. , Saeed, U. , Rizvi, G. , Ross, D. , Clarke, R. and Price, J. , *Execution of 3 level full factorial design to evaluate the process parameters: polymer color properties.* Annual Technical conference of the Society of Plastics Engineers (ANTEC), Orlando, Florida, USA: p. 1-5 ,2012.

127. Ahmad, S., **AlSadi, J.** , Saeed, U. , . and Rizvi,G. , *Process Optimization through Designed Experiments to Achieve Consistency in Output Color of a Compounded Plastic Grade.* Taylor&Francis. **Vol 27 ,24 April 2015**.

128. Roy, N.K., Landau, D. P. and Potter, W. D. , Applied Intelligence. **Vol 20**(3): p. 215–229 , 2004.

129. Mandic, D.P.a.C., J. A. , *Recurrent Neural Networks for Prediction: Learning Algorithms, Architectures and Stability.* Wiley: New York, 2001.

130. Yu, M.C., Bisell, M. A. and Whitehouse, R. S., *The Effect of Carbon Black Dispersion on Polymer Performance.* ANTEC. **3246 , Vol 50,1995**.

131. Whitcomb, P.J.a.A., M. J. , *Robust Design-Reducing Transmitted Variation: Finding the Plateaus via Response Surface Methods.* Annual Quality Congress: p. 642-651 , 1996.

132. Anderson, M.J., and Whitcomb, P. J., *Response Surface Methods (RSM) for Peak Process Performance at the Most Robust Operating Conditions.* Proceeding from International SEMATECH Manufacturing Initiative (ISMI) Symposium on Manufacturing Effectiveness, 2007.

133. Washburn, E., *The Dynamics of Capillary Flow.* Phys. Rev. **Vol 17**(273 ,1921).

134. Xu, J., Hou,Z., and Li, T., *Novel Sample Preparation Method of Polymer Emulsion for SEM Observation.* Microscopy Research and Technique. **Vol 70**: p. 847–850 ,2007.

135. Klanjsek, G.M., Kunaver, M. , Mozeti M. and Hrovat, A. . **148**(1): p. 2203 – 2207 , 2004.

136. Saeed, U., Ahmad, S., **Alsadi, J**., Rizvi,G. and Ross, D., *"Neural Network For Colour Properties Of Polycarbonates", Annual International Conference, PPS-29.* p. Nuremberg, Germany, pp. 1-4, 2013.

137. Ahmad, S., **AlSadi, J**. , Saeed, U. , and Rizvi,G, *Implementation of Box Behnken Design for Optimizating Compounding Process Ensuring Consistant Output Colour of a Polycarbonate Grade, Quality Engineering, Manuscript ID LQEN-2014-0098, Rev1 under review , submitted in July 2014.*

138. **AlSadi, J.**, Ahmad, S. , Saeed, U. , Rizvi, G. , Ross, D. , Clarke, R. and Price, J, *Effects of Processing Parameters on Colour Mismatch During Compounding. Annual Technical conference of the Society of Plastics Engineers (ANTEC), Orlando, Florida, USA ,pp 1-5 , 2012.*

139. Ahmad, S., **AlSadi, J.** , Saeed, U. , Rizvi, G. , Ross, D. , Clarke, R. and Price, J. , *Experimental Study to Investigate Effect Of process variables On Output Colour Of A compounded Plastic Grade*, in *Annual Technical conference of the Society of Plastics Engineers (ANTEC)*. Cincinnati, Ohio, USA. p. 1-8, 2013.

140. Ahmad, S., **AlSadi, J.** , Saeed, U. , Rizvi, G. , Ross, D. , Clarke, R. and Price, J, *Study on effect of Small Perturbations in Colour Formulation on Output Colour of Plastic Grade Compounded with Single Polycarbonate resin*, in *Annual Technical conference of the Society of Plastics Engineers (ANTEC)*. Orlando, Florida, USA. p. 1-5,2012.

141. Ahmad, S., **AlSadi, J.** , Saeed, U. , Rizvi, G. , Ross, D. and Clarke, R. , *Effect Of Small Perturbations In Colour Formulation On Output Colour Of Plastic Grade Compounded With Two Polycarbonate Resins*, in *Annual Technical conference of the Society of Plastics Engineers (ANTEC),* . Cincinnati, Ohio, USA. p. 1-5,2013.

142. Rabbani, M., **AlSadi, J**. , Rizvi,G. , D. Ross, and Ahmed S., *Study on the Effects of processing Parameters on Plastic Colours During Compounding Operations* in *Annual Technical conference of the Society of Plastics Engineers (PPS)*. Marrakech, Morocco. p. 1-4,2011.

143. Rabbani, M., **AlSadi, J**. , Rizvi, G. , Ross, D. and Ahmed, S., *Sensitivity of Colours in Compounding of Plastics to Minute Variations in Pigment Compositions*, in *Annual Technical conference of the Society of Plastics Engineers (PPS)*. Marrakech, Morocco. p. 1-6 ,2011.

144. **Alsadi, J**., Saeed, U. , Rizvi, G. , Ross, D. , Clarke, R. and Price, J. ,, *Effects of Rheological Behaviour on Colour Matching of Two Polycarbonate Resin Blends. Annual Technical conference of the Society of Plastics Engineers (ANTEC), Dubai, UAE ,2014.*

145. **Alsadi, J.**, Saeed, U. , Rizvi, G. , Ross, D. , Clarke, R. and Price, J, *Effects of Processing Parameters on Colour Mismatch and Experimental Design to Optimize the Colour Properties of Polycarbonate,Presenting at UOIT 3rd Annual Graduate Student Research Conference, April 2012.*

Appendix A: Neural Network

Table A–1. The complete dataset used for training (70%), validation (15%), and testing (15%); R=resin, A=additives, P=pigments

Temp (°C)	Speed (rpm)	Feed Rate (kg/hr)	R1	R2	A1	A2	A3	A4	A5	A6	A7	A8	A9	A10	P1	P2	P3	P4	P5	P6	P7	L*	a*	b*
269.0	375.0	501.0	0.3	0.7	0.2	0.2	0.3	0.1	0.8	0.0	0.0	0.0	0.0	0.0	1.8	0.0	0.0	0.1	0.0	0.0	0.0	67.4	1.6	5.0
269.0	375.0	501.0	0.3	0.7	0.2	0.2	0.3	0.1	0.8	0.0	0.0	0.0	0.0	0.0	1.8	0.0	0.0	0.1	0.0	0.0	0.0	67.0	1.5	5.2
269.0	375.0	501.0	0.3	0.7	0.2	0.2	0.3	0.1	0.8	0.0	0.0	0.0	0.0	0.0	1.9	0.0	0.0	0.1	0.0	0.0	0.0	66.8	1.4	5.0
257.0	650.0	150.0	0.3	0.7	0.2	0.2	0.3	0.1	0.8	0.0	0.0	0.0	0.0	0.0	1.8	0.0	0.0	0.1	0.0	0.0	0.0	67.2	1.5	4.9
257.0	650.0	150.0	0.3	0.7	0.2	0.2	0.3	0.1	0.8	0.0	0.0	0.0	0.0	0.0	1.9	1.0	0.0	0.1	0.0	0.0	0.0	67.0	1.5	5.1
297.0	550.0	200.0	0.3	0.7	0.2	0.2	0.3	0.1	0.8	0.0	0.0	0.0	0.0	0.0	1.8	0.0	0.0	0.1	0.0	0.0	0.0	67.1	1.6	4.9
297.0	550.0	200.0	0.3	0.7	0.2	0.2	0.3	0.1	0.8	0.0	0.0	0.0	0.0	0.0	1.9	1.0	0.0	0.1	0.0	0.0	0.0	67.4	1.5	4.8
297.0	550.0	200.0	0.3	0.7	0.2	0.2	0.3	0.1	0.8	0.0	0.0	0.0	0.0	0.0	1.9	1.0	0.0	0.1	0.0	0.0	0.0	67.2	1.5	4.5
297.0	550.0	200.0	0.3	0.7	0.2	0.2	0.3	0.1	0.8	0.0	0.0	0.0	0.0	0.0	1.9	1.0	0.0	0.1	0.0	0.0	0.0	67.2	1.4	4.9
256.0	752.0	225.0	0.3	0.7	0.2	0.2	0.3	0.1	0.8	0.0	0.0	0.0	0.0	0.0	1.8	0.0	0.0	0.1	0.0	0.0	0.0	68.1	1.6	4.8
256.0	752.0	225.0	0.3	0.7	0.2	0.2	0.3	0.1	0.8	0.0	0.0	0.0	0.0	0.0	1.9	1.0	0.0	0.1	0.0	0.0	0.0	67.2	1.4	4.8
256.0	752.0	225.0	0.3	0.7	0.2	0.2	0.3	0.1	0.8	0.0	0.0	0.0	0.0	0.0	1.9	1.0	0.0	0.1	0.0	0.0	0.0	67.3	1.4	4.9
256.0	752.0	225.0	0.3	0.7	0.2	0.2	0.3	0.1	0.8	0.0	0.0	0.0	0.0	0.0	1.9	1.0	0.0	0.1	0.0	0.0	0.0	67.2	1.5	4.8
256.0	752.0	225.0	0.3	0.7	0.2	0.2	0.3	0.1	0.8	0.0	0.0	0.0	0.0	0.0	1.9	1.0	0.0	0.1	0.0	0.0	0.0	67.4	1.7	5.3
246.0	774.0	244.0	0.3	0.7	0.2	0.2	0.3	0.1	0.8	0.0	0.0	0.0	0.0	0.0	1.8	0.0	0.0	0.1	0.0	0.0	0.0	67.2	1.4	5.0
246.0	774.0	244.0	0.3	0.7	0.2	0.2	0.3	0.1	0.8	0.0	0.0	0.0	0.0	0.0	1.9	1.0	0.0	0.1	0.0	0.0	0.0	66.4	1.5	4.3

Temp (°C)	Speed (rpm)	Feed Rate (kg/hr)	R1	R2	A1	A2	A3	A4	A5	A6	A7	A8	A9	A10	P1	P2	P3	P4	P5	P6	P7	L*	a*	b*
246.0	774.0	244.0	0.3	0.7	0.2	0.2	0.3	0.1	0.8	0.0	0.0	0.0	0.0	0.0	1.9	1.1	0.0	0.1	0.0	0.0	0.0	67.3	1.4	4.9
246.0	774.0	244.0	0.3	0.7	0.2	0.2	0.3	0.1	0.8	0.0	0.0	0.0	0.0	0.0	1.9	1.0	0.0	0.1	0.0	0.0	0.0	68.0	1.9	5.6
246.0	774.0	244.0	0.3	0.7	0.2	0.2	0.3	0.1	0.8	0.0	0.0	0.0	0.0	0.0	1.9	1.0	0.0	0.1	0.0	0.0	0.0	67.2	1.5	4.8
262.0	769.0	204.0	0.3	0.7	0.2	0.2	0.3	0.1	0.8	0.0	0.0	0.0	0.0	0.0	1.8	0.0	0.0	0.1	0.0	0.0	0.0	67.3	1.6	5.1
262.0	769.0	204.0	0.3	0.7	0.2	0.2	0.3	0.1	0.8	0.0	0.0	0.0	0.0	0.0	1.9	1.0	0.0	0.1	0.0	0.0	0.0	67.4	1.7	5.3
262.0	769.0	204.0	0.3	0.7	0.2	0.2	0.3	0.1	0.8	0.0	0.0	0.0	0.0	0.0	1.9	1.0	0.0	0.1	0.0	0.0	0.0	66.4	1.5	4.3
262.0	769.0	204.0	0.3	0.7	0.2	0.2	0.3	0.1	0.8	0.0	0.0	0.0	0.0	0.0	1.9	1.0	0.0	0.1	0.0	0.0	0.0	67.3	1.6	4.7
266.0	765.0	200.0	0.3	0.7	0.0	0.0	0.0	0.0	0.0	0.0	0.0	0.0	0.0	0.0	0.1	0.0	0.2	0.1	0.2	0.0	0.0	70.6	4.0	18.2
224.0	700.0	500.0	0.3	0.7	0.0	0.0	0.0	0.0	0.0	0.0	0.0	0.0	0.0	0.0	1.5	0.0	0.0	0.3	0.0	0.0	0.0	63.5	-0.3	-0.2
224.0	700.0	500.0	0.3	0.7	0.0	0.0	0.0	0.0	0.0	0.0	0.0	0.0	0.0	0.0	1.5	0.0	0.0	0.3	0.0	0.0	0.0	63.8	-0.3	-0.2
300.0	222.0	150.0	0.3	0.7	0.0	0.0	0.0	0.0	0.0	0.0	0.0	0.0	0.0	0.0	1.5	0.0	0.0	0.3	0.0	0.0	0.0	63.0	-0.2	-0.2
300.0	222.0	150.0	0.3	0.7	0.0	0.0	0.0	0.0	0.0	0.0	0.0	0.0	0.0	0.0	1.5	0.0	0.0	0.3	0.0	0.0	0.0	62.9	-0.3	0.0
255.0	599.0	474.0	0.3	0.7	0.0	0.0	0.0	0.0	0.0	0.0	0.0	0.0	0.0	0.0	1.5	0.0	0.0	0.3	0.0	0.0	0.0	63.6	-0.5	0.1
255.0	599.0	474.0	0.3	0.7	0.0	0.0	0.0	0.0	0.0	0.0	0.0	0.0	0.0	0.0	1.5	0.0	0.0	0.0	0.0	0.0	0.0	63.6	-0.2	-0.1
255.0	599.0	474.0	0.3	0.7	0.0	0.0	0.0	0.0	0.0	0.0	0.0	0.0	0.0	0.0	1.5	0.0	0.0	0.0	0.0	0.0	0.0	63.6	-0.2	-0.1
255.0	599.0	474.0	0.3	0.7	0.0	0.0	0.0	0.0	0.0	0.0	0.0	0.0	0.0	0.0	1.5	0.0	0.0	0.3	0.0	0.0	0.0	63.5	-0.3	-0.2
255.0	599.0	474.0	0.3	0.7	0.0	0.0	0.0	0.0	0.0	0.0	0.0	0.01	0.0	0.0	1.5	0.0	0.0	0.3	0.0	0.0	0.0	63.8	-0.3	-0.1
275.0	750.0	125.0	0.3	0.7	0.0	0.0	0.0	0.0	0.0	0.0	0.0	0.0	0.0	0.0	1.5	1.0	1.2	0.3	0.0	0.0	0.0	64.5	-0.3	-0.2
275.0	750.0	125.0	0.3	0.7	0.0	0.0	0.0	0.0	0.0	0.0	0.0	0.0	0.0	0.0	1.4	1.1	1.2	0.3	0.0	0.0	0.0	63.7	-0.3	-0.2

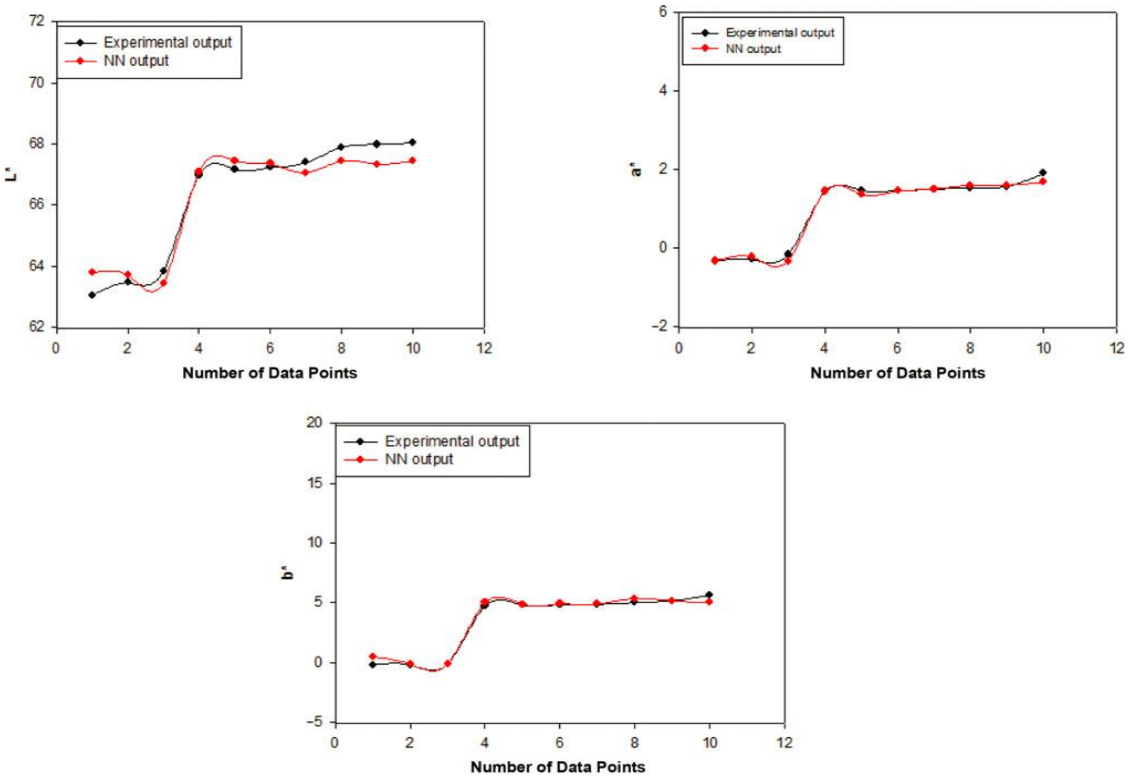

Figure A–1. Comparison of NN and experimental output for colour tristimulus values L*, a*, b*: validation data

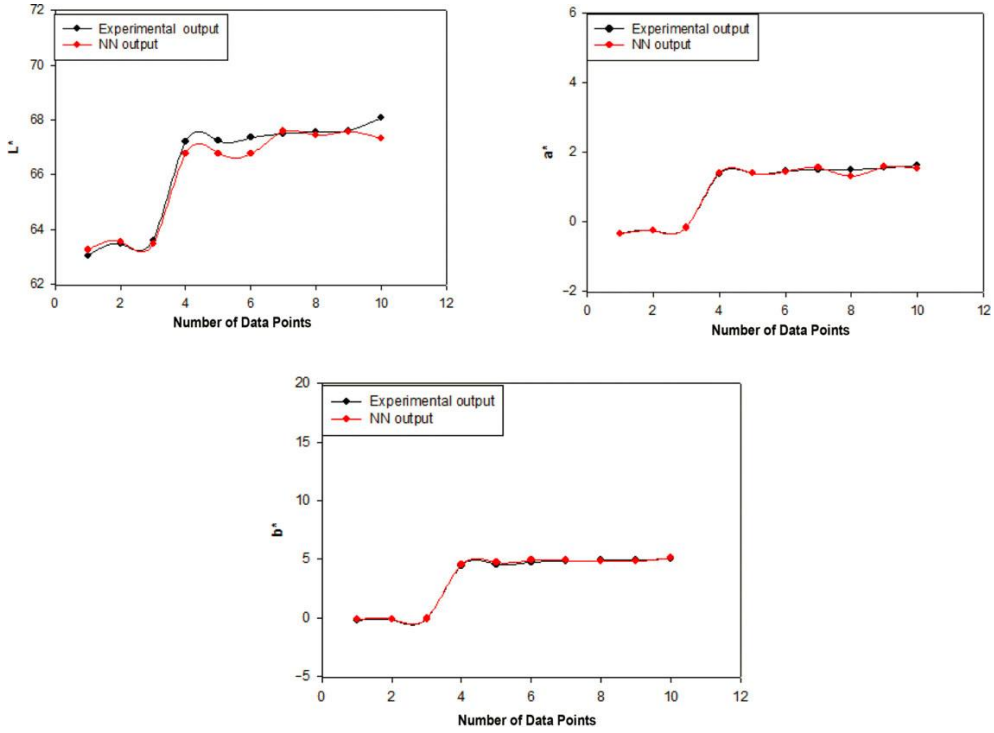

Figure A–2. Comparison of NN and experimental output for colour tristimulus values L*, a*, b*: test data

Table A–2. Weights between the input layer and hidden layer for L*, a*, and b*

Neurons, i	1	2	3	4	5	6	7	8	9	10	11	12	13	14	15	16	17	18	19	20	21	22	23	24	25
1	− 0.44	− 0.80	− 0.35	0.38	0.04	0.09	0.55	− 0.22	− 0.18	0.29	− 0.04	0.38	− 0.26	0.41	0.32	0.29	0.40	0.37	−0.06	0.54	0.34	0.41	−0.20	−0.35	0.05
2	− 0.53	− 0.21	0.15	− 0.28	0.05	0.36	− 0.41	− 0.50	0.12	− 0.51	− 0.35	− 0.23	− 0.31	−0.19	0.70	0.29	0.33	−0.10	−0.28	−0.07	−0.30	0.31	−0.60	−0.78	0.20
3	0.44	0.07	− 0.28	0.09	− 0.42	− 0.47	− 0.13	0.22	− 0.37	0.36	0.02	− 0.10	− 0.33	0.57	0.48	0.33	0.64	−0.44	0.58	−0.37	−0.03	0.46	0.06	0.15	0.25
4	0.17	0.07	0.03	0.35	0.65	0.33	− 0.22	0.38	− 0.56	− 0.17	− 0.30	− 0.12	− 0.36	−0.04	0.46	0.31	0.19	0.60	0.16	0.28	0.14	0.11	−0.02	−0.67	−0.48
5	0.44	0.16	0.04	0.00	− 0.03	0.33	0.04	− 0.53	− 0.25	− 0.11	0.00	− 0.33	− 0.54	0.09	−0.22	−0.56	−0.58	−0.40	0.03	−0.24	−0.30	0.33	0.03	0.06	0.37
6	0.00	0.11	0.69	− 0.21	− 0.36	0.34	0.07	0.01	− 0.60	− 0.03	− 0.05	− 0.55	0.24	0.18	−0.03	0.52	−0.38	0.10	−0.56	0.31	0.44	−0.44	0.08	−0.57	−0.13
7	0.01	0.05	− 0.09	− 0.37	− 0.39	− 0.49	0.37	− 0.05	− 0.14	− 0.46	0.54	0.47	0.09	0.41	0.20	0.04	0.59	0.17	−0.48	0.33	−0.36	0.15	−0.40	−0.20	0.01
8	0.13	− 0.50	0.15	− 0.14	0.46	− 0.50	− 0.09	0.47	− 0.49	0.09	− 0.31	0.00	− 0.16	0.25	−0.41	−0.01	−0.58	−0.51	0.11	−0.01	0.50	−0.31	−0.23	−0.25	−0.25
9	− 0.58	0.59	0.47	− 0.34	− 0.51	0.26	0.43	0.32	0.28	0.43	− 0.36	− 0.43	0.06	0.10	0.08	−0.48	−0.02	−0.61	0.05	−0.27	−0.15	−0.14	−0.27	−0.59	−0.20
10	− 0.51	− 0.06	0.58	0.15	− 0.17	0.57	− 0.17	0.19	0.66	0.23	− 0.17	0.61	0.37	0.78	0.21	0.09	−0.51	0.37	−0.03	−0.32	−0.13	0.37	0.11	0.64	−0.07
11	− 0.20	0.16	0.34	0.32	0.01	0.18	− 0.08	0.48	− 0.29	0.56	0.13	− 0.13	0.48	−0.11	0.30	0.05	0.18	0.39	−0.22	−0.60	−0.67	−0.51	0.58	0.49	0.72
12	0.35	0.36	0.14	0.45	− 0.21	0.20	− 0.05	0.06	− 0.50	− 0.03	− 0.56	− 0.55	0.11	−0.10	−0.11	0.28	0.42	−0.30	−0.40	−0.47	−0.37	0.25	0.07	0.76	−0.15
13	− 0.46	0.19	− 0.53	− 0.51	0.48	0.21	− 0.09	0.34	− 0.26	− 0.45	0.21	0.48	− 0.31	0.37	0.26	0.19	0.05	−0.01	−0.12	0.59	0.15	0.07	−0.19	0.14	0.14
14	− 0.07	− 0.21	0.47	0.38	0.12	0.63	− 0.20	− 0.34	0.50	0.61	0.10	− 0.51	0.23	0.15	0.47	−0.27	−0.10	0.30	0.41	−0.34	0.18	0.08	−0.35	0.35	0.84

Table A–3. Variety of pigments used for experiments with their maximum and minimum concentrations (pph) of polycarbonate resin for 3,500 lots

		Concentration (pph)	
Pigments	**Chemical Name**	**Max**	**Min**
Green pigment 187-B, C.I. pigment blue 36	Cobalt chromite blue-green spinel	0.79	0
Titanium dioxide	Titanium dioxide (80–100%), aluminum hydroxide (1–5%)	12	0
Blue/green pigment	C.I. pigment blue 29 (sodium aluminosilicate)	1	0
Violet pigment	Manganese ammonium pyrophosphate	0.88	0
Carbon black concentrate	Poly (BPA-carbonate) terminated with paracumylphenol	4.95	0
Titanium dioxide pigment	Titanium dioxide (80–99%), amorphous silica (<10%)	8.65	0
Titanium dioxide	Titanium dioxide (80–100%), aluminum hydroxide (1-5%)	12.5	0
Titanium dioxide pigment	Titanium dioxide (80-98%), aluminum hydroxide (0-9%)	2.65	0
Zinc sulfide	Zinc sulfide 100%	11	0
Zinc oxide	Zinc oxide (99.8%), lead (0.05%)	4.32	0
Black pigment1	C.I. pigment black 7 (90–100%)	0.26	0
Black pigment 2	C.I. pigment black 7 (90–100%)	0.46	0
Carbon black pigment 1	Carbon black, amorphous 100%	1.94	0
Carbon black pigment 2	Carbon black, amorphous 100%	1.23	0
Black pigment	BPA polycarbonate, encapped w/P-cumylp (75%), carbon black (25%)	1.99	0
Black pigment	Amorphous silica(1-5%), iron oxide 99%	0.54	0
Black pigment	Amorphous silica(1-9%), iron oxide 90%	0.04	0
Carbon black grade series	Carbon black, amorphous 100%	1.75	0
Black pigment	Polybutylene terephthalate (70–90%), carbon Black (10–30%)	7.06	0
C.I. pigment green 50	Cobalt titanate (100%)	1.32	0
C.I. solvent green 3 (green Pigment)	C.I. solvent green 3 (100%), mercury < 1 ppm	0.5	0
C.I. solvent green 3 (green pigment)	C.I. solvent green 3 (100%), mercury < 1 ppm	0.19	0
C.I. pigment green 7	Copper-phthalocyanine complex (100%)	1	0
C.I. pigment green 7	Copper-phthalocyanine complex (100%)	0.62	0
Tan pigment	Zinc ferrite	0.91	0
Pigment red 101 (dark red iron oxide)	Iron (III) oxide (95%), amorphous silica (4%)	1.35	0
Pigment red 101	Iron (III) Oxide (95%), Aluminum Hydroxide (1-5%)	0.77	0
SPD micropellets of R6110 at 0.1%	C.I. disperse violet 26/31	0.06	0
Red pigment	Iron oxide - red (97-100%)	0.26	0
Red pigment	C.I. solvent red 52 (100%)	0.5	0
Red pigment- 1	Iron oxide – red (>92%)	0.05	0
Red pigment- 2	Iron oxide – red (>92%)	0.93	0
C.I. solvent red 135-1	C.I. solvent red 135 (100%)	0.83	0
C.I. solvent red 135-2	C.I. solvent red 135 (100%)	1.13	0
Red pigment (solvent red 207)	9,10-Anthracenedione, 1,5-bis(cyclohexylamino)-	0.3	0
Red pigment (solvent red 207)	9,10-Anthracenedione, 1,5-bis(cyclohexylamino)-	1	0
Violet pigment	C.I. solvent violet 13(> 97 %)	0.5	0
Permanent blue 15:4-1	Phthalocyanine blue (87–90%), proprietry (8–10%)	1	0
Permanent blue 15:4-2	Phthalocyanine blue (87–90%), proprietry (8–10%)	0.29	0
Violet pigment	C.I. solvent violet 13 (>97 %)	0.33	0
C.I. solvent violet 36	C.I. solvent violet 36 (100%)	0.15	0
Blue pigment-1	C.I. pigment blue 29 (100%)	1	0
Blue pigment-2	C.I. pigment blue 29 (100%)	0.7	0
Blue pigment #60	C.I. pigment blue 60; C.I. 69800	0.04	0
C.I. solvent violet 36	C.I. solvent violet 36 (100%)	0.47	0

		Concentration (pph)	
Pigments	**Chemical Name**	**Max**	**Min**
Blue pigment #104-1	C.I. solvent blue 104 (99%)	0.5	0
Blue pigment #104-2	C.I. solvent blue 104 (99%)	0.85	0
Blue pigment #101	9, 10 Anthracenedione, 1, 4, bis (alkylphenyl) amino (99%)	0.09	0
Blue pigment #28-1	Spinel, aluminum oxide-cobalt blue (100%)	1	0
Blue pigment #28-1	Spinel, aluminum oxide-cobalt blue (100%)	0.88	0
Titanium antimony chromium III dioxide rutile (C.I. pigment brown 24)-1	Titanium antimony chromium III dioxide rutile (C.I. pigment brown 24) (100%)	2.04	0
Titanium antimony chromium III dioxide rutile (C.I. pigment brown 24)-1	Titanium antimony chromium III dioxide rutile (C.I. pigment brown 24) (100%)	0.85	0
Yellow pigment #14	Nickel antimony titanium yellow rutile (99%)	1.84	0
Yellow pigment #53-1	Nickel antimony titanium yellow rutile (99%)	1.92	0
Yellow pigment #53-2	Nickel antimony titanium yellow rutile (99%)	1.9	0
C.I. pigment yellow #183	C.I. pigment yellow 183 (100%)	0.7	0
Pigment yellow 163-1	C.I. solvent yellow 163 (100%)	0.98	0
Pigment yellow 163-2	C.I. solvent yellow 163 (100%)	0.89	0
Pigment orange 60	C.I. solvent orange 60 (100%)	0.91	0
C.I. solvent yellow 93-1	C.I. solvent yellow 93 (100%)	1.11	0
C.I. solvent yellow 93-2	C.I. solvent yellow 93 (100%)	0.74	0
C.I. pigment yellow 138	Quinophthalone yellow; C.I. pigment yellow 138 (100%)	0.32	0
C.I. disperse yellow 201	Propanedinitrile, [[4-[[2-(4-cyclohexylphenoxy)ethyl]ethylamino]- 2 methylphenyl]methylene (100%)	0.4	0
Pigment orange 107/47-1	C.I. disperse orange 47	0.73	0
Pigment orange 107/47-2	C.I. disperse orange 47	0.56	0

Table A–4. Concentration (ppH gm of polycarbonate resin) of lots with experimental and test (neural network) L*, a*, and b*

	White		Black				Green					Red		Yellow			Violet				Experimental			Test (Neural Network)		
Lot No.	**P1**	**P2**	**P1**	**P2**	**P3**	**P4**	**P1**	**P2**	**P3**	**P4**	**P5**	**P1**	**P2**	**P2**	**P3**	**P4**	**P1**	**P2**	**P3**	**P4**	**L***	**a***	**b***	**L***	**a***	**b***
1	0.05	0	0	0.01	0	0	0	3.08	0	0	0	0	0	0	0	0	0	0	0.63	0	44.21	–21.13	20.15	44.25	–21.1	20.13
2	1.57	0	0	0.15	0	0	0	0	0	0.07	0	0	0	0	0	0	0	0.05	0	0	38.65	–4.08	5.8	38.63	–4.17	5.68
3	1.06	0	0	0	0	0	0	0	0	0	0	0	0	0	0	0	0	0	0	0	76.44	0.14	3.25	76.43	0.11	3.25
4	0	1.64	0	0	0	0	0	0	0	0	0	0	0	0	0	0	0	0	0	0	72.75	–1.31	–1.69	72.76	–1.28	–1.44
5	0.87	0	0	0	0	0	0	0	0	0	0	0	0	0	0	0	0	0	0	0	71.96	–0.88	1.62	72.16	–0.85	1.55
6	0.28	0	0	0	0	0	0	0	0	0.05	0	0	0	0	0	0	0	0	0	0	34.61	0.65	–27.62	34.46	0.6	–27.62
7	2.05	0	0	0	0.08	0	0	0	0	0	0	0	0	0	0.05	0	0	0	0	0	88.96	0.03	3.76	88.85	0.01	3.8
8	0.01	0	0	1.9	0	0	0	0	0	0.01	0	0	0	0	0	0.01	0	0	0	0	28.57	0.23	–1.15	28.48	0.14	–0.22
9	1.02	0	0	0	0.08	0	0	0	0	0	0.13	0	0	0	0	0	0	0	0	0	73.47	–20.57	–16.26	73.53	–20.51	–16.26
10	0.87	0	0	0	0	0	0	0	0	0	0	0	0	0	0	0	0	0	0	0	70.96	–0.92	1.5	71.18	–0.89	1.42
11	2.32	0	0	0	0	0	0	0	0	0	0	0	0	0	0	0	0	0	0	0	96.08	–1.23	3.12	96.01	–1.21	3.1
12	0.9	0	0	0.23	0	0	0	0	0	0	0	0	0.08	0	0.95	0	0	0	0	0	34.67	–0.03	–1.6	34.57	–0.09	–1.58
13	3.26	0	0	0.01	0	0	0.01	0	0	0	0	0	0.01	0	0	0	0	0	0	0	76.73	1.12	2.97	76.96	1.06	2.99
14	0	0	0	0	0	0	0	0	0	0	0	0	0	0	0	0	0	0	0	0	95.83	–0.3	2.77	95.42	–0.29	2.86
15	1.25	0	0	0.01	0	0	0	0.02	0	0	0	0	0	0	0	0	0	0	0	0	68.1	–0.1	6.06	68.28	–0.12	6.03
16	2.73	0	0	0	0	0	0	0	0	0	0	0	0	0.03	0	0	0	0	0	0	94.51	–0.63	2.99	94.35	–0.61	3
17	2.05	0	0	0	0.08	0	0	0	0	0	0	0	0	0	0.05	0	0	0	0	0	88.76	0	3.97	88.65	–0.02	4.01
18	0.28	0	0	0	0	0	0	0	0	0.49	0	0	0	0	0.05	0	0	0	0.11	0	42.71	–36.15	10.36	42.7	–36.21	10.35
19	0	0	0	0	0	0.83	0	0	0	0	0	0	0	0	0	0	0	0	0	0	26.74	–0.11	–0.52	26.82	–0.12	–0.46
20	0	0	0	0	0	0	0	0	0	0	0	0	0	0	0	0	0	0	0	0	95.84	–0.29	2.78	95.43	–0.27	2.87
21	0.38	0	0	0	0.02	0	0	0	0	0	0	0	0	0	0.43	0.14	0	0	0	0	79.77	4.19	68.51	79.82	4.26	68.12
22	0	0	0	0	0	0	0	0	0	0	0	0	0	0	0	0	0	0	0	0	92.7	–0.44	4.98	92.35	–0.41	5.02
23	0.38	0	0	0	0.02	0	0	0	0	0	0	0	0	0	0.43	0.14	0	0	0	0	79.78	4.16	68.52	79.83	4.23	68.12
24	0	0	0	0	0	5.52	0	0	0	0	0	0	0	0	0	0	0	0	0	0	27.7	–0.02	–1.12	27.89	–0.02	–1.09
25	2.23	0	0	0.01	0	0	0	0	0	0	0	0	0	0	0	0	0	0	0	0	67.14	5.2	17.07	66.5	4.57	16.86
26	0.73	0	0	0	0.03	0	0	0	0	0	0	0	0.13	0	0	0	0	0	0	0	46.84	41.02	25.39	46.99	41.03	25.28
27	0.42	0	0	0	0	0	0	0	0	0	0	0	0	0	0	0	0	0	0	0	46.31	48.33	25.95	46.23	48.18	25.89
28	0	0	0	0	0	4.39	0	0	0	0	0	0	0	0	0	0	0	0	0	0	27.43	–0.08	–1.26	27.55	–0.09	–1.23
29	0.08	0	0	0	0.07	0	0	0	0	0	0	0	0	0	0	0	0.2	0	0	0	46.81	45.23	25.66	46.64	45.07	25.54
30	0.85	0	0	0	0.18	0	0	0	0	0.07	0	0	0	0	0	0	0	0	0.5	0	58.39	–36.66	36.43	58.52	–36.06	36.53

	White		Black				Green					Red		Yellow			Violet				Experimental			Test (Neural Network)		
Lot No.	**P1**	**P2**	**P1**	**P2**	**P3**	**P4**	**P1**	**P2**	**P3**	**P4**	**P5**	**P1**	**P2**	**P2**	**P3**	**P4**	**P1**	**P2**	**P3**	**P4**	**L***	**a***	**b***	**L***	**a***	**b***
31	0.5	0	0	0.1	0	0	0	0.72	0	0	0	0	0	0	0.66	0	0.32	0	0	0	36.56	–2.64	5.18	36.41	–2.56	5.23
32	0	0	8.39	0	0	0	0	0	0	0	0	0	0	0	0	0	0	0	0	0	27.63	–0.14	–0.91	27.74	–0.16	–0.78
33	1.75	0	0	0.16	0	0	0	0	0	0.08	0	0	0	0	0	0	0	0.06	0	0	38.7	–4.04	6.43	38.66	–4.14	6.31
34	0.72	0	0	0.01	0	0	0	0	0	0	0	0	0	0	0	0	0	0	0	0	61.53	1.88	4.26	61.73	1.85	4.32
35	0.66	0	0	0	0.01	0	0.11	0	0	0	0	0.06	0	0	0	0	0	0	0	0	70.83	–1.76	–4.05	70.89	–1.77	–3.93
36	0	0	0	0	0.13	0	0	0	0	0	0	0	0	0	0	0	0.03	0	0	0	42.26	44.03	21.49	42.38	43.98	21.56
37	1.97	0	0	0.13	0	0	0	0	0	0.02	0	0	0	0	0.05	0	0	0	0	0	41.33	–1.47	–4.31	41.35	–1.61	–4.31
38	0	0	0	0	0	3.65	0	0	0.08	0	0	0	0	0	0	0	0	0	0.14	0	28.42	–0.2	–1.14	28.43	–0.16	–1.15
39	0.13	0	0	0	0.04	0	0	0	0	0	0	0	0	0	0	0	0	0	0.03	0.2	41.75	42.48	22.95	41.79	42.47	22.9
40	0.71	0	0	0.05	0	0	0	0.07	0	0	0	0	0	0	0	0	0	0	0	0	41.76	–0.38	1.82	41.85	–0.41	1.93

Appendix B: Glossary

I. Data Mining & Neural Network

Data mining: The process of efficient discovery of non-obvious valuable patterns from a large collection of data.

Decision Trees: A class of data mining and statistical methods that form tree like predictive models.

On-Line Analytical Processing (OLAP): Computer-based techniques used to analyze trends and perform business analysis using multidimensional views of business data

OLAP operations:

- **Rollup:** increasing the level of aggregation
- **Drill-down:** decreasing the level of aggregation or increasing detail
- **Slice:** selection
- **Dice:** projection
- **Pivot:** re-orienting the multidimensional view of data

Error rate: A number that reflects the rate of errors made by a predictive model. It is one minus the accuracy.

Genetic algorithm: A method of solving optimization problems using parallel search, based on Darwin's biological model of natural selection and survival of the fittest.

Model: A description that adequately explains and predicts relevant data but is generally much smaller than the data itself.

Neural Network: A computing model based on the architecture of the brain. A neural network consists of multiple simple processing units connected by adaptive weights.

Regression: Analysing technique data to determines a mathematical equation that minimizes some measure of the error between the prediction from the regression model and the actual data.

Bias: The net input (or bias) is proportional to the amount that incoming neural activations must exceed in order for a neuron to fire.

Backpropagation (generalised delta-rule): A name given to the process by which the Perceptron neural network is "trained" to produce good responses to a set of input patterns. In light of this, the Perceptron network is sometimes called a "back-prop" network

Sigmoid function: An S-shaped function that is often used as an activation function in a neural network.

Epoch: One complete presentation of the training set to the network during training.

Learning rule: The algorithm used for modifying the connection strengths, or weights, in response to training patterns while training is being carried out.

Learning algorithm: An optimization procedure that adjusts the weights connecting the nodes to minimize the difference between the output and the target (the desired result)

Threshold: A quantity added to (or subtracted from) the weighted sum of inputs into a neuron, which forms the neuron's net input. Intuitively, the net input (or bias) is proportional to the amount that the incoming neural activations must exceed in order for a neuron to fire.

Weight: In a neural network (NN), the strength of connection between two neurons. Weights may be positive (excitatory) or negative (inhibitory). The thresholds of a neuron are also considered weights, since they undergo adaptation by a learning algorithm.

Data divisions:

- **Training set:** used to adjust the weights on the neural network.

- **Validation set:** used to minimize over fitting

- **Test data:** After the successful training of the network, the network was tested with the test data

GDM: Gradient descent with momentum (GDM): Generally faster than training. Can be used in incremental mode training.

GD: The batch gradient descent. Basic gradient descent; slow response; can be used in incremental mode training.

GDX: Batch variable learning rate

RP: Resilient backpropagation. Simple batch mode training algorithm with fast convergence and minimal storage requirements.

Multilayer networks typically use sigmoid transfer functions in the hidden layers. Sigmoid functions are characterized by the fact that their slope must approach zero as the input gets large. This causes a problem when using steepest descent to train a multilayer network with sigmoid functions, since the gradient can have a very small magnitude; and therefore, cause small changes in the weights and biases, even though the weights and biases are far from their optimal values. The purpose of the resilient backpropagation (Rprop) training algorithm is to eliminate these harmful effects of the magnitudes of the partial derivatives.

SCG: Scaled conjugate gradient.

This algorithm is too complex to explain in a few lines, but the basic idea is to combine the model-trust region approach (used in the Levenberg-Marquardt algorithm described later), with the conjugate gradient approach.

LM: Levenberg-Marquardt (least squares curve fitting). Fastest training algorithm for networks of moderate size. Has memory reduction feature for use when the training set is large.

II. Response Surface Methods (RSM)

Adequate Precision: This is a signal-to-noise ratio. It compares the range of the predicted values at the design points to the average prediction error. Ratios greater than 4 indicate adequate model.

Adj R-squared: A measure of the amount of variation around the mean explained by the model, adjusted for the number of terms in the model.

Analysis of Variance (ANOVA): A method, based on the F-distribution, for testing the null hypothesis of no treatment effects. Also can be defined as a statistical technique which subdivides the total variation of a set of data into component parts associated with specific sources of variation for the purpose of testing a hypothesis on the parameters of a model.

Center points: Experiments runs with all numerical factor levels set at the midpoint of their high and low settings.

Curvature: A measure of departure of the response surface from a planar surface. Curvature is indicated if the average of the factorial points is different from the average of the center points.

Degrees of Freedom: The number of independent comparisons available to estimate a parameter. Usually the number of model parameters minus 1.

Design Model: The design model is the model that the experiment was designed to estimate when the design was first created.

Degrees of Freedom (DF): The amount of information available from replicated points attributed to the blocks, generally equal to one less than the number of blocks.

Design of Experiments (DOE): A change of many or several factors that affect process responses, in a minimum number of runs; simultaneously optimize several responses; build empirical models to predict response behaviour as a function of process factors

Factor: Experimental variables selected for inclusion in the predictive model.

Factorial: A series of runs in which combinations of factor levels are included.

Full Factorial Designs: perform a power analysis to evaluate differences detected in designed experiments evaluate the impact of adding replicates and centre points on power examine the impact of outliers on results and residual plots

Fractional factorial: An experimental design which includes only a subset of all possible combinations of factor levels, causing some of the effects to be confounded.

Fractional Factorial Design: Reduce the number of experimental runs using fractional factorial designs, apply sequential experimentation to fit a model, use centre points to improve power, test for curvature, and estimate pure error.

F-Value: Test for comparing curvature or lack of fit variance with residual (pure) error variance. If the variances are close to the same, the ratio will be close to one and it is less likely that lack of fit is significant.Itis calculated by curvature Mean Square divided by Residual Mean Square.

Interaction: The effect that occurs when the combined change in two factors produces an effect greater (or less) than that of the sum of effects expected from either factor alone. An interaction occurs when the effect one factor has depends on the level of another factor.

Lack of Fit (LOF): This is the variation of the data around the fitted model. If the model does not fit the data well, the test will show significant. The result of experimentation should be a model that will adequately predict the response within the design space. A small F value and high p value (greater than 0.1) are good in this test. If a model has a significant lack of fit it is not a good predictor of the response and should not be used.

Linear Model: A polynomial model containing only linear or main effect terms.

Mean: Overall average of all the response data.

Mean Square: Estimate of the term variance, calculated by the term sum of squares divided by term degrees of freedom.

Model: The model is the empirical mathematical model that is fit to the data. Polynomial models are used in DESIGN-EXPERT. In the ANOVA the Model term is the source of variation accounted for by the model terms.

Outlier: An outlier is a design point where the response does not fit the model. Suspected outliers should be examined for possible errors in response measurement or recording or in the conduct of that particular experiment. Outliers should not be dismissed - the response may be desirable and may lead to an important discovery.

Polynomials: Factorial polynomial models are limited to intercept, first order linear and order interaction terms, where n is the number of factors.

Predicted R-squared: Measures the amount of variation in new data explained by the model. Predicted R-squared = 1 - SSPRESS/(SStotal - SSblocks-SScurvature).

Predicted Value: The value of the response predicted by the mathematical model

Probability of a Larger F-Value: If the F ratio -the ratio of variances - lies near the tail of the <F>distribution then the probability of a larger F is small and the variance ratio is judged to be significant. Usually, a probability less than 0.05 is considered significant.

p-Value: Probability value, usually relating the risk of falsely rejecting a given hypothesis.

Pred R-squared: A measure of the amount of variation in new data explained by the model. The predicted R-squared and the adjusted R-squared should be within 0.20 of each other. Otherwise there may be a problem with either the data or the model.

Pure Error: Amount of variation in the response in replicated design points.

Quadratic Model: A polynomial model containing linear and two-factor terms.

Regression Analysis: A method by which data is fitted to a mathematical model.

Replicate: Replication of design points provides an estimate of pure error in the design. Replication means running the experiment at least twice from scratch. More replicates provide better estimates of error.

Residual Error: The difference between the observed response and the value predicted by the model for a particular design point.

R-squared: A measure of the amount of variation around the mean explained by the model.

Std Dev (Root MSE): Square root of the residual mean square. Consider this to be an estimate of the standard deviation associated with the experiment.

Sum of Squares: Pure error sum of squares from replicated points.

95% CI High and Low: These two columns represent the range that the true coefficient should be found in 95% of the time. If this range spans 0 then the coefficient of 0 could be true, indicating the factor has no effect. The predictive model is listed in both actual and coded terms.

III. Colour

Absolute white: A white solid with known spectral reflectance data identified as “reference white” used in practice for all measurements of absolute reflectance. When calibrating a spectrophotometer, often a white ceramic plaque is measured and used as the absolute white reference. In theory, a material that perfectly reflects all light energy at every visible wavelength.

Absorb/Absorption: Dissipation of the energy of electromagnetic waves into other forms (e.g., heat) which results of its interaction with matter. Decreases in directional transmittance of incident radiation result in modification or conversion of the absorbed energy.

Achromatic colour: A neutral colour that has no hue (white, gray or black).The "hueless" colours black, gray, and white, that is, the whole range of gray levels between black and white. In ISO Definition: Perceived colours devoid of hue. The colour names white, gray and black are commonly used or, for transmitting objects, colourless and neutral. (Source: ISO 9241-8 (1997-10-00) ISO/TC 159)

Figure B–1. Achromatic colours

Additive Colour: Colour space based on the three primary colours red (R), blue (B) and green (G) used for additive colour mixing. Televisions and computer monitors use RGB to reproduce colour.

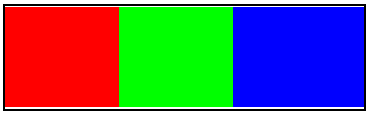

Figure B–2. The three primaries of the RGB colour space are red, green, and blue

Any colour can be produced by adding the colours of the three colour channels RGB (Red, Green, and Blue). If the colours of two of the colour channels are mixed in equal proportions, new base colours are created. Blue and green add up to a bright, light blue called cyan. Magenta, a bright pink, is made by mixing red and blue. Red and green together make yellow. If red, green, and blue light are mixed equally together at full power, you get white light. (Adapted from WWW.LINOCOLOUR.COM)

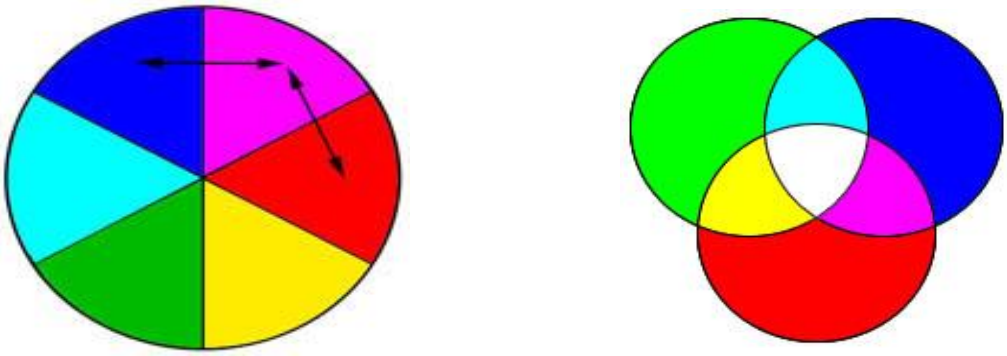

Figure B–3. Mixing two colours additively leads to a lighter colour; if red, green, and blue light are mixed equally together at full power, you get white light (from WWW.MICA.EDU)

Additive primaries: Red, green and blue light. When all three additive primaries are combined at 100% intensity, white light is produced. While combining the three additive primaries at varying intensities, a gamut of different colours is produced. Combining two primaries at 100% produces a subtractive primary, cyan, magenta or yellow:

100% red + 100% green = yellow

100% red + 100% blue = magenta

100% green + 100% blue = cyan

Appearance: An object's or material's manifestation through visual attributes such as size, shape, colour, texture, glossiness, transparency, opacity, etc.

Artificial daylight: Term loosely applied to light sources, frequently equipped with filters that try to reproduce the colour and spectral distribution of daylight

Brightness: The dimension of colour that refers to an achromatic scale, ranging from black to white. It is also called lightness, luminous reflectance or transmittance.

L*: Indicate lightness and darkness on CIE 1964 colour space

a*: Represents red to green axis on CIE 1964 colour space

b*: Represents yellow to blue axis on CIE 1964 colour space.

C*: Abbreviation for chromaticity.

Chroma/Chromaticity: The intensity or saturation level of a particular hue, defined as the distance of departure of a chromatic colour from the neutral (gray) colour with the same value. Synonym for Saturation

Chromatic Colours: The "colourful" colours like, red, green, blue, yellow, purple, etc.

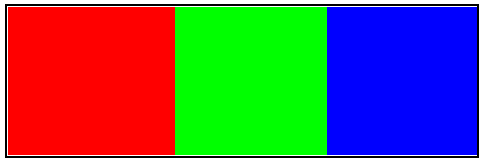

Figure B–4. The chromatic primaries of additive colour mixing

Chromaticity diagram (CIE): A two-dimensional graph of the chromaticity coordinates (x as the abscissa and y as the ordinate), which shows the spectrum locus (chromaticity coordinates of monochromatic light, 380-770nm). It has many useful properties for comparing colours of both luminous and non-luminous materials.

CIE (Commission Internationale de l'Eclairage): The International Commission on Illumination, is the primary international organization that determines standards for colour and lighting and developed the **NORM COLOUR SYSTEM** and the **LAB COLOUR SPACE** (Lab Colour System, or CIELAB Colour System).

CIE 1976 L*a*b* colour space: A uniform colour space utilizing an Adams-Nickerson cube root formula, adopted by the CIE in 1976 for use in the measurement of small colour differences.

CIELAB (or CIE L*a*b*, CIE Lab): Colour space is defined by the **CIE** based on one channel for **LUMINANCE** (lightness) (L) and two colour channels (a and b). The values L*, a* and b* are plotted using Cartesian coordinate system. Equal distances in the space approximately represent equal colour differences. Value L* represents lightness; Value a* represents the red/green axis; and value b* represents the yellow/blue axis. The axis extends from green (-a) to red (+a) and the b axis from blue (-b) to yellow (+b). The brightness (L) increases from the bottom to the top of the three-dimensional model. (From **WWW.LINOCOLOUR.COM**)

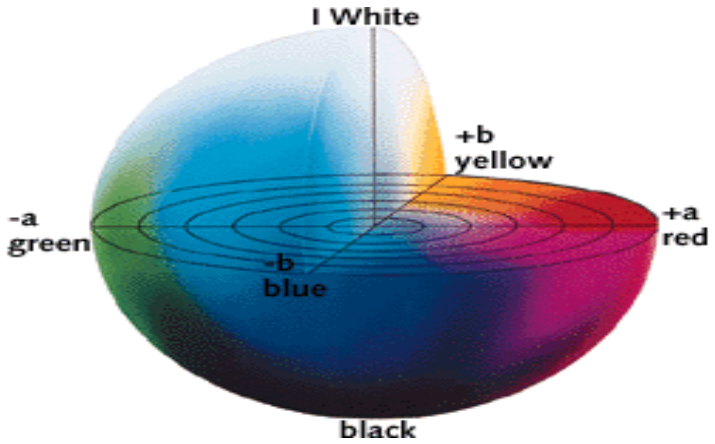

Figure B–5. The CIELAB colour space

CMC (Colour Measurement Committee of the Society of Dyes and Colourists of Great Britain): Organization that developed and published in 1988 a more logical, ellipse-based equation based on L*C*h° colour space for computing DE (see delta E*) values. It is considered as an alternative to the rectangular coordinates of the CIELAB colour space.

Colour: One aspect of appearance; a stimulus based on visual response to light, consisting of the three dimensions of hue, saturation and lightness.

Colour difference: The difference between two colours under specified conditions as magnitude and character.

Colour model: A colour-measurement scale or system that is numerically specifies the perceived attributes of colour. Used in computer graphics applications and by colour measurement instruments.

Colour space: Three dimensional solid enclosing all possible colours with coordinates for red, green and blue. The dimensions may be described in various geometries, giving rise to various spacing within the solid. It integrates brightness into the picture; the colour triangle must be transformed from a two-dimensional triangle into a spatial body known as colour space.

Colour specification: Tristimulus values, chromaticity coordinates and luminance value, or other colour-scale values, used to designate a colour numerically in a specified colour system.

Colour temperature: A measurement of light colour radiated by a black body while it is being heated. This measurement is expressed in terms of absolute scale, or degrees Kelvin. Lower Kelvin temperatures such as 2400K are red; higher temperatures such as 9300K are blue. Neutral temperature is white, at 6504K.

Colourants: Materials used to create colours — dyes, pigments, toners, waxes, phosphors.

Colour Additive: Colour includes white, black, and gray. In addition, any chemical that reacts with another substance and causes formation of a colour

Colourimeter: An optical measurement instrument that responds to colour in a manner similar to the human eye — by filtering reflected light into its dominant regions of red, green and blue.

Colourimetric: Relating to values giving the amounts of three coloured lights or receptors — red, green and blue.

Colourist: A skilled person in the art of colour matching (colourant formulation), also knowledgeable concerning the behavior of colourants in a particular material; a tinter/shader (q.v)

Contrast: The level of variation between light and dark areas in an image.

Cultural Variations in the Meaning of Colours: See figure below.

Culture	Red	Blue	Green	Yellow	White
USA, Europe	Danger	Manliness, sweet, calm, Authority	Safety, safe, sour	Caution, Cowardice	Purity
France	Nobility	Freedom, Peace	Criminality	preliminary	Neutrality
Egypt, Arab Nations	Death	Virtue, Faith, Truth	Fertility, Strength	Happiness, Welfare or Wealth	Joy
India	Life, Creativity		Welfare or Wealth, Fertility	Success	Death, Purity
Japan	Anger, Danger	Shame, Despicableness	Future, Youth, Energy	Grace, Dignity, Nobility, childish, joyful	Death
China	Happiness, Joy, Festivity	Sky, Clouds	Ming dynasty, royal, Honor	Birth, Wealth, Strength or Power	

Figure B–6. Cultural variations in the meaning of colour (http://www.swiss-miss.com/2005/08/page/2)

D65: The CIE standard illuminant that represents a colour temperature of 6504K. This is the colour temperature most widely used in graphic arts industry viewing booths. See Kelvin (K).

Daylight illuminants (CIE): Series of illuminant spectral power distribution curves based on measurements of natural daylight and recommended by the CIE in 1965. Values are

defined for the wavelength region 300 to 830nm. They are described in terms of the correlated colour temperature.

Delta (delta E*): A symbol used to indicate deviation or difference. – The total colour difference computed with a colour difference equation. In colour tolerance, the symbol DE is often used to express Delta Error.

Dye: A soluble colourant — as opposed to pigment, which is insoluble.

Electromagnetic spectrum: The massive band of electromagnetic waves that pass through the air in different sizes, measured by wavelength. Different wavelengths have different properties, but most are invisible — and some completely undetectable — to human beings. Only wavelengths that are between 380 and 720 nanometers are visible, producing light. Waves outside the visible spectrum include gamma rays, x-rays, microwaves and radio waves.

Gloss: An additional parameter to consider when determining a colour standard, along with hue, value, chroma, the texture of a material and whether the material has metallic or pearlescent qualities. Gloss is an additional tolerance that may be specified in the Munsell Colour Tolerance Set. The general rule for evaluating the gloss of a colour sample is the higher the gloss unit, the darker the colour sample will appear. Conversely, the lower the gloss unit, the lighter a sample will appear. Gloss is measured in gloss units, which use the angle of measurement and the gloss value (e.g. 60° gloss = 29.8). A 60° geometry is recommended by the American Society for Testing and Materials (ASTM) D523 standard for the general evaluation of gloss.

HSL, HSV, HSB: – Hue, Saturation, Luminance (also known as Hue, Saturation, Value or Hue, Saturation, Brightness): A system for describing the physical perception of colour, in terms of tint (hue, colour tone), perceived narrowness of the spectrum (saturation, chroma), and luminance (brightness, value). Hue determines the position on the colour wheel or colour circle, Saturation is the purity of the colour, and Luminance the range of lightness to darkness of the colour. Hue can be changed by moving position on the colour circle:

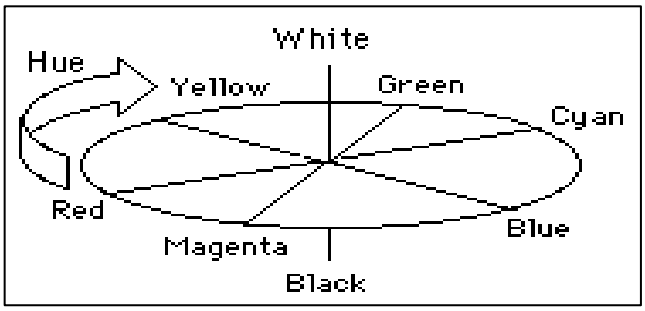

Figure B–7. Hue changes by moving position on the colour circle (from Hyper Physics)

Hue: The first element in the colour-order system, defined as the attribute by which we distinguish red from green, blue from yellow, etc. Munsell defined five principal hues (red, yellow, green, blue and purple) and five intermediate hues (yellow-red, green-yellow, blue-green, purple-blue and red-purple.

Luminance: The amount of visible light incident that comes to the eye from a surface. Reflectance is the proportion of incident light that is reflected from a surface. Luminance, illuminance, and reflectance, are physical quantities that can be measured by physical devices.

Illuminant A (CIE): Incandescent illumination, yellow-orange in colour, with a correlated colour temperature of 2856K. It is defined in the wavelength range of 380 to 770nm.

Illuminant C (CIE): Tungsten illumination that simulates average daylight, bluish in colour, with a correlated colour temperature of 6774K.

Light: Electromagnetic radiation of which a human observer is aware through the visual sensations that arise from the stimulation of the retina of the eye. This portion of the spectrum includes wavelengths from about 380 to 770nm.

Metamerism: A phenomenon exhibited by a pair of colours that match under one or more sets of illuminants.

Munsell Colour System: The colour identification of a specimen by its Munsell hue, value and chroma as visually estimated by comparison with the Munsell Book of Colour.

Nanometer (nm): Unit of length equal to 10-9 meter (a.k.a. one billionth of a meter, or a milli-micron).

Observer: The human viewer who receives a stimulus and experiences a sensation from it. In vision, the stimulus is a visual one and the sensation is an appearance.

Reflectance: The ratio of the intensity of reflected radiant flux to that of incident flux

Scattering: Diffusion or redirection of radiant energy encountering particles of different refractive index. Scattering occurs at any such interface, at the surface, or inside a medium containing particles.

Spectrophotometer: Photometric device that measures spectral transmittance, spectral reflectance or relative spectral emittance.

Spectrophotometric curve: A curve measured on a spectrophotometer; a graph with relative reflectance or transmittance (or absorption) as the ordinate, plotted with wavelength or frequency as the abscissa.

Spectrum: Spatial arrangement of components of radiant energy ,wavelengths, wave number or frequency.

Standard observer (CIE): 1) A hypothetical observer having the tristimulus colour-mixture data recommended in 1931 by the CIE for a 2° viewing angle. A supplementary observer for a larger angle of 10° was adopted in 1964. 2) The spectral response characteristics of the average observer defined by the CIE. Two such sets of data are defined, the 1931 data for the 2° visual field (distance viewing) and the 1964 data for the annular 10° visual field (approximately arm's length viewing). By custom, the assumption is made that if the observer is not specified, the tristimulus data has been calculated for the 1931 or 2° field observer. The use of the 1964 data should be specified.

Total reflectance: Reflectance of radiant flux reflected at all angles from the surface, thus including both diffuse and specular reflectances.

Transparent: Describes a material that transmits light without diffusion or scattering.

Tristimulus colourimeter: An instrument that measures tristimulus values and converts them to chromaticity components of colour.

Value: Indicates the degree of lightness or darkness of a colour in relation to a neutral gray scale. The scale of value (or V, in the Munsell system of colour notation) ranges from 0 for pure black to 10 for pure white.

IV. Digital Optical Microscope technology (DOM)

3D Display Function: A major advantage of digital microscopes over optical microscopes is their ability to easily create 3D images. The 3 dimensional profiles of observation targets are often unclear when using only 2 dimensional images. The ability to create 3 dimensional images from a "stack" of 2 dimensional images in the Z-axis is one of the most important functions of digital microscopes.

Data Storage/Recording: Most microscope systems require a separate PC for storing image files. The VHX-1000 is equipped with a built-in hard drive, CD-R/RW drive, ethernet port, and multiple USB ports, providing several ways for a user to catalog images and data.

Digital Microscopes: All-in-one microscope systems that integrate an LCD monitor PC, camera, optics, light source, and software into a portable, standalone observation device. There are generally two types of digital microscopes: low-cost, USB systems and all-in-one, research grade systems.

Variable-angle Observation System: Stand and stage system that allows a user to tilt the camera and lens around a sample (up to 90 degrees) while also rotating 360 degrees about the object. More capable units provide for an on-axis tilt, keeping the object in the center of the field-of-view while tilting about it. Adjustable lens and stage height accommodates larger samples not suitable for conventional microscopes.

Dia: The 50% (D50) of each mode is calculated after determining the minimum and maximum sizes contributing to the specific peak under consideration. For two modes, each

will have a separate 50%.When only one mode is present, the Dia will equal the 50% of the particle distribution.

MA: Mean diameter, in microns, of the "area distribution" is calculated from the volume distribution. This area mean is a type average that is less weighted (also less sensitive) than the MV to changes in the amount of coarse particles in the distribution. It represents information on the distribution of surface area of the particles of the distribution.

MV: Mean diameter in microns of the "volume distribution" represents the center of gravity of the distribution.

Percentiles: Values are selectable over the range 1% to 99% in 1% increments.

SD: Standard Deviation in microns, also known as the Graphic Standard Deviation (σg), is one measure of the width of the distribution. It is not an indication of variability for multiple measurements.

RMS Residual: (Root mean square) Microtrac performs calculations to provide particle size distributions. The calculation is completed when software-decided least error is attained.

Vol: The calculated contribution in percent of each peak to the total volume of the distribution.

V. Rheology

Bingham Model or Bingham Equation: A simple rheological model that relates shear stress and shear rate and quantifies yield stress and high-shear viscosity.

Carreau Model or Carreau Equation: A relative of the Cross Model that is often fitted to viscosity vs shear rate profiles.

Casson Model or Casson Equation: A commonly used rheological model that quantifies yield stress and high shear viscosity, typically used for inks and molten chocolate.

Complex Modulus: The overall resistance to deformation of a material, regardless of whether that deformation is recoverable (elastic) or non-recoverable (viscous).Symbol G*.

Complex Viscosity: Complex Modulus divided by Angular Frequency.

Cross Model or Cross Equation: A rheological model commonly fitted to viscosity vs shear rate profiles

Crossover Frequency: In an oscillatory (or dynamic) frequency sweep, the frequency at which the elastic and viscous moduli cross, usually marking the transition from the terminal (viscous) region to the rubbery plateau (elastic) region).

Dilatancy Shear Thickening: non-Newtonian behaviour where viscosity increases with increasing shear rate.

Elastic Modulus: The contribution of elastic (solid-like) behaviour to the complex modulus. Symbol G'.

Loss Modulus: Another name for Viscous Modulus. Symbol G".

Loss Tangent: Another name for Tan Delta

Newtonian Fluid: A fluid which exhibits a viscosity that is independent of the current shear conditions.

Non-Newtonian Fluid: A fluid which exhibits a viscosity that is dependent upon the shear conditions.

Power Law Model: A useful rheological model that describes the relationship between viscosity or shear stress and shear rate over the range of shear rates where shear thinning occurs in a Non-Newtonian fluid. Quantifies overall viscosity range and degree of deviation from Newtonian behaviour.

Pseudoplastic: Same as shear-thinning

Relaxation Time: A time constant describing the rate of relaxation of stresses in a material (eg a viscoelastic fluid) that has been deformed to a defined strain.

Rheopexy: Time dependent viscosity increase at constant shear rate – often known as anti-thixotropy.

Shear Rate: The rate of change of shear stress. The velocity gradient perpendicular to the direction of shear flow (dv/dx). Units 1/s or s-1

Shear Stress: The shear force per unit area. Symbol s or t. Units of Pascals (Pa)

Shear Strain: A unit-less quantity, the relative displacement of the faces of a sheared body (for example a layer of fluid) divided by the distance between them.

Shear Thinning: Viscosity decrease with increasing shear rate. Shear-thinning is the most common form of non-Newtonian behaviour and is seen in suspensions, emulsions, polymer solutions and gels. The change in viscosity with shear rate for some materials can span several orders of magnitude, thus emphasising the adage that for most products "viscosity is a plot, not a dot".

Storage Modulus: Another name for Elastic Modulus. Symbol G'.

Tan Delta: The tangent of the phase angle – the ratio of viscous modulus to elastic modulus and a useful quantifier of the presence and extent of elasticity in a fluid.

Thixotropy: Time dependent viscosity change at constant shear rate. A thixotropic fluid is a shear-thinning fluid that takes a finite time to reach an equilibrium viscosity following a step change in the applied shear rate.

Thermoplastics: Polymer that turns to a liquid when heated and freezes to a very glassy state when cooled sufficiently

Thermosets: Polymer that irreversibly cure

Viscoelasticity: The phenomenon of exhibiting both elastic (solid-like or energy storing) and viscous (liquid-like or energy dissipating) properties.

Viscosity: The resistance of a fluid to flow. In shear deformation viscosity is the ratio of applied shear stress to resulting shear rate.Typcally reported in units of Poise (P) and centipoise (CP) or Pascal seconds (Pa.s) or milliPascal seconds (mps.s). Symbol is typically h.

Viscous Modulus: The contribution of viscous (liquid-like) behaviour to the Complex Modulus. Symbol G".

Zero-shear Viscosity: The viscosity at the limit of low shear rate. In other words, the maximum plateau value attained as shear stress or shear rate is reduced. Zero-shear viscosity is effectively the viscosity of a product whilst at rest. For that reason, in the case of a dispersion, an elevated continuous phase zero-shear viscosity can play a vital role in inhibiting ongoing sedimentation or creaming processes.